LASER SCANNING CYTOMETRY FOR THE DETECTION OF FLUORESCENT MICROSPHERES AND BACTERIA

BY

DAVID A. LADNER

B.S., New Mexico Institute of Mining and Technology, 2003

THESIS

Submitted in partial fulfillment of the requirements
for the degree of Master of Science in Environmental Engineering in Civil Engineering
in the Graduate College of the
University of Illinois at Urbana-Champaign, 2005

Urbana, Illinois

ABSTRACT

Low pressure membrane systems are effective in removing turbidity and pathogens from drinking water. Membrane integrity can be compromised through improper installation, wear, age, or other factors that produce small holes or tears in the membrane structure. Operators easily detect large breaches in integrity, but small breaches can go undetected allowing pathogens to enter the permeate stream. The aim of this project is to develop a device capable of detecting small breaches in membrane integrity by enumerating bacteria that pass through compromised membranes. The device uses principles of cytometry, where bacteria are stained with a fluorescent dye, illuminated with a laser, and detected with a photomultiplier tube. The prototype laser scanning cytometer (LSC) uses inexpensive components, such as a 635-nm laser common in supermarket scanners and CD players. Significant effort has been expended to develop the prototype motion control and data processing software, using fluorescent microspheres as bacterial surrogates. Bacterial staining procedures were investigated to find the best staining method to accurately and consistently count bacteria. The device has proven effective in both microsphere and *Escherichia coli* detection, as compared with fluorescence microscopy.

To Mom and Dad and all our ancestors who paved the way.

ACKNOWLEDGMENTS

Directly involved in bringing this project to completion were members of Mark M. Clark's research group. Ben Lee created our prototype device leaving a clear path for its optimization. Katie Thompson taught me microbiological methods and gave insight through many discussions. Jeffrey White, Laser and Spectroscopy Facility Director, Frederick Seitz Materials Research Laboratory, UIUC, gave valuable technical advice concerning lasers and signal processing. Mark Clark and Gary Durack had the initial ideas for this membrane integrity project. Mark provided occasional course correction to keep his students on track, but mostly, he let us explore without stifling our creativity. Project funding was provided by the Korea Institute of Science and Technology. Indirect help was given through Won-Young Ahn, Melvin Koh, Angela Koh, Li Liu, Susana Kimura, Adrienne Mennitti, and Kim Milferstedt. Trips to the Dairy Queen were just as important as control runs to keep me focused. Finally, I would like to thank my fiancé, Miriam Nibley. I began writing this thesis in her home and I am completing it shortly after our engagement. She has been the thread of enjoyment recently woven into the tapestry of my days here in Illinois.

TABLE OF CONTENTS

TABLE OF CONTENTS vi

Introduction 1

Literature Review 2
- Membrane Integrity Monitoring 2
- Bacterial Detection and Counting 3
- Laser Scanning Cytometry 5
- Bacterial Staining 6
- Microspheres 8
- Signal Processing 8
  - *Peak Counting 9*
  - *Digital Filtration 9*

Microspheres 12
- Materials and Methods 12
  - *Microspheres and Filters 12*
  - *Prototype Components 13*
  - *Scanning Program 15*
  - *Focusing 16*
  - *Signal Processing 16*
  - *Fluorescence Microscopy 17*
  - *Experimental Design 17*
- Results 18
- Discussion 25

Bacteria 28
- Materials and Methods 28
  - *E. coli Sample Preparation 28*
  - *Staining, Filtering, and Mounting 30*
  - *Scanning Program 40*
  - *Focusing 41*
  - *Laser Power and PMT Optimization 43*
  - *Signal Processing 43*
    - Cell Counting 43
    - Digital Filtration 44

Fluorescence Microscopy *54*
Experimental Design... *54*
Results and Discussion 55

Additional Experiments **60**
Bioreactor Effluent... 60
Lake Water 62

Conclusions and Future Work.. **66**

Appendices.. **69**
Appendix A: Procedure for Reviving and Storing Freeze-Dried *E. coli* cultures 70
Appendix B: Labview Scanning Programs 72
Stage Scanning Program.. *73*
High Resolution Scanning Program *79*
Positioning Program... *84*
Appendix C: Matlab Signal Processing Programs 89
Counting Program used for Microspheres *90*
Counting Program used for Bacteria........................... *93*
Digital Filtering Program.. *95*
Appendix D: Fluorescence Microscope Settings 97

Bibliography **99**

Introduction

The Korea Institute of Science and Technology funded this research project in an attempt to develop an on-line membrane integrity verification method. The membranes in question were microfiltration or ultrafiltration membranes having the capacity to remove bacteria and other small particles from drinking water. Membrane modules can become damaged through improper installation, wear, or degradation over time. Currently there are several different methods used in industry to monitor membrane integrity. Benjamin Lee performed a thorough literature review and proposed a novel method of membrane integrity verification (Lee, 2003). The method was filtration of membrane permeate, staining with fluorescent dye, and scanning with a device designed to detect fluorescently labeled bacteria. The presence of bacteria on the filter indicated a breach in membrane integrity. Mr. Lee designed and built a prototype device for bacterial detection. He was able to demonstrate proof of concept by detecting large concentrations of bacteria on the membrane surface. The next phase of the project, explained in the present thesis, was to optimize the prototype device making it more accurate and reliable as a membrane integrity verification method. As the literature was reviewed, it was determined that the prototype developed was very similar to laser scanning cytometry devices used in medical and microbiological research. The prototype is referred to hereafter as a laser scanning cytometer (LSC).

Aside from the Literature Review, this work is divided into two main sections: Microspheres, and Bacteria. In the Microspheres section are found experiments employing fluorescently labeled microspheres as bacterial surrogates. Microspheres were used because they were simpler to handle and gave more distinct signals than bacteria. Two size classes of microspheres were involved in prototype optimization. The Bacteria section deals with optimization of the prototype using *Escherichia coli*. The optimal parameters for detection of microspheres were not necessarily optimal for bacterial detection. Using bacteria also added the necessity for optimizing the bacterial staining protocol.

Literature Review

This thesis comprises a combination of several fields of study. Because membrane integrity was the original motivation, a discussion of membrane integrity monitoring methods is included. A much more thorough discussion is found in the thesis by Benjamin Lee (2003). The papers cited here augment Mr. Lee's literature review, without unnecessary repetition. A review of bacterial detection and counting is included to compare methods currently available to the LSC method proposed. Microsphere counting is treated separately, as there are significant differences between microspheres and bacteria. LSC is reviewed as it applies to microbiology, along with a mention of flow cytometry, which is directly related to LSC. Staining of bacteria using fluorochromes is reviewed to determine the most effective methods. Finally, the field of digital signal processing is presented to give a background on the methods used to derive meaningful information from LSC data.

Membrane Integrity Monitoring

Lee (2003) reported that membrane integrity monitoring methods fell in two classes: direct and indirect methods. Direct methods were the pressure hold test, diffusive air flow test, sonic sensing analysis, and bubble point test. Indirect methods were turbidity and laser turbidimetry, particle counting, particle monitoring, and microbial analysis. The current work focuses on the last of the indirect methods, microbial analysis. Ultimately, microbial analysis is the most important membrane integrity verification. Membranes are expected to remove pathogens, so testing for these pathogens must be undertaken to prove the membrane effectiveness. In many scientific studies of integrity monitoring methods, the techniques are compared to microbial removal efficiency to verify that the monitoring was adequate (Jacangelo et al., 1991; Hong et al., 2001; Kitis et al., 2003). However, Farahbackhsh et al. (2003) reported that none of the indirect monitoring tests had been well correlated with microbial removal.

Drinking water treatment plant operators currently use microbial analyses according to regulations. These are typically bacterial culture methods which require a lengthy incubation time. The culture method can detect compromised membranes, as was the case for a study of nanofiltration (Seyde et al., 1999), but the tests do not provide real-time information. Once a breach is detected, the affected water would have already reached consumers. For microbial analysis to be effective it would have to be both sensitive and fast (Crozes et al., 2002).

Bacterial Detection and Counting

As was noted for drinking water treatment plants, bacterial detection and counting is often performed with methods that require an incubation time, such as the plate count method. Not only is the plate count method slow, but manual counting is tedious. Some researchers have automated the method with a video counting device, but the need for an incubation time of at least one day remains (Shaw & Haddix, 2004). A bacterial detection strategy that does not require incubation has been sought by many researchers. One of the latest successful attempts is an adenosine triphosphate assay (Deininger & Lee, 2001). ATP is a key molecule in cellular metabolism, so its detection indicates microbial presence. The ATP assay was able to detect bacteria in 5 minutes, and had a detection limit of about 200 cells per filtered volume of water (usually 0.1 to 10 ml). A similar test detected another cellular metabolism molecule, 4-methylumbeliferyl-B-D-galactose (Eckner et al., 1999). This enzyme can be detected in four hours, and was more sensitive than the ATP test, detecting coliforms down to 1 colony-forming unit per ml (cfu/ml). A more specific method for bacterial detection is rapid PCR. Rapid analytical devices have been developed to find particular species of pathogens (States et al., 2004). This came to the forefront after the terrorist attacks of September 11, 2001, when water security became a major concern for plant operators.

Fluorescence and/or luminescence was the principle for detection in the ATP assay and the enzyme test. Fluorescence is the principle behind another long-standing method, flow cytometry (FCM). FCM is usually used for analysis of eukaryotic cells in medical studies. Some researchers have seen its promise as a prokaryotic cell counter. Pinder et al. found that FCM counts requiring just a few minutes per sample correlated very well with plate counts that required two days of incubation (Pinder et al., 1990). The drawback was that FCM could only count accurately if at least 100 cfu/ml were present.

It has been shown that direct counting of bacteria with fluorescence microscopy can detect more bacteria than plate counts, as some bacteria do not grow in laboratory culture media. Hobbie and coworkers (1977) developed a direct count method that is widely used in microbiological studies. Nuclepore membranes were used to collect bacteria and the fluorochrome acridine orange (AO) was used for cell labeling. Other stains were developed, also, and will be discussed later. Perhaps the most comprehensive review of direct counting methods was done by Kepner and Pratt (1994). They reviewed over 220 papers describing direct counts with fluorescence microscopy and outlined a detailed procedure for its implementation. The procedure involved sample collection, selection of membrane filters, the use of a backing filter to support the membrane, dispersion of bacteria from environmental samples, stain concentration, staining time (stain duration), and counting methods. Kepner and Pratt recommended that 400 cells be counted per filter, falling within a minimum of 20 fields of view. However, they also reported that most studies in the literature used 10 fields. Sub-sample replication (at least in triplicate) was also encouraged. To provide adequate comparison of different studies, they specified which details of the direct count procedure should be reported in any publication. The type of information required included the following:

- Preservative: Type, final concentration, and storage conditions.
- Stain: Type, final concentration, and duration of staining.
- Filters: Type and nominal pore size.
- Counting: Count strategy (minimum number of cells and/or grids), total magnification used.

As a follow-up to these recommendations, it has been suggested that the average number of bacteria per microscope field also be included in the list of required data types (Lisle et al., 2004).

The bacterial counting and enumerating methods described above have advantages and disadvantages. Plate counts are standard and well understood, but are slow. ATP and enzyme assays are fairly fast, but are not well-understood, as they are a new technology. FCM is fast and fairly well-understood, but requires high cell concentrations. Fluorescence microscopy is well understood, fast, and can detect low cell concentrations (especially by filtering higher water volumes), but requires expensive equipment and skilled operators. When discussing the needs of membrane integrity monitoring, none of these methods are adequate. However, there is an emerging technology that has promise to be fast, sensitive to low concentrations, easy to use, and relatively inexpensive: laser scanning cytometry.

Laser Scanning Cytometry

Laser scanning cytometry (LSC, also known as solid phase cytometry) is a microbiological tool developed within the past decade to examine cells at the population level (Darzynkiewicz et al., 1999; Katsuragi & Tani, 2001). LSC is similar to FCM and fluorescence microscopy in that bacteria are detected and characterized using fluorescent dyes. LSC, like microscopy, detects bacteria captured on a slide or membrane, while FCM carries cells past a detector in a stream of fluid. Currently it is not practical to buy an LSC device simply to count bacteria, as the technology is new and quite expensive. However, it could be possible to develop an LCS device with relatively inexpensive components that is effective in bacterial enumeration.

One of the first devices that could be classified as an LSC was called the Cytodisk, developed in the 1980s (Degrooth et al., 1985). The Cytodisk employed a disk with V-shaped grooves, similar to a phonograph record. A solution containing fluorescent microspheres was placed on the disk and allowed to dry, causing the microspheres to settle to the bottom of the grooves. The Cytodisk had a needle to track its course and a fiber optic line attached to the needle for illumination and collection of fluoresced light. The device was effective for microsphere characterization and the researchers were hopeful for continued development with cells.

A few years later, an LSC was developed for detection of cells on a microscope slide (Kamentsky & Kamentsky, 1991). This device was used for DNA measurements and compared well with FCM. The LSC was superior, however, in that it was able to measure the same cells more than once, whereas FCM samples were discarded after one run. A very similar LSC device was called the Microvolume Laser Scanning Cytometer (MLSC). The distinguishing feature of this design was the collection of cells in very small (microvolume) capillary channels in order to align them before scanning (Walton et al., 2000). This device was used mostly for blood cell experiments with biological markers. It required a high degree of image processing, which was described in detail by other researchers (Norton et al., 2000). A similar method was used in another LSC experiment, but to select the cells of interest, they were labeled with ferromagnetic nanoparticles and fluorescent probes. Using a magnetic field, blood cells were pulled toward one end of a capillary channel to separate them from the rest of the constituents in the blood (Tibbe et al., 1999). Counts compared well with a hematology analyzer and FCM.

The design that has risen above the others and is most widely used in LSC research today is the Chem*Scan RDI* (also referred to as Chem*Scan* or Scan *RDI*).[1] The Chem*Scan RDI* was proven to be as effective as flow cytometry for eukaryotic cell analysis. With the Chem*Scan* the operator can examine the cells with a built-in microscope after scanning, which makes it more attractive than FCM (Mignon-Godefroy et al., 1997). The device was used in development of a 210-minute test for *E. coli* in drinking water, where enzymes were used to label *E. coli* specifically, without labeling other bacteria (Van Poucke & Nelis, 2000). There was 90% agreement between Chem*Scan* and plate count methods, but the Chem*Scan* was able to detect between 1 and 11 *E. coli* in 100 ml of sample, while two plate count methods were negative. Another study reported that total bacteria were counted in a 30-minute test, with results being as good or better than the R2A agar plate count method (Broadaway et al., 2003). A rapid LSC method for *Legionella pnuemophila* detected between 10 and 100 bacteria per liter (Aurell et al., 2004). This was more sensitive than culture methods, as LSC sometimes detected bacteria when the culture method did not. The Chem*Scan* has been compared with fluorescence microscopy, as well. Lisle et al. (2004) determined that it was less biased and showed better repeatability than fluorescence microscopy, especially for low concentrations of *E. coli.*

The Chem*Scan RDI* LSC device fills the role of a quick, easy-to-use, and sensitive bacterial detection device. Its one disadvantage is cost, as the machines are quite expensive. However, the technology has proven itself and the only hurdle remaining is to make it affordable.

Bacterial Staining

With either fluorescence microscopy or LSC, staining of the bacteria with fluorochromes is a necessary step. Two key factors are dye concentration and staining time (stain duration). A thorough literature review of direct bacterial counting reported that DAPI and Acridine Orange stains are widely-used (Kepner & Pratt, 1994). Figure 1 shows stain duration compared with stain concentration for the literature reviewed.

---

[1] Chemunex, Ivry-sur-Seine, France

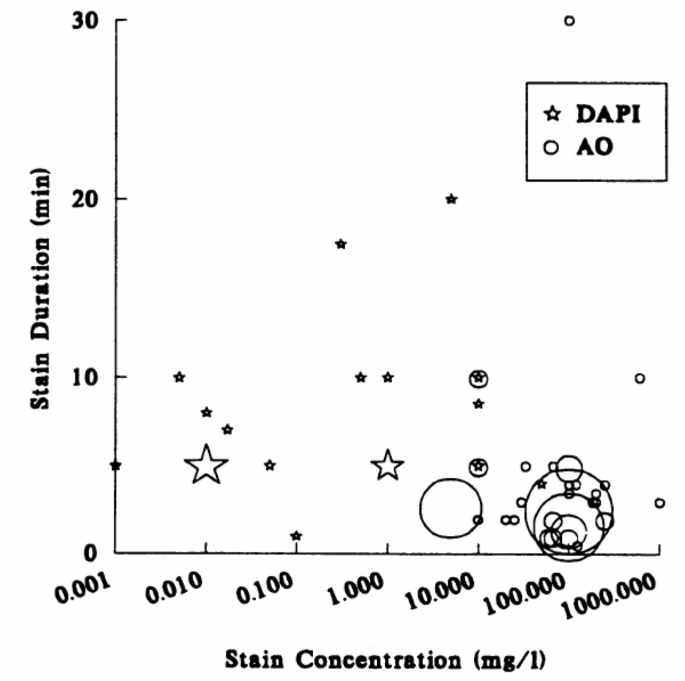

Figure 1: Stain duration compared with stain concentration for studies using DAPI and Acridine Orange (AO). The size of the symbol represents the number of studies, ranging from one to ten. (Source: Kepner & Pratt, 1994).

In order to decrease the cost of LSC devices, the laser should be low power and inexpensive. Red diode lasers emitting light at a high wavelength (635 nm) fit these specifications. For the diode laser to be effective, the stain must be excitable in the 635-nm range. Researchers have found several possibilities: EK4, LL585, oxazine 750, LD700, and rhodamine 800 (Latt et al., 1984; Shapiro & Stephens, 1986). Molecular Probes[2] also developed a high wavelength stain that binds easily with nucleic acid. This is called SYTO 62.

A wide range of SYTO stains have been developed, all binding to nucleic acid. These have been used for direct count and various other fluorescence microscopy applications. The stains attach to all types of nucleic acid, not just DNA. Many different stain concentrations and stain durations have been employed, as described in Table 1.

---

[2] Eugene, Oregon

Table 1: Studies in the literature have employed SYTO stains at various concentrations and stain durations, as shown here.

Stain Used	Stain Concentration	Stain Duration	Reference
SYTO 62	25 µM	—	(Farinas et al., 2001)
SYTO 17	1 µM	60 minutes	(Comas & Vives-Rego, 1997)
SYTO 13	1 µM	5 minutes	(Guindulain & Vives-Rego, 2002)
SYTO 13	2.5 µM	20 minutes	(Guindulain & Vives-Rego, 2002)
SYTO 13	1 µM	10 minutes	(Comas-Riu & Vives-Rego, 2002)
SYTO 13	0.05, 0.5, and 2.5 µM	10 minutes	(Guindulain et al., 1997)
SYTO 13	2.5 µM	15 minutes	(Lebaron et al., 2001)

Microspheres

Polymer microspheres have become popular in water research applications because of their usefulness as surrogates for pathogens such as bacteria and viruses that can be difficult and dangerous to handle. Microspheres have been used to simulate viruses in reverse osmosis and nanofiltration integrity monitoring (Acker et al., 2001; Kitis et al., 2003), *Giardia* cysts in ozone disinfection (Chiou et al., 1997), bacteria and colloidal contaminants in groundwater transport, (Niehren & Kinzelbach, 1998; Fang & Logan, 1999) and *Cryptosporidium parvum* oocysts in granular media filtration (Dai & Hozalski, 2003). Microspheres are widely used for blood flow measurements in mammals (Thein et al., 2000). They have also served as indicators of microfiltration membrane integrity (Carr et al., 2003). In these studies, FCM, luminescence spectrometry, laser turbidimetry, and fluorescence microscopy were used for microsphere enumeration. It seems that in most any device or system where microbes are being studied, microspheres can serve as surrogates during optimization of the device or characterization of the system. LSC is no exception, as microspheres have been used to calibrate and develop LSC and similar devices in the past (Degrooth et al., 1985; Varga et al., 2004).

Signal Processing

In cytometry applications, large amounts of data are collected. Signal processing is an important step to make sense of the information. There are two areas of signal processing that come into play during the laser scanning cytometry proposed: peak counting and digital filtration.

Peak Counting

In laser scanning cytometry, the photo multiplier tube (PMT) outputs a voltage signal to the data processor. When a cell is encountered, fluoresced light causes the PMT to output a higher voltage. If the laser (or other excitation light source) spot is wide enough, the microsphere or bacterial cell will be detected in several consecutive data points along the track, forming a peak. It will also be detected in two or more adjacent tracks. Thus there should be some type of signal processing to determine which data points belong to a single microsphere or cell. No specific information on peak counting procedures was found in the literature, so a method was invented for this project.

Digital Filtration

Digital filtration involves more advanced data manipulation than peak counting. Digital filtration techniques are ubiquitous in electronic devices, such as cellular telephones, radios, and television; anything that sends or receives information via arrays of data will necessarily be filtered to distinguish the information from background noise. It would be easy to get lost in the technical terms and jargon of the digital signal processing (DSP) world, except for a very useful book on the subject by Stephen W. Smith (1999). Smith explains DSP in terms that an engineer who is unfamiliar with the field can understand.

To understand DSP, one must realize that all signals can be evaluated in the *time domain* or the *frequency domain*. People are generally familiar with the time domain. The signal from a cardiac monitor and the lines on an oscilloscope are a few examples; the data are sampled at specific intervals of time. Signals can also be sampled at specific intervals of space, like measuring the temperature variation along a metal rod with sensors placed at every centimeter. This is also generically defined as a time domain signal.

The frequency domain deals with information contained not in the temporal variation of the data, but in the frequency of the signal. For frequency domain information, there must be some kind of periodic or oscillating signal with many data points. We are familiar with frequency information found in sound, as our ears detect the high and low pitch of musical instruments. We are also familiar with the electromagnetic spectrum, where we "tune in" our radio to a specific station.[3]

The bells of a clock tower provide an analogy for time domain and frequency domain signal interpretation. If a sensor were detecting the vibrations from the bells one might analyze the data to determine when the bell was struck. There would be a "blip" in the data at the point at which oscillation begins. This is interpretation of data in the time domain. One might also want to know the pitch of the sound produced by the bell. For that, the signal would have to be analyzed over several periods of oscillation to determine how rapidly the cycles were occurring. This is frequency domain signal analysis.

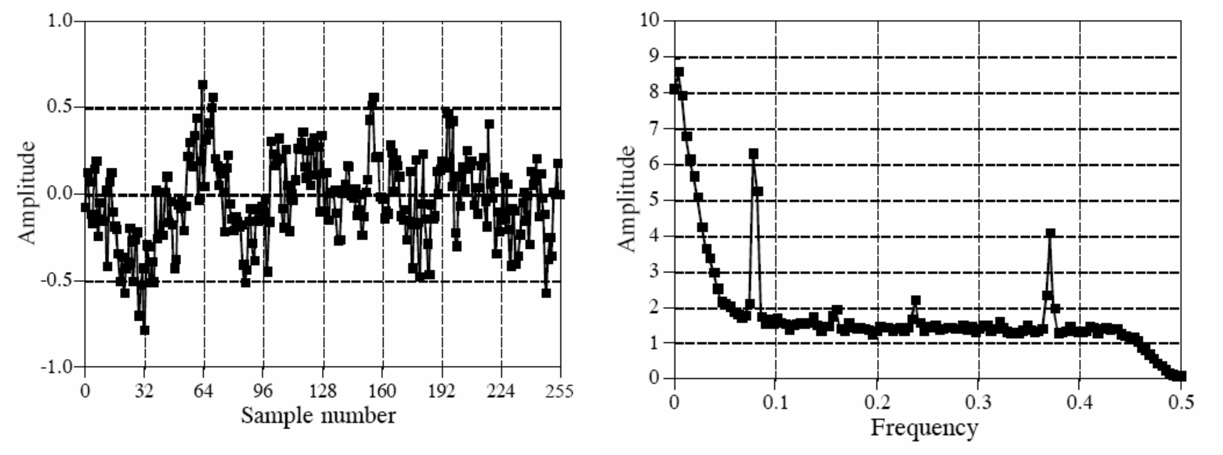

a **b**

Figure 2: A signal viewed in the time domain (a) and transformed to the frequency domain (b). The frequency domain is actually an averaged result of more data points than are displayed in the time domain; this is in order to see clear peaks. Here both Y axes are labeled Amplitude, but these are distinct scales. In the time domain the amplitude measures the strength of the signal at a given point, while in the frequency domain the amplitude measures the significance of periodicity at the given frequency (Source: Smith, 1994, page 171).

One important key to understanding signals is to realize that any signal can be analyzed in either the time domain or the frequency domain. For time domain analysis one might plot the voltage, intensity, or any parameter of interest, verses the time, distance, or sample number, as shown in Figure 2a. For frequency domain analysis, the amplitude is plotted verses the frequency, as shown in Figure 2b. It is important to realize that Figure 2b has the same information as contained in Figure 2a, but it has been transformed into the frequency domain using a mathematical operation called the Fourier Transform. To find the sample number containing the lowest point, one would work in the time domain and see that it is sample number 32. If one wanted to find where oscillations in the data were occurring, we would use the frequency domain data and see the two distinct peaks at 0.08 and 0.37, representing significant oscillations at those frequencies. It is hard to pick these out of the time domain signal, but the frequency domain makes them apparent. Thus, it is clear that some information is found in the time domain, while other information is in the frequency domain, even though the signal is from the same original data set.

---

[3] The radio example is interesting in that it highlights the difference between analog and digital signal processing. Old radios, where one had to turn the knob until the signal came in clearly, were analog signal processors. They blocked competing radio stations using the electronics in the radio to focus on one frequency. New radios employ digital filtration where they take the analog signal from the airwaves, digital it, and filter out competing signals with algorithms and mathematical operations. We would probably all agree that digital filtration is superior in this application; we would rather just punch in the station number than have to tweak that little knob.

In LSC, information travels from the PMT to the data acquisition card via an analog voltage signal. The card converts the analog signal to a digital signal for processing. This digital signal is then in the time domain. Because the encounter between the laser and bacteria or microspheres occurs very fast and covers only a few data points, the information is found in the high frequency portion of the data. The low frequency information is unnecessary, but sometimes low frequency oscillations can cause difficulty in counting. Thus, one way to filter the signal is to convert the PMT data into the frequency domain, remove the low frequency portion, and convert it back into the time domain. This constitutes a high-pass filter; the high frequencies are allowed to pass, while the low frequencies are removed. Thus, any low frequency perturbation in the original data will not hinder counting of data peaks.

Microspheres

Materials and Methods

Microspheres and Filters

Polystyrene microspheres of 2-µm diameter were obtained from Molecular Probes. These were custom prepared with dark red dye having an excitation maximum of 660 nm and an emission maximum of 680 nm. Additional polystyrene 10-µm and 2-µm microspheres were obtained from Duke Scientific.[4] These microspheres were dyed with red fluorescent dye having an excitation maximum of 670 nm and an emission maximum of 700 nm. Spectra for both microspheres are shown in Figure 3.

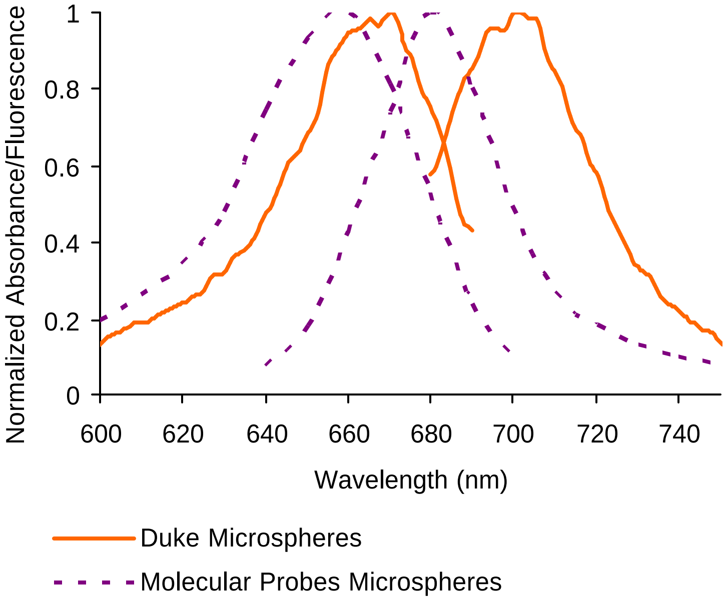

Figure 3: Excitation and emission spectra for Duke and Molecular Probes microspheres. The left peak is the excitation peak, the right is emission.

The Duke 10-µm microspheres were received in powder form, dispersed in deionized water with sodium dodecyl sulfate (SDS), and diluted to varying concentrations. Both Duke and Molecular Probes 2-µm microspheres were diluted from stock solutions using deionized water.

---

[4] Palo Alto, California

Glass fiber filtration of Molecular Probes microspheres helped remove aggregates and provide monodisperse solutions.

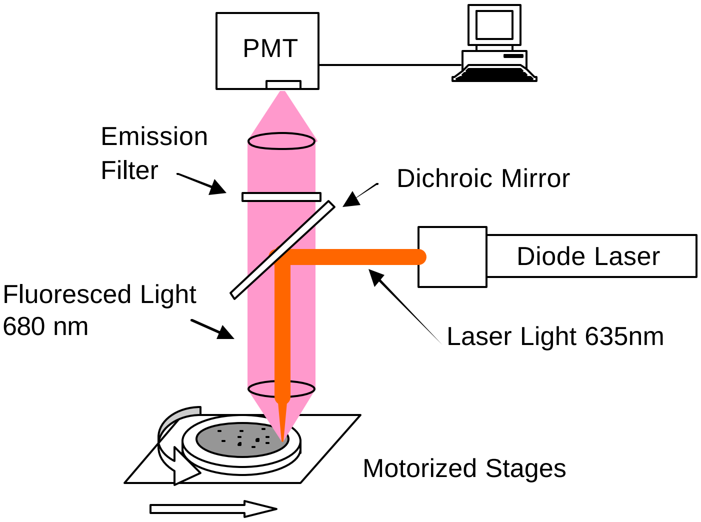

Figure 4: Diagram of the prototype laser scanning cytometry device.

Microsphere solutions were diluted to a wide range of concentrations using deionized water. For filtration, a sample size between 0.1 and 1 mL was pipetted into 5 mL of water held in a column above a 25-mm diameter polycarbonate, track-etched membrane[5] with a 0.2-µm pore size. Microspheres were allowed to disperse in the water column and the solution was pulled through the membrane under vacuum. The wet membrane was then placed on a microscope coverslip, the water causing adhesion between glass and membrane, which held the membrane flat for consistent scanning. For some samples, a 0.33-M sucrose solution was used in place of the water column during filtration in order to provide better adhesion between the membrane and coverslip after drying.

Prototype Components

Membranes were scanned in the prototype LSC device to detect microspheres on the surface. As shown in Figure 4, scanning was done with fixed laser light directed onto the moveable scanning stage. The laser used was a 635-nm wavelength diode laser,[6] which is a common type for applications such as CD players and supermarket scanners. Power to the laser was variable between 0 and 10 mW with scans typically performed at 1 mW. Beam size was 1.3 mm with a divergence of 0.75 mrad. The membrane was supported by motorized stages[7] that moved in linear and rotary directions to allow scanning of the entire membrane surface. Stages were powered with a servo amplifier system[8] and controlled with a motion controller card[9] installed in a desktop PC. The card also performed data acquisition. Supporting the motorized stages were two manual translational stages[10] used to focus and align the membrane under the laser.

---

[5] Isopore™ membranes, Millipore, Billerica, Massachusetts

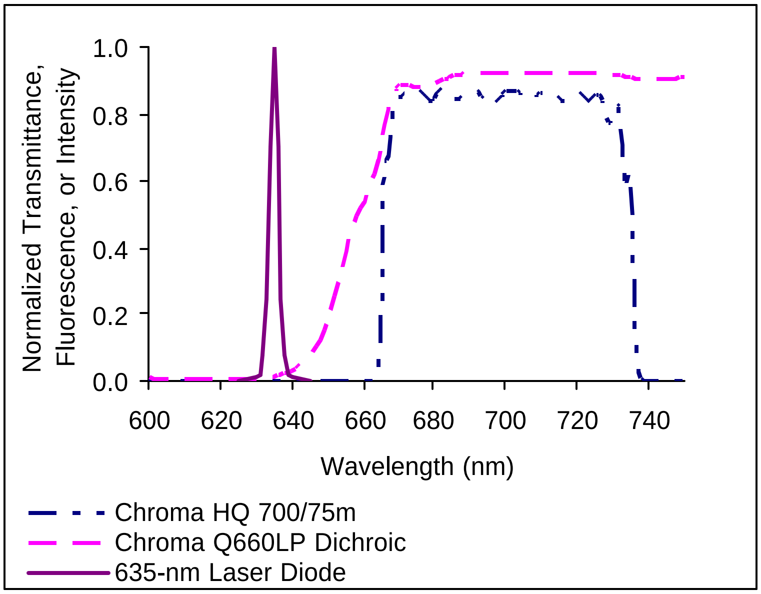

Figure 5: Comparison of spectra for prototype components.

Laser light was directed onto the membrane with a dichroic beamsplitter.[11] Upon encountering a microsphere, fluoresced light (higher wavelength) passed through the beamsplitter, while laser light (lower wavelength) reflecting off the membrane surface was blocked. The dichroic wavelength separation was imperfect, so an emission filter[12] was used to further separate fluoresced light from reflected light. The light spectrum of the laser and the transmission spectra of the beamsplitter and emission filter are shown in Figure 5.

---

[6] Circular Beam Diode Lablaser, Coherent, Santa Clara, California
[7] MM-3M-EX and MM-3M-R stages, National Aperture, Salem, New Hampshire
[8] MC-4SA Milti-Axis Servo Amplifier, National Aperture, Salem, New Hampshire
[9] 7344 motion controller card, National Instruments, Austin, Texas
[10] TSX-1D Doevetail Stage, Newport Corporation, Irvine, California
[11] Q660LP, Chroma, Rockingham, Vermont
[12] HQ700/75m, Chroma, Rockingham, Vermont

Two lenses[13] were used in the prototype. These were both 12-mm diameter lenses with 12-mm effective focal lengths and an anti-reflectance coating. One lens focused laser light onto the membrane and collected fluoresced light from the microspheres. The other lens focused fluoresced light onto the receptor of a photomultiplier tube[14] (PMT). The PMT was custom fit with a detection tube that was optimal for near-infrared response. A variable voltage source powered the PMT and amplified its signal. Typically, the voltage was set between 0.2 and 0.45 mV. Analog signals from the PMT were collected by the motion control/data acquisition card for digitizing and processing. With computer programs written specifically for the prototype, microspheres were counted and their location on the membrane was recorded.

Scanning Program

Computerized control of motorized stages and data acquisition were accomplished using LabView[15] software. Scans were performed similar to a CD or DVD, in that the laser was focused onto the surface of a circular membrane rotating under the laser. The laser position was controlled by the motorized stages in terms of polar coordinates (r, ?), with the linear stage controlling the radial coordinate (r) and the rotary stage controlling the angular coordinate (?). Scans were performed by continuously spinning the rotary stage and moving the linear stage so that the laser scanned from the edge of the membrane toward the center. In some scans the linear stage was moved in a stepwise manner where the user determined the step size. Often, 0.2 mm was the step size, creating about 60 tracks (concentric circles) for data collection over the 12.5-mm membrane radius. Alternatively, the linear stage could be moved continuously at a user-defined velocity giving a spiral scanning pattern, instead of concentric circles. In order to allow faster data collection, some scans covered only part of the membrane surface. The user defined an inner and outer radius (i.e. 2 and 4 mm) so only the membrane surface in that range was scanned.

The PMT delivered an analog voltage signal to the data acquisition card, where the signal was sampled and digitized. In some scans, the sampling rate was set by the user-defined resolution of the scan. For instance, the user defined the resolution to be 0.1 mm, so the program sampled the voltage signal every 0.1 mm along the track. In other scans, the sampling rate was not set by the user, but was determined by the speed of the program. This yielded higher sampling rates and, on average, the distance between samples was 0.009 mm (9 µm).

---

[13] Tech Spec PCX, Edmunds Optics, Barrington, New Jersey
[14] HC120-01 module with R6357 detection tube, Hamamatsu, Bridgewater, New Jersey
[15] Labview 6.1, National Instruments, Austin, Texas

For higher resolution scans (more data points per membrane area) a separate program was developed to look at a very small section of the membrane. This program moved the stage in 2.5-µm increments to cover a grid size specified by the user. At each location a number of PMT readings (typically 1000) were taken and the mean value was calculated. These scans required more time than typical stage scanning, but allowed close analysis of single microspheres. Because the mean value of many readings was used, sampling variations due to electronic or random noise were minimized. These scans were used to focus the stage and characterize the laser spot size.

Focusing

Focusing is important because when objects are not in focus, they can appear larger than they really are, as anyone using a microscope can observe. This is the *halo effect* and has been seen in other particle counting and particle sizing applications (Kramer & Clark, 1996). For maximum signal-to-noise ratio in microsphere fluorescence, a well focused (small and intense) laser spot was desired. This was found by adjusting the stage height to change the object distance (i.e. the distance between the object lens and the membrane). High resolution scans of a single 2-µm microsphere were performed and scan data were converted into images using a Matlab[16] program. From the images, spot size and intensity were characterized and the optimum focus obtained.

Signal Processing

Scan data included PMT values and Cartesian coordinates. Data were saved to a text file to be processed with programs written in Matlab. The counting program created a histogram of PMT data and used the mode as the background PMT level. The mode was valid as a background level because most of the data in a typical scan were background.

---

[16] Matlab 7, Mathworks, Natick, Massachusetts

With the background calculated, a threshold PMT voltage level was set as a multiple of background (typically 110%). The program found all data points lying above this threshold and considered those to be part of a microsphere peak. If points were grouped closely together, they were considered to be part of the same peak. Each peak, with its spatial information, was placed in an array of counted microspheres. Thus the program output consisted of microsphere locations and the magnitudes of their peaks.

Fluorescence Microscopy

Fluorescence microscopy was used to verify prototype microsphere counts. Membranes were examined using a fluorescence microscope[17] illuminated with a mercury lamp.[18] The excitation filter, emission filter, and beamsplitter[19] were optimal for near-infrared fluorescence. The transmission spectra for the emission filter and beamsplitter were very similar to the emission filter and beamsplitter used in the prototype (Figure 5). The spectrum for the excitation filter is not shown but has practically no transmittance above 660-nm wavelength. The microscope objectives[20] used were 10x and 100x magnification. Images of microspheres on the membrane surface were taken with a digital camera.[21] Images were processed and microspheres were counted using microscope software.[22]

Experimental Design

To determine whether microspheres or random points were being counted by the prototype, 10-µm Duke microspheres were localized on a small area (about 4 mm^2) of a membrane by carefully placing small drops of solution on the membrane surface. Before placement, a sucrose solution (0.74 mM) was filtered through the membrane so that upon drying it adhered to the coverslip on which it was placed. The microspheres were diluted in the same sucrose solution. With fluorescence microscopy at 100x magnification, 25 micrographs of the membrane were tiled together to create a single image. MCID software processed the image to count the microspheres present. The same membrane was scanned with the prototype.

---

[17] Axiovert 100, Zeiss, Thornwood, New York
[18] HBO 50-watt mercury short-arc lamp, Msscientific, Berlin, Germany
[19] D640/20, D680/30, and 660dclp, Chroma, Rockingham, Vermont
[20] Plan-NeoFluar 10x (0.3 numerical aperture, air medium) and 100x (1.3 numerical aperture, oil medium), Zeiss, Thornwood, New York
[21] CoolSNAPfx, Photometrics, Tucson, Arizona
[22] MCID Elite, Imaging Research Inc., St. Catharines, Ontario, Canada

Resolution was set at 0.001 mm and track spacing was adjusted to 0.02 mm. The scan, covering an annulus of 4.0 to 6.7-mm radii, was set at 90 degrees-per-second rotary speed, and lasted 12 minutes. Laser power was set at 0.09 mW. The detected microspheres were counted in Matlab and an image was created similar to the microscope image. The two images were compared to evaluate if the microscope and prototype gave similar results.

Repeatability of prototype counting was evaluated through scanning of a single membrane 11 times in succession. One mL of a 7600 microspheres per mL, 2-µm Duke microsphere solution was pipetted into 5 mL of deionized water and filtered through the membrane. Immersion oil was used to help adhere the microspheres to the membrane. Scans were performed with 1-mW laser power, 90 degrees-per-second rotary stage speed, and 0.005-mm/s linear stage speed. An annular section of the membrane between 3 and 4.5-mm radii was scanned.

Molecular Probes microspheres were used to evaluate prototype counting performance over a range of concentrations. Varying concentrations were made through serial dilutions of a microsphere stock solution into deionized water. For scanning, laser power was again 0.1 mW and rotary speed was 90 degrees-per-second. The membrane surface scanned was and annulus of 6.45 to 6.50-mm. Resolution and track spacing were set at 0.001 mm. Fluorescence microscopy was used to verify the concentrations.

Further counting performance evaluation was performed with Duke 2-µm microspheres. These were also diluted in deionized water and filtered onto membranes in varying concentrations. Scanning used 0.10-mW laser power and 90 degrees-per-second rotary speed. Sampling was as fast as the program would allow. Linear stage speed was 0.005 mm/s and the scans covered an annulus of membrane area from 1.5 to 2.5-mm radii.

Results

Figure 6 shows an image of a single 2-µm microsphere taken with a high resolution scan. This was the most focused (smallest spot size) of several similar images taken while focusing the laser on the membrane. There was an approximately Gaussian or skewed Gaussian distribution of light intensity over the spot cross section. For counting purposes, only the part of the laser spot intense enough to initiate fluorescence above 110% of background was important. Figure 6 shows this portion with arrow bars. The spot is roughly elliptical, with a length of 26 µm and a width of 14 µm.

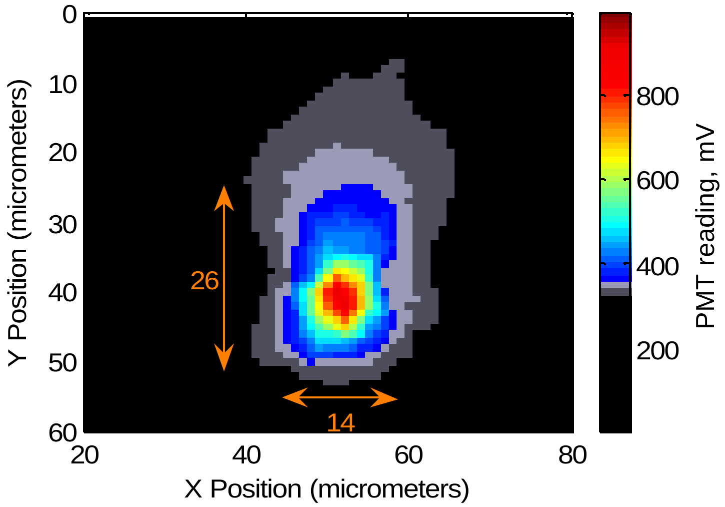

Figure 6: Image of a single 2-µm Duke microsphere from a high resolution prototype scan. Arrows indicate where the size (in micrometers) of the laser spot that is greater than 110% of background.

Output from a typical scan of several microspheres is shown in Figure 7. For clarity, the figure shows only a portion of the annulus scanned, covering 23 tracks. The peaks in the scan data indicate microsphere locations. Track spacing was set so that no microspheres would be missed between tracks. In Figure 7 it can be seen that most microspheres were detected in at least two adjacent tracks.

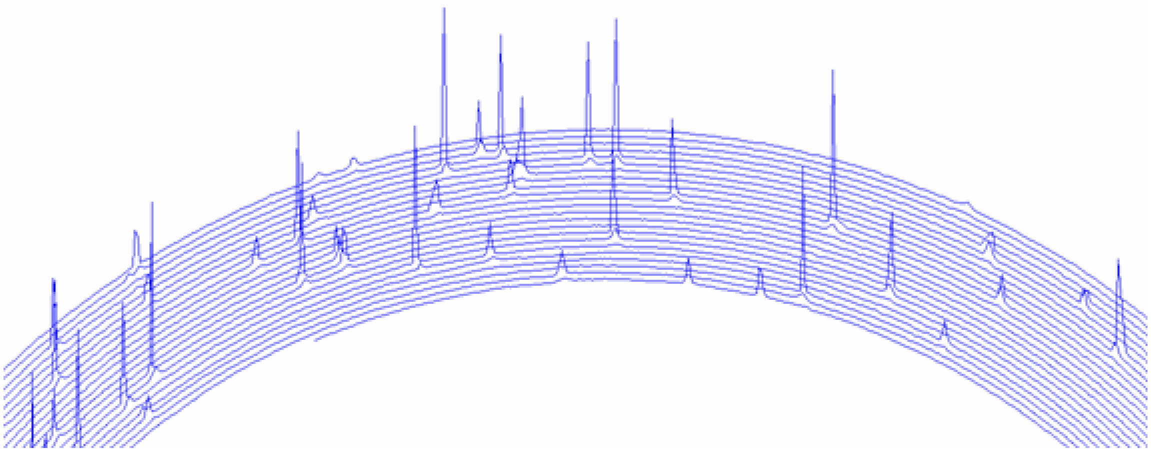

Figure 7: Typical output from a scan of 2-µm microspheres on a membrane surface. For clarity, only part of the scan data is shown. Peaks indicate microspheres.

Figure 8 shows the two images created with fluorescence microscopy and scan data. MCID counted 90 microspheres in the microscope image while prototype software counted 80 microspheres in the scan. The microscope image was sharper and well focused. The prototype laser spot size was larger than the microspheres, so resolution was lower than the microscope and the microspheres appeared larger and somewhat out of focus.

Results of repeatability experiments are shown in Figures 9, 10, and 11. The background increased over time until reaching a steady value. The number of points above threshold decreased over time. Background and the number of points above threshold had coefficients of variation (CV) of 2.93 and 4.97, respectively (calculated as the standard deviation over the mean, multiplied by 100). The CV for counted microspheres was only 0.57.

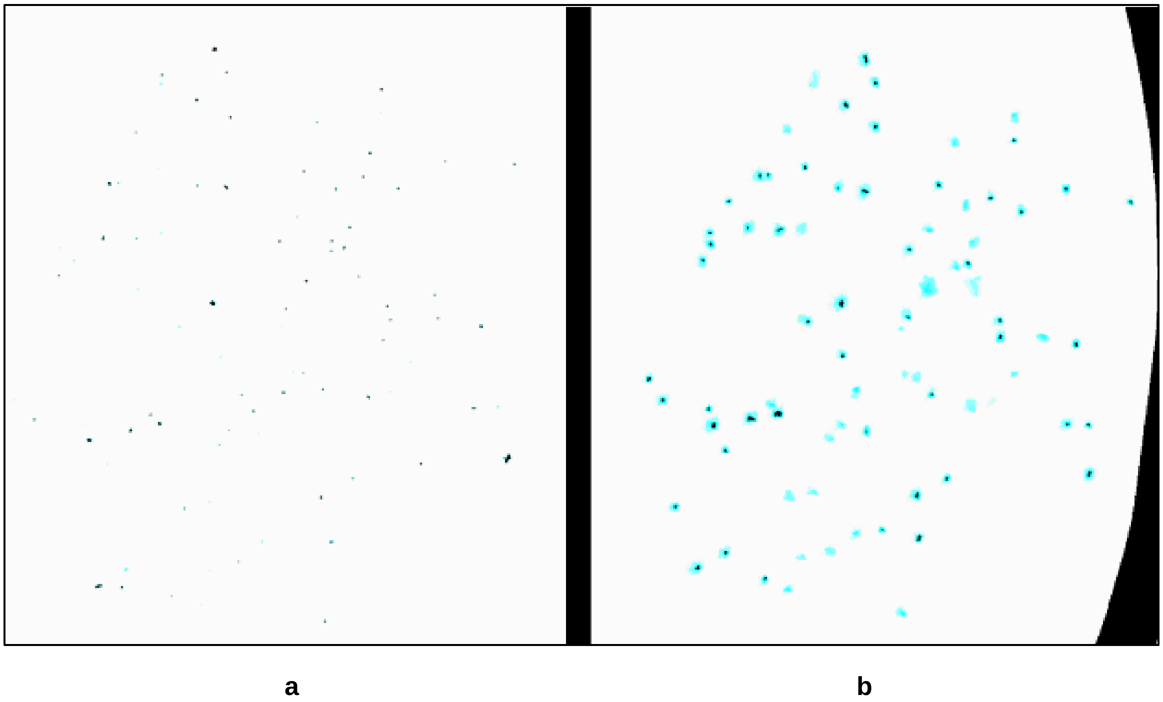

Figure 8: Comparison of (a) fluorescence microscope image and (b) LSC Prototype image of several 10-µm Duke microspheres.

Prototype counts were compared with fluorescence microscope direct counts for both Molecular Probes and Duke 2-µm microspheres. Figures 12 and 13 show the results. The prototype appeared to count more effectively with Duke microspheres. Duke microspheres gave taller peaks than Molecular Probes microspheres (data not shown), indicating that Duke microspheres were more easily detected by the prototype. For both types of microspheres, the prototype counting effectiveness tailed off above about 200 microspheres per square millimeter (µS/mm^2).

For further analysis, the Duke microsphere counts for the microscope and prototype are shown separately in Figures 14 and 15, respectively. The X-axes show the theoretical microsphere concentration, based on dilution calculations. Comparing data sets, the prototype was at least as good as the microscope for the range of about 5 to 200 µS/mm^2. Both methods were more variable at concentrations below 5 µS/mm^2. The microscope was shown to count with accuracy up to about 1000 µS/mm^2, but the prototype underestimated the microsphere concentration above 200 µS/mm^2.

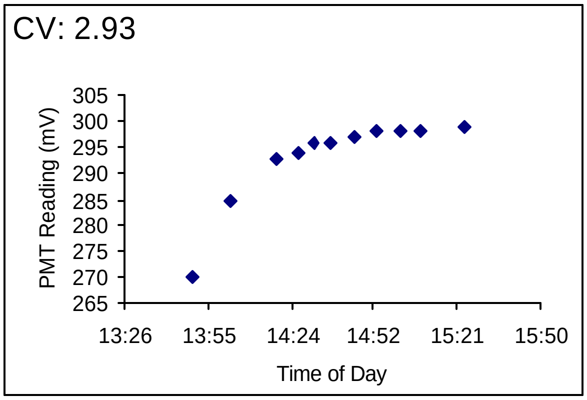

Figure 9: Background PMT level for 11 consecutive scans of the same membrane.

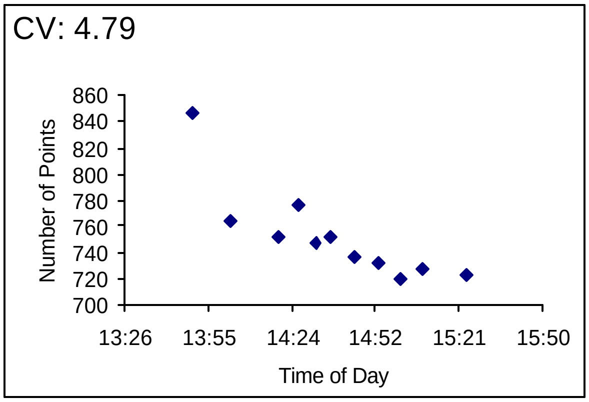

Figure 10: Number of data points detected above the threshold of 110% of background in 11 consecutive scans of the same membrane.

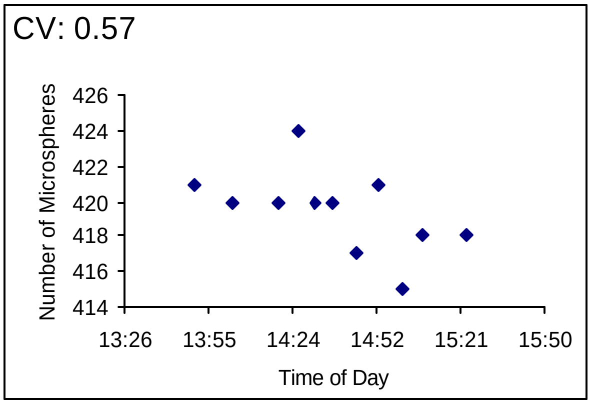

Figure 11: Number of microspheres counted in 11 consecutive scans of the same membrane.

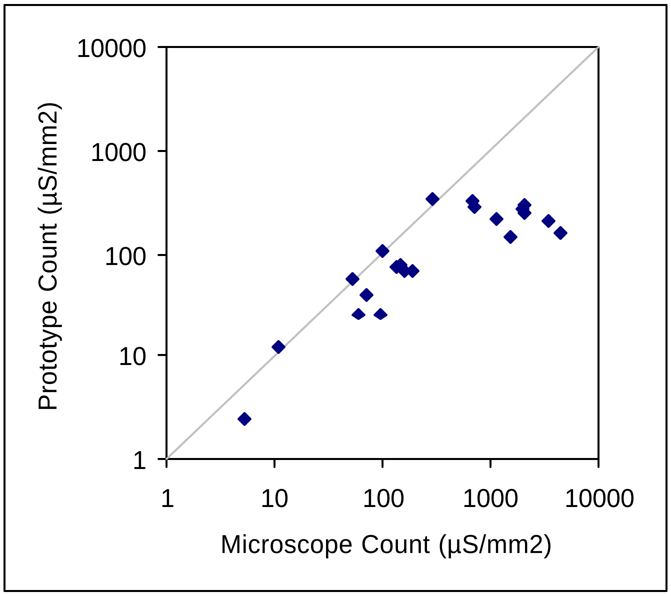

Figure 12: Prototype counts compared to direct counts for Molecular Probes 2-µm microspheres.

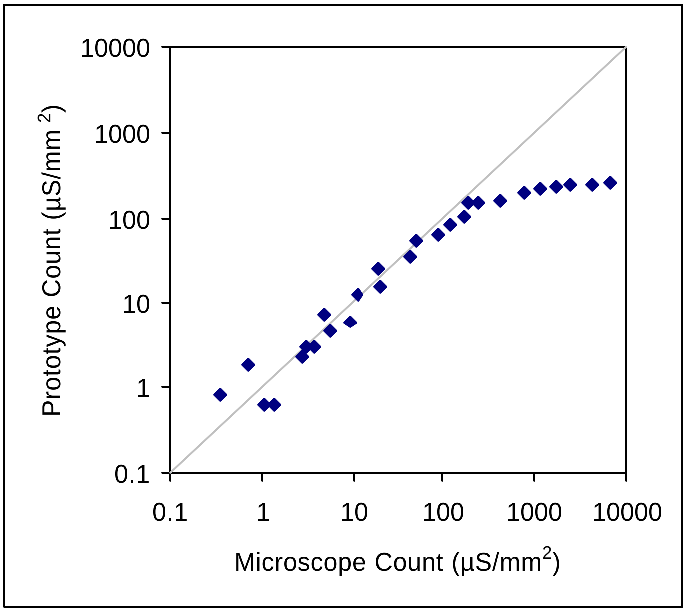

Figure 13: Prototype counts compared with direct counts for Duke 2-µm microspheres.

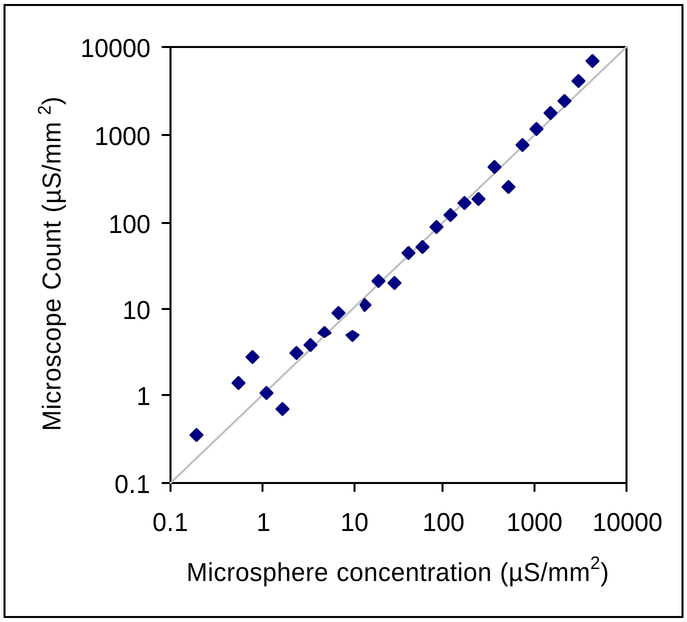

Figure 14: Fluorescence microscope direct counts for Duke 2-µm microspheres.

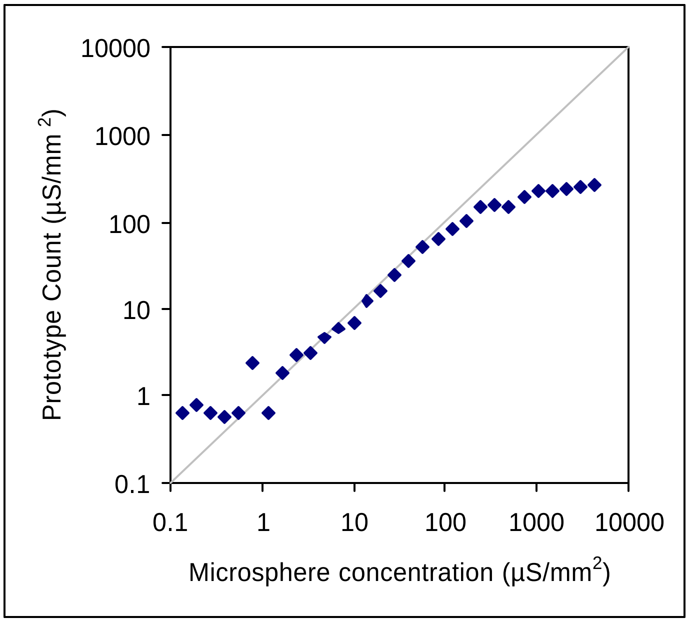

Figure 15: Prototype counts for Duke 2-µm microspheres.

Discussion

It was possible to characterize the distribution of laser light intensity over the spot formed on the membrane. A perfect laser would have a Gaussian intensity distribution over a circular spot. Lower quality lasers can have a widely varying intensity distribution and the spot shape may not be perfectly circular, as was seen in the prototype (Figure 6). Spot size and intensity varied as the focus was changed. This was an important parameter because it determined the track spacing and sampling frequency (points per distance) needed to provide complete coverage of the membrane surface. Ideally, the track spacing and distance between data points along the track would be just less than the spot size so that the most membrane surface could be covered with the fewest data points. Higher resolution scans (more frequent sampling) provided more accurate information, but required more time to scan and to process the data. An example was shown in Figure 8 where the prototype imaging was compared to microscope imaging. This required a 12-minute scan time and gave more information than necessary to simply enumerate microspheres. Most of the scans required 4 or 5 minutes. They did not cover the entire membrane surface, but linear correlations between counts and concentrations were obtained, so the scans were adequate. With improved sampling speed and careful adjustment of track spacing, more accurate and consistent correlations are expected in the future.

The prototype failed to count properly when microspheres were very close to one another (coincidence error). As seen in Figure 8, microspheres in small groups were sometimes counted as one. This was due in part to the laser spot size. Because the spot was about 26 µm wide, it could not resolve microspheres closer than 26 µm apart. More important than the spot size, however, was the prototype counting software. As explained in the Materials and Methods section, the counting software found all data points greater than a defined threshold level to be part of a microsphere peak. If two points were within 50 µm of one another, they were considered to belong to a single microsphere. The value of 50 µm was used because early in prototype development it was seen that single microspheres were being counted more than once and the 50-µm setting helped avoid this. The ramification was that when two microspheres were closer than 50 µm apart, they were counted as one. Theoretically, then the highest concentration of microspheres that the counting software could handle was about 500 µS/mm^2, as calculated in Equation 1.

$$\frac{1mS}{p\cdot\left(50mm/2\right)^2}\cdot\frac{1000^2\,mm^2}{mm^2}=509\frac{mS}{mm^2} \qquad [1]$$

It appears from Figures 12, 13, and 15, that the actual counting accuracy for the prototype was in fair agreement with Equation 1, as coincidence errors began to be evident around 200 to 300 μS/mm^2.

It was seen that the background level increased to a steady state over time (Figure 9). The PMT needed time to warm up and level off to give consistent readings. It was this background level variation that was believed to adversely affect the number of points above threshold (Figure 10). The threshold was 110% of background, so a lower background lowered the threshold and more peaks were counted. The number of points above threshold might have also decreased due to photobleaching (decreased fluorescence after prolonged light exposure) of the microspheres. Regardless, the prototype software was fairly consistent in the number of microspheres counted, as was evident from the low CV reported for microsphere counts (Figure 11). For about 420 microspheres present the counts were always within plus or minus 5 microspheres.

Duke microsphere counts were more consistent than Molecular Probes counts (Figures 12 and 13) because Duke spheres were more easily detected. This was probably due to the different emission spectra for the two kinds of microspheres. Duke Microspheres emitted light at longer wavelengths than Molecular Probes spheres. The cutoff wavelength for the dichroic and filter in the prototype was about 665 nm (Figure 5). Duke Microspheres had a larger portion of their emission spectra above this cutoff than did Molecular Probes spheres (Figure 3). Thus, the prototype filters were more compatible with the Duke microspheres than with the Molecular Probes microspheres. This is not a reflection on the quality of Molecular Probes microspheres compared to Duke; the particular Duke microspheres purchased simply had a more appropriate emission spectrum for the present application.

Both microscope and prototype counts showed variability in counting accuracy. This may have been due to randomness inherent in the methods. Both methods only covered a portion of the membrane surface. With microscopy, at most 20 frames were taken for each sample, which was less than 3% of the membrane surface onto which microspheres were deposited. Because fast scan times were desired, the prototype also covered a small surface area. In Molecular Probes experiments, scans covered just over 1% of the membrane surface. In Duke experiments, scans covered about 7% of the surface. The counts over that area were assumed to be typical for the entire membrane. At small microsphere concentrations there were sometimes one or two microspheres in one frame and none in another. This non-homogeneity led to more variability at low concentrations, especially below 5 µS/mm^2, which is evident in Figures 14 and 15.

The prototype LSC device performed well for the 5 to 200-µS/mm^2 range and further improvements are expected. This leads to the question of whether it is practical to expect that a similar device could be manufactured on a large scale and be economically feasible. Diode lasers like the one used in the prototype LSC are used in applications such as super market scanners and compact disk players. They are much more common and less expensive compared to helium-neon lasers typically used in cytometry applications. The PMT in the prototype was the same as those used in other cytometry devices, but other devices typically use two or more PMTs, while the prototype used only one. Multiple PMTs can help in data analysis and confirmation that a data peak is a microsphere, but it was shown that a single PMT was sufficient in this application. Motorized stages, computer equipment for data analysis, lenses and optical filters are all expensive, but CD players and simple microscopes already employ similar components. It is not unreasonable that with proper development an LSC device could be manufactured that would be similar in cost to these common instruments. Such a device could be a useful tool in experiments where microspheres are used frequently and must be enumerated quickly and accurately. It is also possible that the present or similar devices could be commercialized for rapid determination or frequent monitoring of microbiological water purity.

Bacteria

Much of the work done for this thesis was in the development of adequate methods to provide consistent results in scanning experiments. Thus, experiments were performed to determine which methods were most appropriate. These experiments and their results will be described in each section of the Materials and Methods, in order to give a justification for the method that was found to be most appropriate. The Results and Discussion section will provide a brief summary of overall result of the experiments, which will be a description of the final bacterial counting capability of the prototype LSC.

Materials and Methods

E. coli Sample Preparation

Escherichia coli was chosen as the model bacteria for LSC experiments because it is a common species for research studies and is fairly easy to culture. *E. coli* stock was obtained from the American Type Culture Collection[23] (ATCC) in freeze dried form. The specific *E. coli* strain used was *Escherichia coli* (Migula) Castellani and Chalmers MG 1655. The samples were revived from freeze-dried state according to ATCC methods. This resulted in 24 slants of *E. coli* colonies kept in refrigeration, which were used for all experiments. Appendix A contains the detailed procedure employed, from an intra-laboratory report by Katherine Thompson.

The procedure for creating stock solutions from stored slants was to remove cells from the slants and inoculate a vial of Luria Berari Medium (LB broth). The LB broth was made according to the following recipe (ATCC 1065LB).

Luria Berari (LB) Medium

1. Measure ~800 ml distilled, deionized water
2. Add 10 g bacto-tryptone
3. Add 5 g yeast extract
4. Add 10 g NaCl
5. Adjust pH to 7.5 with NaOH
6. Add water to bring total volume to 1 L
7. Autoclave at liquid cycle for 20 minutes

---

[23] Manassas, Virginia

It was not immediately obvious how to most effectively remove cells from the slants. In the slants, some colonies grew on the surface, while some grew deep in the media, which was a gelatinous solid. Three inoculation methods were used. The first method employed a wire loop to remove a small chunk of media containing a suspended colony and place it in LB broth. The second method was to gently scrape a colony on the surface of the slant using a plastic, disposable inoculation loop and swirling this in LB broth to disperse bacteria. It was found that the chunk of media with a suspended colony did not effectively inoculate the broth. Perhaps the cells remained in the media and were not able to disperse in solution. The gently scraped colony was effective for inoculation and this method was used several times. It was important to find a slant with a colony growing on the surface and scrape directly in that colony to insure inoculation.

In the ATCC method, the inoculated broth was stored at 37º C for 20 hours to let the bacteria grow. When the inoculation was successful, the solution appeared cloudy after incubation. It was found that the exact time of incubation could vary, as some samples were more cloudy than others even after the same incubation time. Leaving the solution in incubation much more than 16 hours appeared to result in large flocs of bacteria, making them difficult to disperse in solution. Because of this, incubation times were usually kept to about 16 hours, but were sometimes longer. Bacterial solutions were verified by placing a small drop on a microscope slide and examining with 200x magnification (20x objective, 10x eyepiece) in a standard light microscope. In an effective inoculation, many bacteria could be seen moving rapidly about the solution. In some cases, very long rod-shaped bacteria were present, indicating contamination of the *E. coli*, which were smaller rod-shaped bacteria. Contamination was not a hindrance to experiments, so no significant effort was spent trying to keep samples pure.

In many laboratory studies, bacterial suspensions are washed by centrifugation, decanting of supernatant, and re-suspension of bacteria in clean buffer (see Appendix A). Because a laboratory centrifuge was not available, washing and re-suspension were performed by filtration instead of centrifugation. *E. coli* solution in LB broth was filtered through a 0.2-µm pore size polycarbonate membrane.[24] Typically, the broth volume was 5 ml. However, if the cell concentration was high, filtration was time-consuming, so smaller volumes were used. Higher volumes were used for low-concentration solutions. After filtration, the bacteria remained on the membrane surface and were re-suspended by spraying phosphate buffered saline (PBS) solution directly onto the membrane and filling to 5 ml. Again, more or less PBS could be used, as desired. The PBS solution was made according to the following recipe:

---

[24] These membranes were the same as those used for filtration and scanning, Isopore™ membranes, Millipore, Billerica, Massachusetts

Phosphate Buffered Saline (PBS) Solution

1. Pour 800 ml DI water into autoclavable container
2. Add 8 g NaCl
3. Add 0.2 g KCL
4. Add 1.44 g Na_2HPO_4
5. Add 0.24 g KH_2PO_4
6. Adjust pH to 7.4 using HCl
7. Add DI water to bring total volume to 1 L
8. Autoclave at liquid cycle for 20 minutes

It was found (in experiments described later) that material as big or bigger than bacteria in the LB broth was stained by SYTO 62, causing errors in bacterial enumeration. In subsequent experiments, LB media and PBS solution were filtered through the 0.2-µm membrane before being used, as suggested in flow cytometry literature (Braga et al., 2003). This greatly reduced or eliminated interference by particles in the bacterial size range.

It was reported in the literature that a formalin (37% formaldehyde, in solution) fixative could aid in keeping bacterial numbers constant over time by stopping their growth and minimizing cell lyses (Kepner & Pratt, 1994). Formalin was not used in early experiments, but in latter experiments it indeed seemed to help keep bacterial flocs from forming in solution, leading to more consistent counts. It had the added advantage of making the odor from bacterial samples more bearable. It became standard practice to fix cell samples with 2% (volume : volume) formalin after incubation. This was done either in the LB broth mixture or after washing with PBS.

Staining, Filtering, and Mounting

In initial experiments with *E. coli*, the sample preparation method used was to filter the sample, add SYTO stain, wait 5 minutes, filter again, place on stage with immersion oil, and scan. This method proved to be ineffective for many reasons, and a systematic approach was taken to optimize the staining, filtering, and mounting of *E. coli* samples for the prototype LSC.

It was also necessary that the method be appropriate for direct counting with fluorescence microscopy, in order to verify cell concentrations.

There is no standard method for staining of bacteria for laser scanning cytometry. As reported in the literature review, there are several papers on staining of bacteria for direct counting using DAPI or Acridine Orange. There are also a few studies using SYTO stains, and only one study using SYTO 62. The procedures found in all of these studies were combined and experiments were performed to find the most reasonable and appropriate procedure for staining bacteria with SYTO 62 for the LSC.

Table 2 is a matrix of the experiments performed to determine which steps in filtering and staining were causing problems. Problems were identified by comparing the background of different scans (Figure 16). An above-normal background indicated a filtration scheme leading to fluorescence of material other than cells. Counts were also compared for each scan (Figure 17). No sample in this series contained bacteria, so any data points counted were false positives.

To determine the effect of wet or dry scanning, Figure 18 was produced. Water content had a distinct effect on the background; the background level decreased when the membrane was scanned wet. However, since each scan lasted several minutes, the membrane often began to dry. This resulted in an increased background level during the scan and flawed counts. This is evident in Figure 19.

Table 2: Steps used in a series of scans to determine which aspects of the staining and filtering method were problematic. An X indicates that the step was employed in the given scan. The water content column indicates whether the filter was allowed to dry before scanning or was scanned while still wet.

Scan #	5 mL DI	5 mL PBS	5 mL 0.33-mM Sucrose	5 mL LB Broth	0.5 mL 0.05-mM SYTO 62	Water Content
2005-01-22a*						
2005-01-22b*						
2005-01-22c*						
2005-01-22d†						
2005-01-22e†						
2005-01-22f	X					Wet
2005-01-22g	X					Dry
2005-01-22h	X					Dry
2005-01-22q	X					Dry
2005-01-22i		X				Wet
2005-01-22j		X				Dry
2005-01-22k			X			Wet
2005-01-22l			X			Dry
2005-01-22m				X		Wet
2005-01-22n				X		Dry
2005-01-22o					X	Wet
2005-01-22p					X	Dry
2005-01-22r					X	Dry
2005-01-22s					X	Dry
2005-01-22t					X	Dry
2005-01-22u		X			X	Dry
2005-01-22v			X		X	Dry
2005-01-22w	X	X	X		X	Dry
2005-01-22x	X	X	X	X	X	Dry

* Scans of the empty stage, with no membrane.

† Scan of a new, unused membrane.

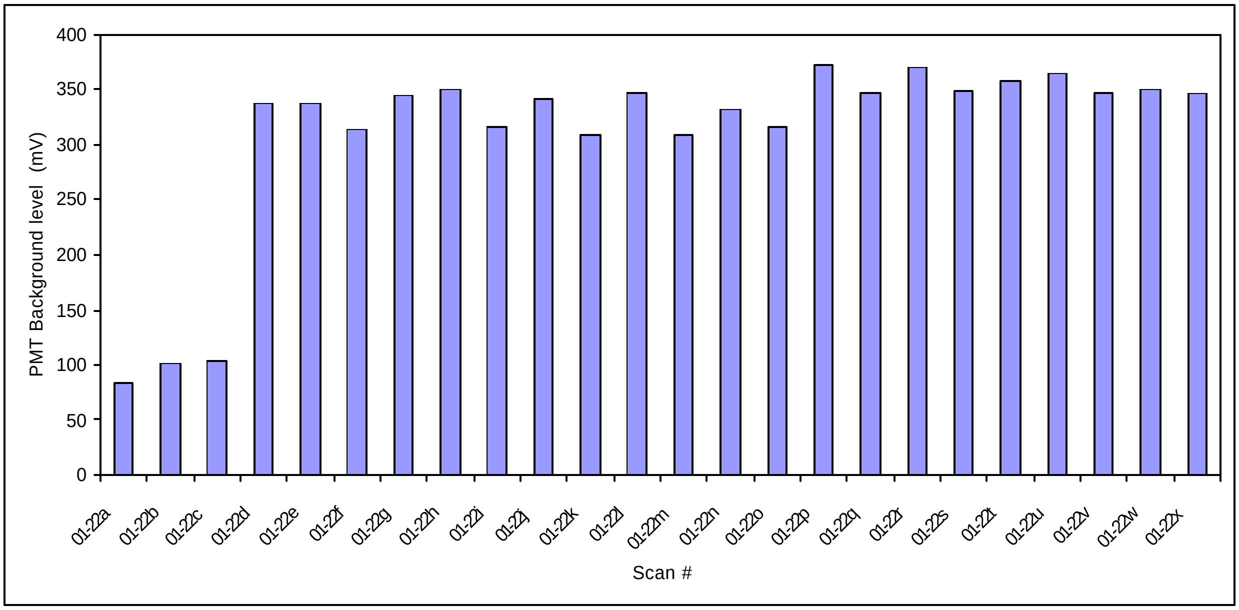

Figure 16: Background level for each scan in the series listed in Table 2.

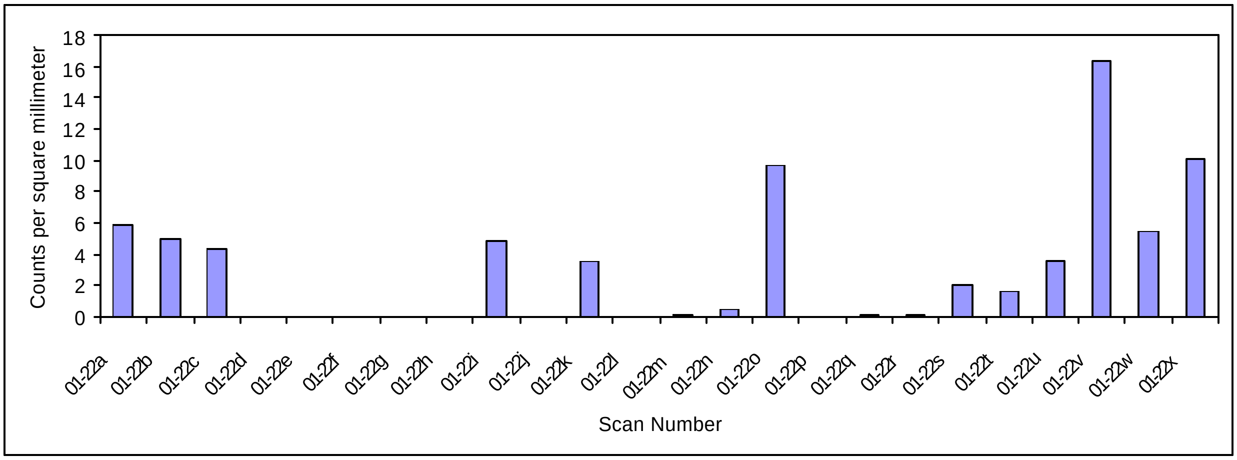

Figure 17: Counts per square millimeter for each scan in the series listed in Table 2.

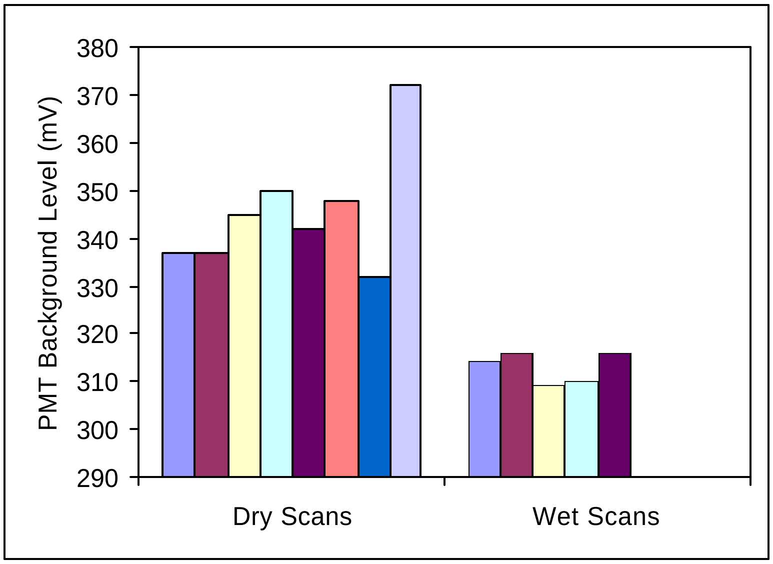

Figure 18: Background levels for the scans in Table 2, with data grouped to distinguish between scans performed with a dry membrane and scans performed with a wet membrane.

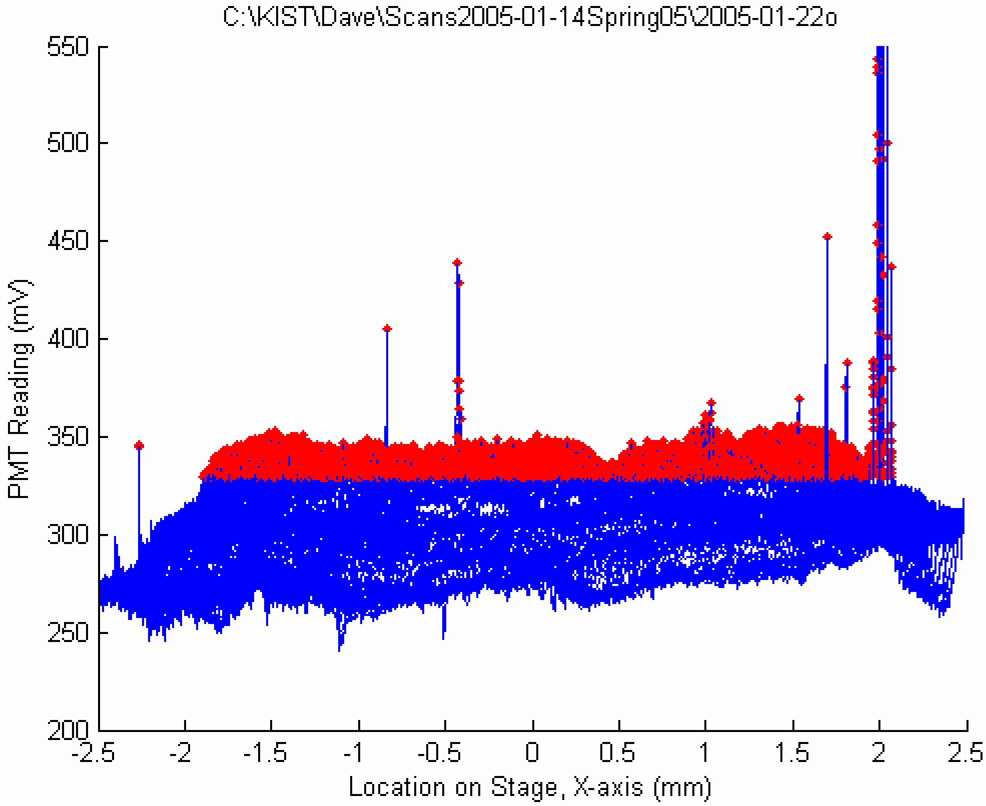

Figure 19: Data from scan 2005-01-22o, which was a wet membrane scan. Red indicates peaks counted. Scans began on the outside and move inward. Due to drying over the time of the scan, the PMT reading was increased, leading to false counts on the inner portion of the membrane.

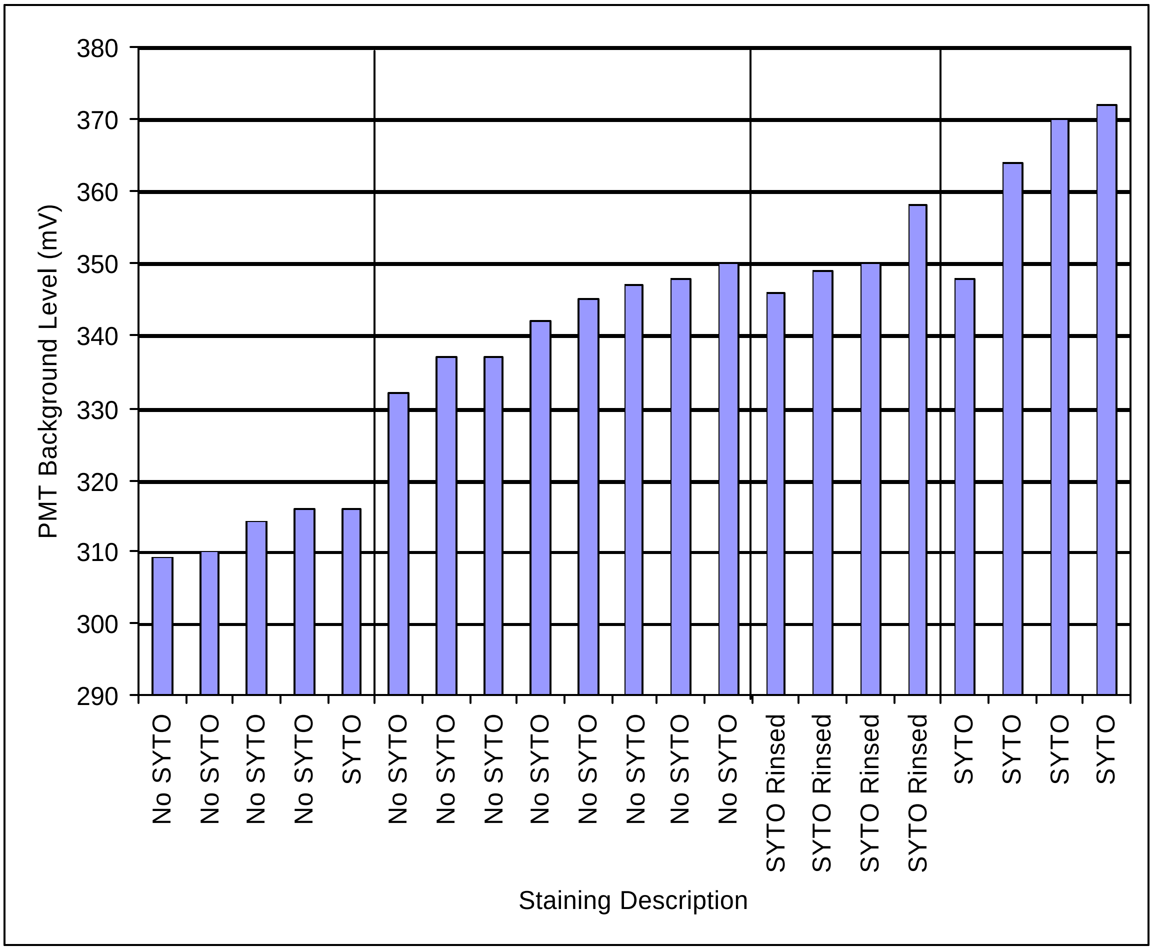

Figure 20: Background levels for scans listed in Table 2, with data grouped first in terms of wet (green background) or dry (pink background) and then by staining method. "No SYTO" indicates that no SYTO 62 stain was used. "SYTO Rinsed" is for scans where SYTO 62 was applied and subsequently rinsed. "SYTO" indicates scans where SYTO 62 was applied and not rinsed away before scanning.

The effect of SYTO 62 stain on the background is elucidated in Figure 20. Leaving STYO stain on the membrane caused an increase in background. Even when rinsed off after staining, an increase in background was observed. From this it was determined that the optimal staining strategy to insure the lowest possible background would be to stain cells before they were filtered.

The other important finding from this series of staining tests is that even when no bacteria or microspheres were present, SYTO 62 application caused the prototype to have positive counts. This is apparent in Figure 21.

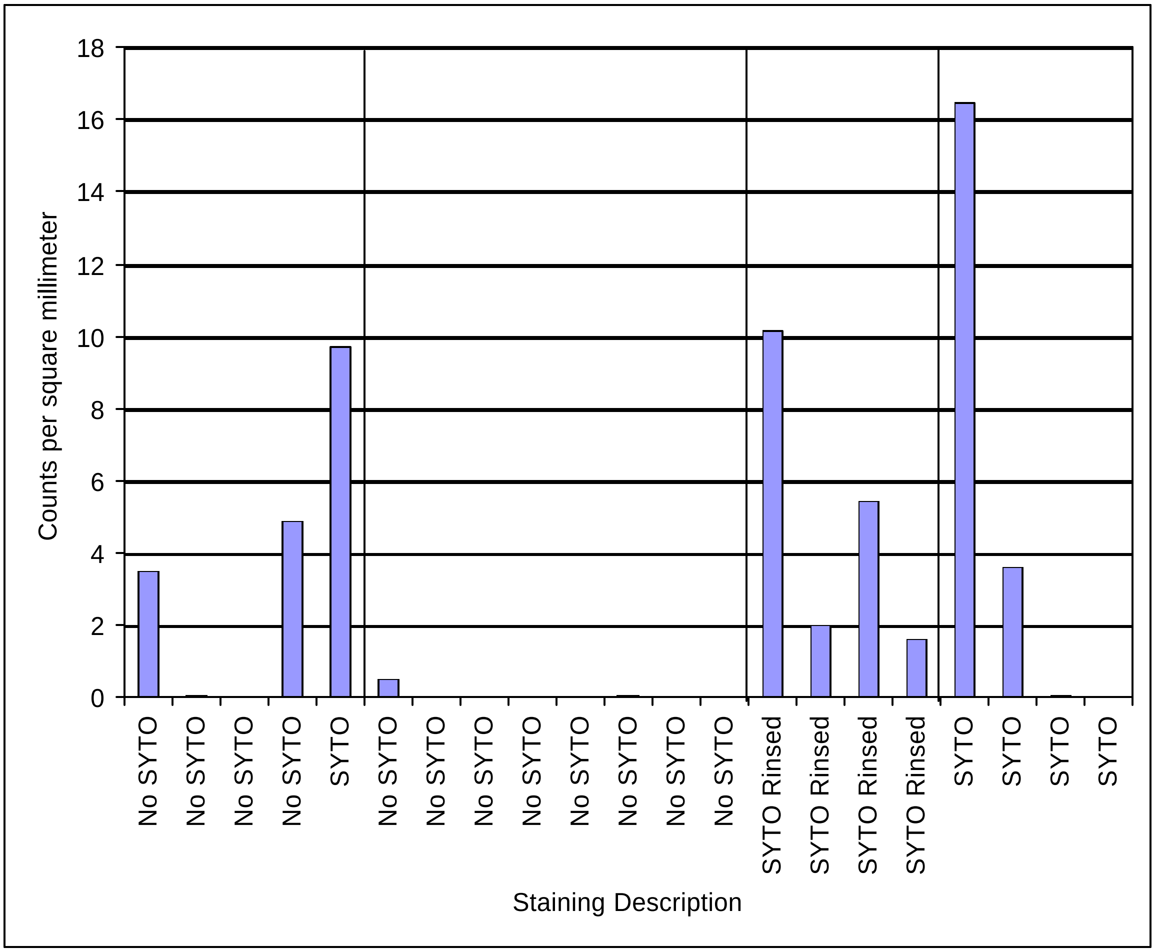

Figure 21: Counts per square millimeter for scans listed in Table 2, with data grouped first in terms of wet (green background) or dry (pink background) and then by staining method. "No SYTO" indicates that no SYTO 62 stain was used. "SYTO Rinsed" is for scans where SYTO 62 was applied and subsequently rinsed. "SYTO" indicates scans where SYTO 62 was applied and not rinsed away before scanning.

In Figure 21 it is clear that the dry membrane scanning method with no SYTO 62 added gave the least false positives (all counts in the figure are false positives, as no cells or bacteria were added). Whether SYTO 62 was rinsed away or not, applying SYTO 62 usually yielded a false positive. This was probably due to particles from the air or on the surface of glassware being filtered onto the membrane. The stain was not specific to nucleic acids, so many particles besides bacterial cells were labeled and fluoresced during scanning.[25] It was preferable, then, to stain the bacteria before filtration, so that contaminant particles would not be stained.

It should be mentioned here that the use of a backing filter was recommended in the literature (Kepner & Pratt, 1994). This was not used in many of the early experiments, but was employed later. This was a glass fiber filter, cut to size and placed between the membrane and the filter stage. The backing filter provided a more evenly distributed vacuum. When the backing filter was used, the membranes dried more thoroughly on the filter stage than when the backing filter was not used. Also, with the backing filter the membranes appeared flatter, with fewer ridges and divots on the membrane, leading to more consistent scanning.

---

[25] For example, SYTO 62 was found to be very useful in staining hydrophobic polysulfone particles (Won-Young Ahn, Intra-laboratory report.)

In the above experiments, the difference between wet and dry scanning was elucidated. However, mounting the membrane wet or dry still gave inconsistent counts among sub-samples. It was decided that a careful analysis of mounting methods should be performed to determine the optimal scheme. Table 3 reports the observations for each mounting method. The mounting method yielding the best results was one that did not cause color variation (which led to variability in light absorbance and reflectance) over the surface of the membrane, was clean and easy to handle, was easily transferable between prototype scanning and microscope scanning, and yielded a flat membrane. The details of this mounting method will be given at the end of this section.

Table 3: Comparison of various mounting methods.

Mounting Method	**Result**
Drop of 0.02-M sucrose	Membrane adhered moderately, but better on one edge. Color was mostly homogeneous, but darker where adherence was better.
Dipped in 0.02-M sucrose	Membrane adhered slightly, but was not completely flat. Color was homogeneous.
Dipped in 0.01-M sucrose	Membrane adhered only on the edges. Color was homogeneous.
Dipped in 0.002-M sucrose	Membrane did not adhere. Color was heterogeneous on the edges.
Dipped in Milli-Q	Membrane did not adhere. Color was homogeneous.
Drop of Milli-Q	Membrane did not adhere. Discoloration found on edges (something besides water must have been present.)
Drop of immersion oil	Membrane adhered. Oil below the membrane in the middle caused a raised area. Color was homogeneous.
2 Drops of immersion oil	Membrane adhered. Oil leaked out onto paper. Surface seemed rough for some reason. Color was homogeneous.
Dipped in immersion oil	Membrane adhered, but floated on a layer of oil, causing elevation differences. Color was homogeneous.
Oil sandwich, pressed gently	Membrane adhered between coverslips. Oil leaked out. Color was homogeneous.
Oil sandwich pressed firmly	Membrane adhered between coverslips. Oil leaked out. Color was homogeneous. (This was the same result as gently pressed, but quicker.)
Small drops (from syringe) oil sandwich	Membrane adhered between coverslips. Oil did not leak out. Color was homogeneous. This seemed like the best mounting method.
Small drops (from syringe) oil sandwich (repeated)	Membrane adhered between coverslips. Oil did not leak out. Color was homogeneous. Again, this seems optimal.

The reviewed literature examined several stain concentrations and stain durations for DAPI, Acridine Orange, and SYTO stains. Considering the literature, and realizing that the lowest stain concentration and lowest stain duration would yield the lowest cost and shortest analysis time, it was decided that final stain concentrations (the concentration of stain after addition to the sample) of 0.5-µM or 1-µM SYTO 62 would be adequate. It was expected that higher stain concentration would result in a higher signal-to-noise ratio, but because SYTO 62 stock was limited and the lower (0.5 µM) concentrations gave sufficient results, no careful analysis of fluorescence intensity with different stain concentrations was attempted.

Based on the literature review, a 5-minute stain duration seemed to be sufficient, so this was used as the minimum stain duration. However, when staining one sample and doing scans of three consecutive sub-samples, the latter sub-samples were stained much longer (at least 8 minutes) than the first sub-sample. To determine if this had an effect on the counting variability among sub-samples, a sample of *E. coli* solution was stained with a final concentration of 0.5-µM SYTO 62. Sub-samples were filtered and scanned at approximately 2-minute intervals. Figure 22 shows the number of cells counted per square millimeter of membrane area for the time series. There was a great deal of variability and no clear relationship between stain duration and the number of cells counted, but the shortest stain duration (2 min, 30 sec) gave a high count compared with the latter data points, so it was presumed that staining occurred very quickly. In this experiment it seemed there was a significant problem with contamination by LB broth particles, so the data were still inconclusive for bacterial cell staining. However, it was decided that a 5-minute stain duration was sufficient, as there was no clear advantage for longer durations.

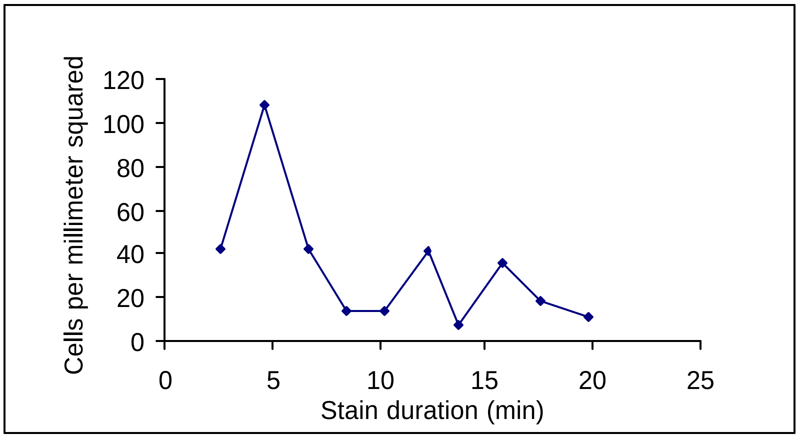

Figure 22: Prototype counts for varying stain durations.

Based on the experiments described, a staining, filtering, and mounting method was developed. This may not be optimal for all water sources or experimental design needs, but this was the most effective method found thus far:

Sample Preparation

- Add formalin (37% formaldehyde) to sample immediately after collection.

Staining

- Place 0.5 ml of sample in a small (2-ml) centrifuge vial.
- Add 0.5 ml of 1-µM SYTO 62 (for a final concentration of 0.5 µM).
- Place sample in the dark for at least 5 minutes.

Filtering

- Place backing filter (glass fiber, cut to fit) on filter stage.
- Place a new membrane on the backing filter and clamp to filter column.
- Add 5 ml of DI water to the filter column.
- Place a cover (small beaker or equivalent) over the filter column to minimize airborne particulate collection.
- Add 0.2 ml of stained sample to the filter column.
- Apply vacuum and filter, allowing time (~10 to 30 seconds) after filtration for membrane to dry.

Mounting

- Remove the membrane from the filter stage and place it under a lid to prevent airborne particulate collection and light exposure.
- Allow the membrane to dry thoroughly, as can be determined by the color change from dark to light.
- Using a syringe and needle, place a small drop of Type FF (non-fluorescing) immersion oil on a 25 by 25-mm No. 1 glass coverslip.
- Place the dry membrane on the coverslip over the immersion oil.

- Place another small drop of immersion oil on the surface of the membrane.
- Place another coverslip on top of the membrane and squeeze or press with a non-scratching object (such as plastic tweezers) to remove air bubbles. There should be just enough immersion oil to completely cover the membrane when pressed, without leaking outside of the coverslips.
- Keep the mounted membrane in the dark until scanning.

Scanning Program

The scanning program for stained bacteria was basically the same as was used for fluorescent microspheres. However, the optimal scanning parameters varied slightly because of subtle differences between microspheres and bacteria. Microspheres fluoresced brightly and were detected by a spot of 14 by 26 µm (Figure 6), so a track width of 20 µm was used. Usually, at least two data points along the track could detect the microsphere and it would be seen in two or more tracks. Thus, the optimal scheme was to scan a narrow annulus of membrane area with many tracks and be sure that all the microspheres in that annulus were counted.

Bacteria, however, did not fluoresce as brightly as microspheres, so they were usually only detected in one track and by one data point. Scanning the narrow annulus was no longer useful, as many bacteria were still missed between tracks. Attempts were made at narrowing the annulus even further to catch all bacteria, but this decreased the total membrane surface area scanned. Because the distribution of bacteria on the membrane was non-homogeneous (a result of uncontrollable randomness in the filtering), the counts from sub-sample to sub-sample varied widely. It was decided that the tracks would be widened to cover more membrane surface for the same scan time. This led to more consistency between sub-sample counts.

The Lab-View scanning program front panel and block diagram are displayed in Appendix B. Note that the program was changed in many aspects from the program used by Ben Lee (2003). This new program was written to achieve faster data acquisition by removing many of the calculations from the loop structure. Also, the graphical displays were eliminated to minimize processor load; the graphs were no longer used for data analysis, as they were replaced by Matlab signal processing programs. Optimal scanning parameters for *E. coli* enumeration were: linear stage velocity, 0.0275 mm/s; rotary stage velocity, 90 degrees-per-second; inner radius, 1 mm; and outer radius, 6.5 mm.

Focusing

As was seen for microspheres, proper focus was required to obtain the maximum laser intensity and increase the signal-to-noise ratio in *E. coli* experiments. Several scans of the same *E. coli* sample were run at varying focal lengths (stage heights). Both the background and counts per square millimeter ware calculated for each scan and are plotted in Figures 23 and 24, respectively. One drawback to this method was that scanning the same section of membrane several times could cause photobleaching of the sample. To investigate this effect, one annulus was scanned while the stage height was increased, then a different annulus was scanned while stage height was decreased, and a third annulus was scanned while increasing again. The data are separated into segments of increasing and decreasing stage height, in order to evaluate the photobleaching effect.

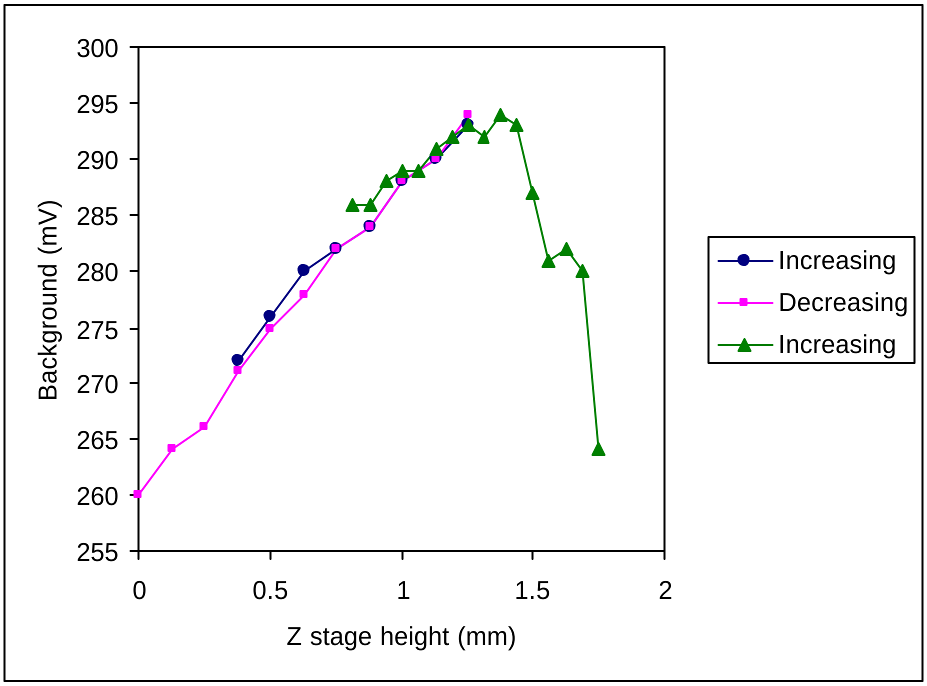

Figure 23: Background PMT readings for several consecutive scans of the same membrane at different stage heights (focal distances). The data is separated into three segments where stage height was increased, decreased, then increased again. A different annulus on the membrane surface was scanned for each data segment.

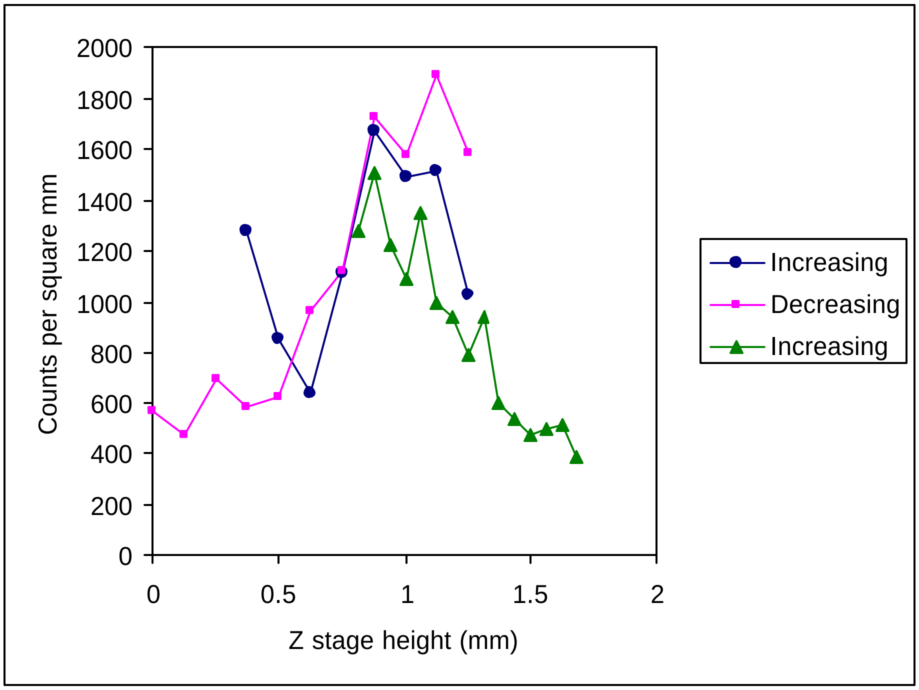

Figure 24: Counts per square millimeter for the scans of Figure 23.

The stage height yielding the highest background level was about 1.4 mm. This was presumably the point of greatest laser spot intensity. However, it was more important to achieve the highest counts. Counting was more varied with respect to stage height, but the best counts were in the 0.8 to 1.25 mm range. This range of data was recounted and the signal-to-noise ratio was calculated (Figure 25). Regardless of photobleaching, the stage height of 0.875 mm yielded high signal-to-noise ratios and consistent counts. This was chosen as the optimal stage height, which was presumably the point where the laser spot was most focused. Note that photobleaching probably had an affect on these scans, as the high counts came toward the beginning of each series. However, it was still fairly clear which stage height gave the optimal focus.

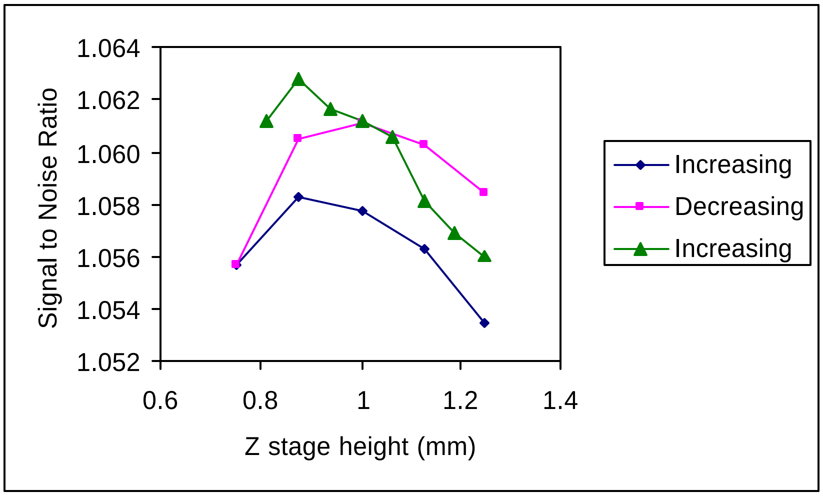

Figure 25: Signal-to-noise ratios calculated for several consecutive scans of the same membrane at different stage heights (focal distances). These were a few of the same scans used in Figures 23 and 24.

Laser Power and PMT Optimization

In microsphere experiments, the laser power was set to 1 mW. The microspheres were bright enough that any higher laser power would max out the PMT signal. With bacteria, a higher laser power was needed, but anything above 3 mW etched the dry-mounted membrane. Higher laser power was possible only with the oil sandwich mounting method. The background increased greatly as power increased, but fluorescence signals also increased, leading to better counts and a higher signal-to-noise ratio. Thus, the maximum laser power of 10 mW was optimal.

The PMT voltage was another adjustable parameter. As with laser power, the lower PMT voltage settings were adequate with microspheres. However, since bacteria yielded a much smaller signal, the PMT voltage was set at the maximum manufacturer-suggested level of 45 mV.

Signal Processing

Cell Counting

The program used to count microspheres found all the data points lying above a certain threshold (usually 110% of background) and counted them as a part of a data peak. It then determined which points were part of a single peak based on proximity to one another. Many data points could have indicated a single microsphere and the program took that into consideration. However, a detailed look at a scan of a dilute bacterial solution yielded Figure 26, where it appeared that even points that were separated from one another were being counted together. In most of the counts, there was only one data point. This suggested that the bacteria were not bright enough to be detected unless the center of the laser spot was on the cell. Effectively, the spot size was reduced. The counting program was subsequently changed so that all data points above the threshold were counted as separate bacteria. The program underwent several modifications over the life of the project, with the final bacterial counting program given in Appendix C.

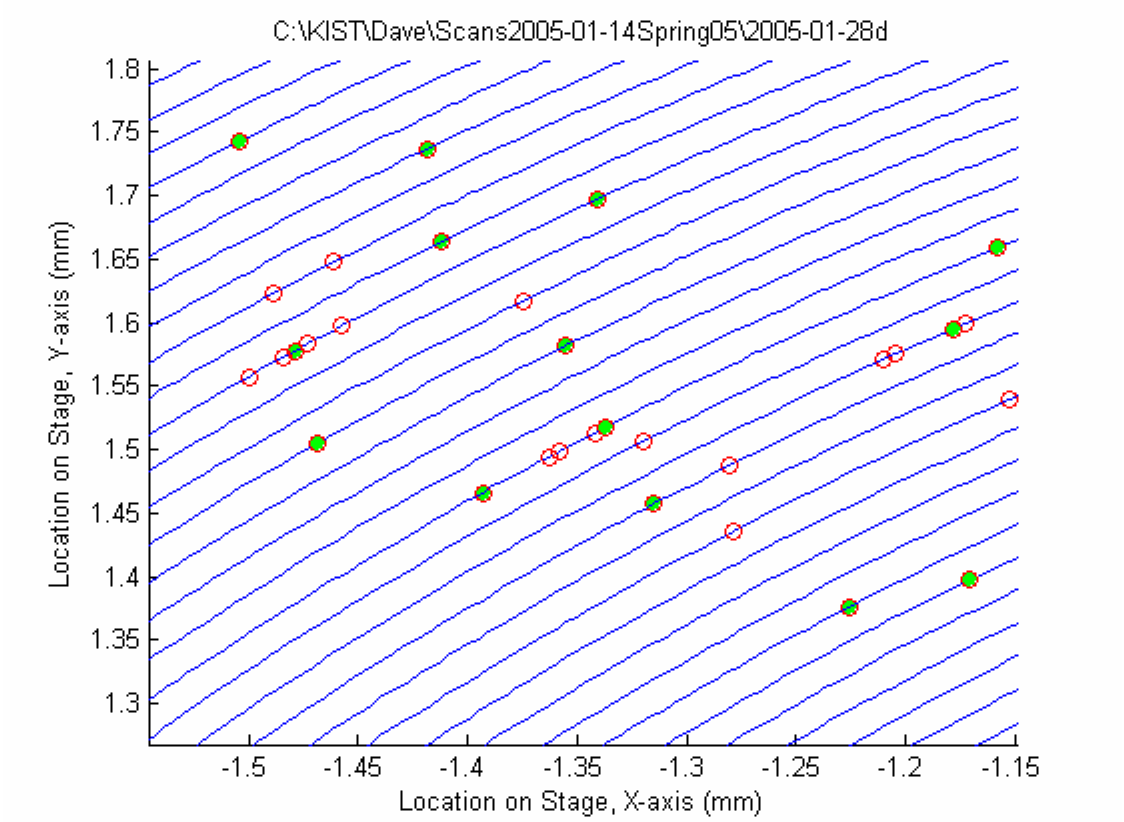

Figure 26: Magnified view of data from a scan of a dilute bacterial solution. Red circles indicate points that lay above the counting threshold. Circles filled with green indicate the maximum point in the group, counted as a cell location.

Digital Filtration

In early scanning experiments there was a significant oscillatory component in the data, as shown in Figure 27. Not all scans were this pronounced, but to some extent an oscillation was always present. This was probably due to the rotary stage being slightly misaligned and not exactly on the horizontal plane, so that one side rose higher than the other as the stage rotated. Supporting this hypothesis is the fact that background changes greatly with varying stage height (Figure 23).

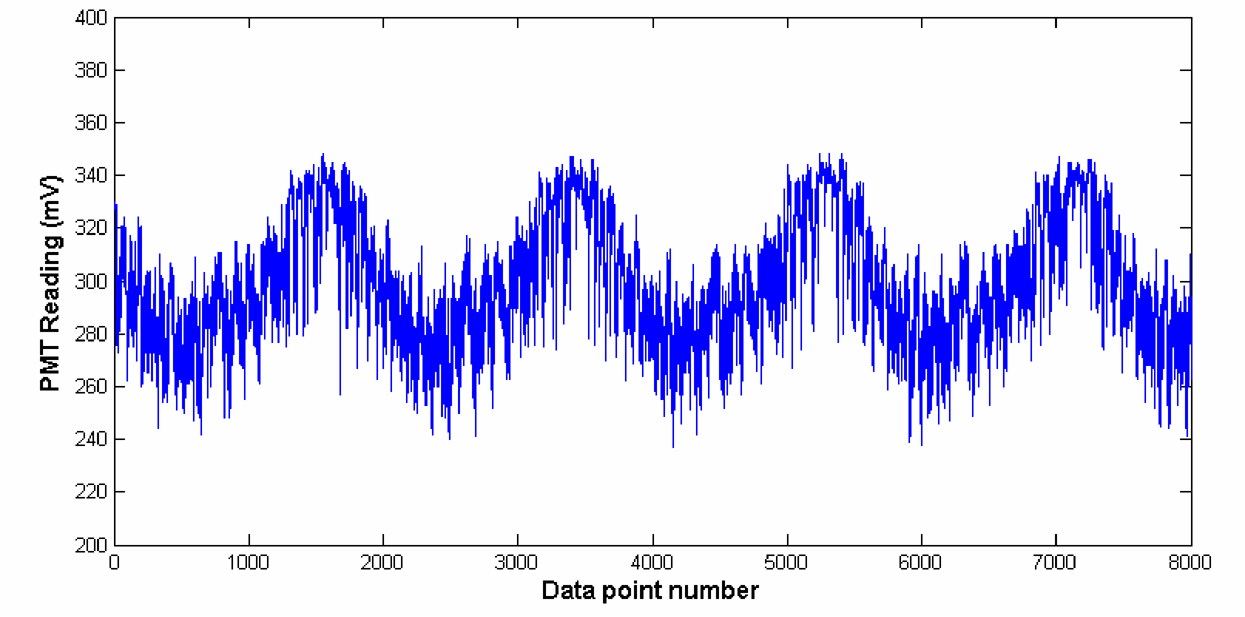

Figure 27: Scan data showing a strong oscillation.

Because this oscillatory signal occassionally had a significant amplitude (about 80 mV in Figure 27) relative to fluorescing bacteria, counts were affected. To remove the oscillation, the stage could have been realigned, but such fine adjustments to the horizontal level were impractical at that time. Thus, digital filtration was attempted.

As explained in the literature review, digital filtration can remove low frequency oscillations. A program was written in Matlab, which used the Fast Fourier Transform to convert the data to the frequency domain, filter out the low frequency portion, and convert it back to the time domain for further counting. The digital filtering program code is given in Appendix C. The user had the ability to prescribe how much of the low frequency data to remove. The graphical output from this program is shown in Figure 28. Note in Figure 28 that the filtered data do not oscillate nearly as much as the original data. The digital filtration was thus effective in straightening the signal.

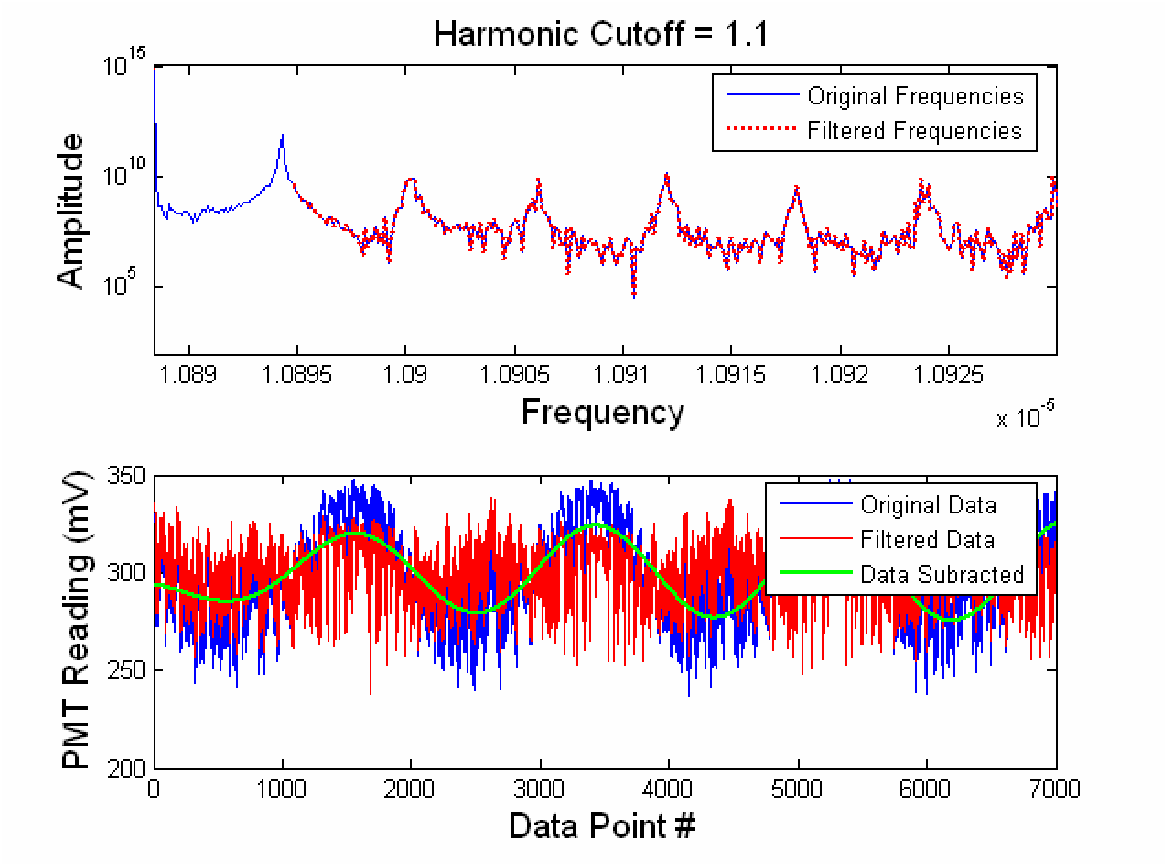

Figure 28: Graphical output from digital filtering program. The top pane is a magnified view of a small portion of the power spectrum. Harmonic cutoff is the user-defined filter setting. In this case it was set at 1.1, so the program removed all frequencies below 1.1 times the frequency of the first harmonic.

To test the effectiveness of digital filtration, a series of scans were performed on samples of *E. coli* of varying concentration. The samples were stained for at least one hour in 1-µM (final concentration) SYTO 62. Half the samples were stained overnight, as the experiment covered two days. This was before optimization of the mounting method, so the membranes were mounted dry and laser power was set at 1 mV. Scanning covered an annulus of 1.5 to 2.5 mm, with 50 tracks. After scanning, samples were counted using fluorescence microscopy. The correlation coefficient (R) between scan counts and microscope counts was 0.77. A program was written to re-count the prototype data for varying levels of digital filtration. This program was very similar to the counting program for bacteria in Appendix C, but was set in a loop structure to run multiple times. In the program, the variable “lowband” was defined as the fraction of original data filtered out by the digital filter. Concurrent with varying digital filtration, the threshold PMT reading for counting was analyzed. This was done with the variable “bgcutoff.” The bgcutoff variable was multiplied by the background (automatically determined) to yield the threshold. All values above this threshold were counted. The results of this series of experiments are shown in Figure 29, with additional views in Figure 30. Note that lowband equal to 0.07 yielded the best correlation coefficient. This means that when five to 10 percent of the low frequency information was cut out of the data set, prototype counts and microscope counts corresponded best. For the counting threshold, the highest correlation coefficient was obtained at bgcutoff equal to 1.015.

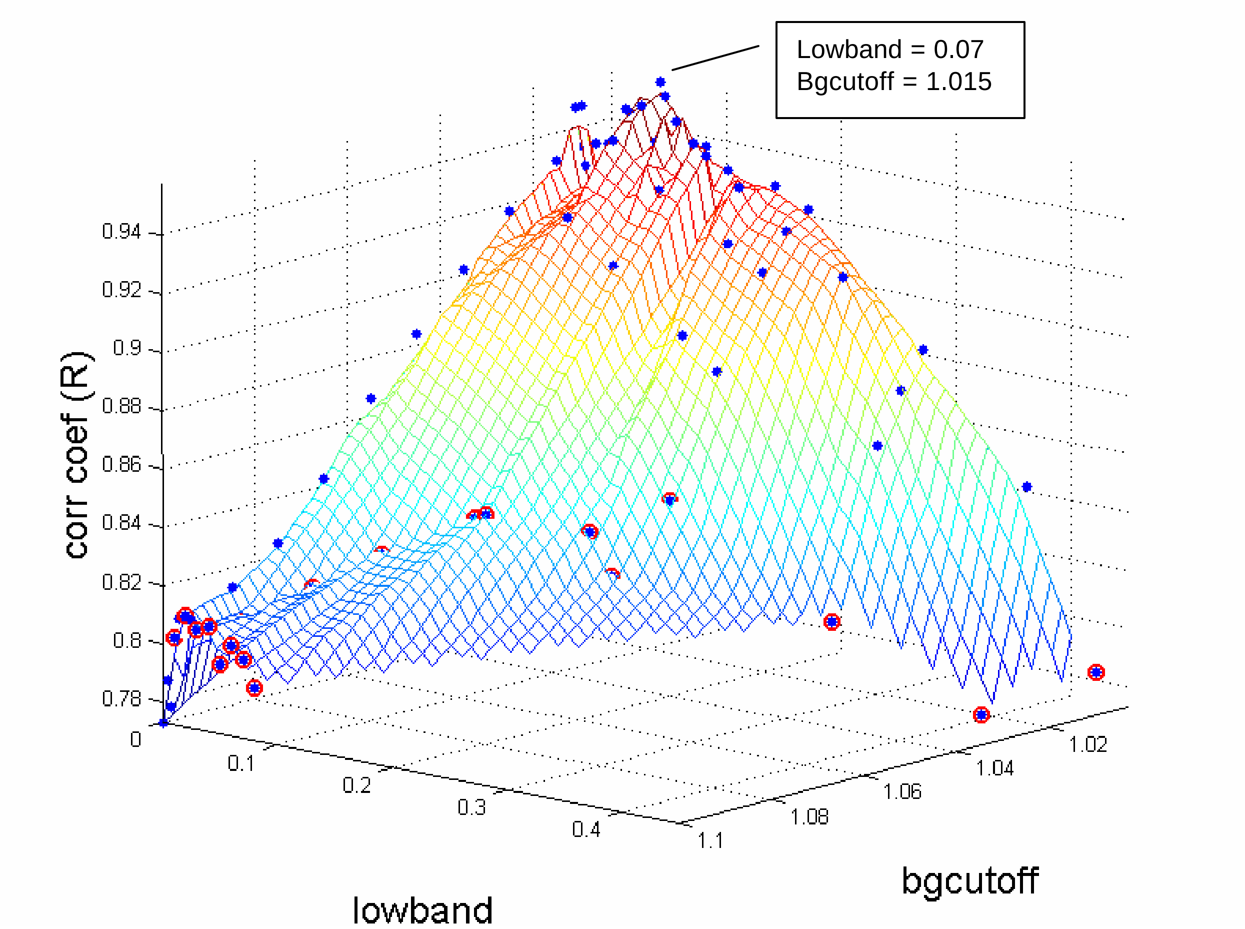

Figure 29: 3-dimentional plot of correlation coefficients varying according to lowband and bgcutoff. Each data point represents the correlation coefficient between prototype and fluorescence microscope counts of 15 samples. Data points circled in red correspond with lowband and bgcutoff values yielding zero counts in the blank membrane experiment of Figure 31.

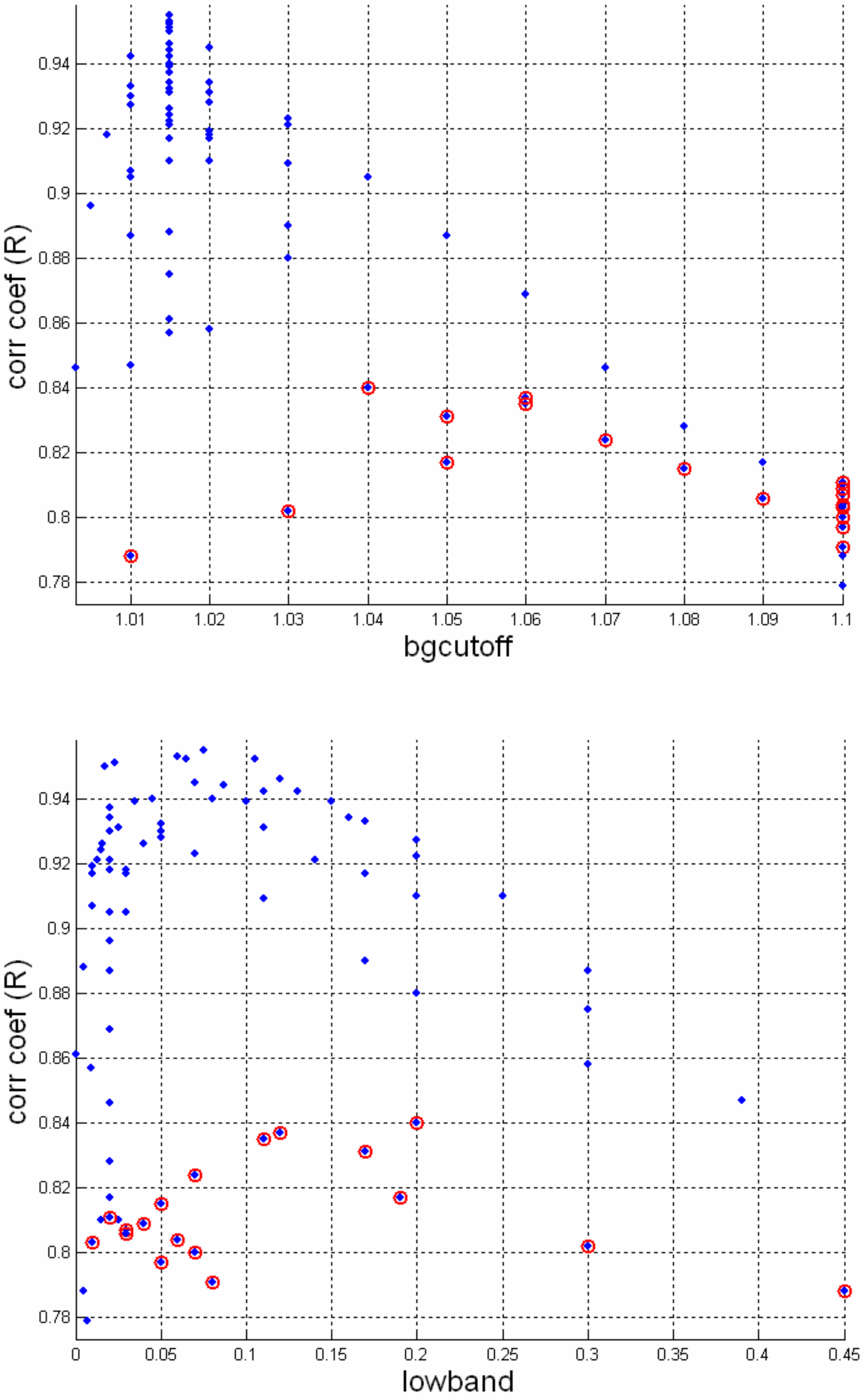

Figure 30: Alternate views of the data plotted in Figure 29.

It was feared that the optimal bgcutoff and lowband values determined were actually too low to be practical. With those levels, false positives would be encountered. To determine where false positives could be avoided, a scan was performed on a membrane that had no bacteria. Counts were again taken over a wide range of bgcutoff and lowband values. Figure 31 shows that at low bgcutoff and lowband values, counts (false positives) were increased. The appropriate range to work in, then, was the range where zero counts were detected. This zero-counts zone is indicated by green data points. Notice that as bgcutoff was increased, lowband could be lowered. As lowband was increased, bgcutoff could be lowered.

The red circles in Figures 29 and 30 indicate the data points that lay within the zero counts zone of Figure 31. Thus, the most appropriate bgcutoff was not 1.015, but 1.04. Likewise, the most appropriate lowband value was not 0.07, but 0.2. Together, these gave a correlation coefficient of 0.84.

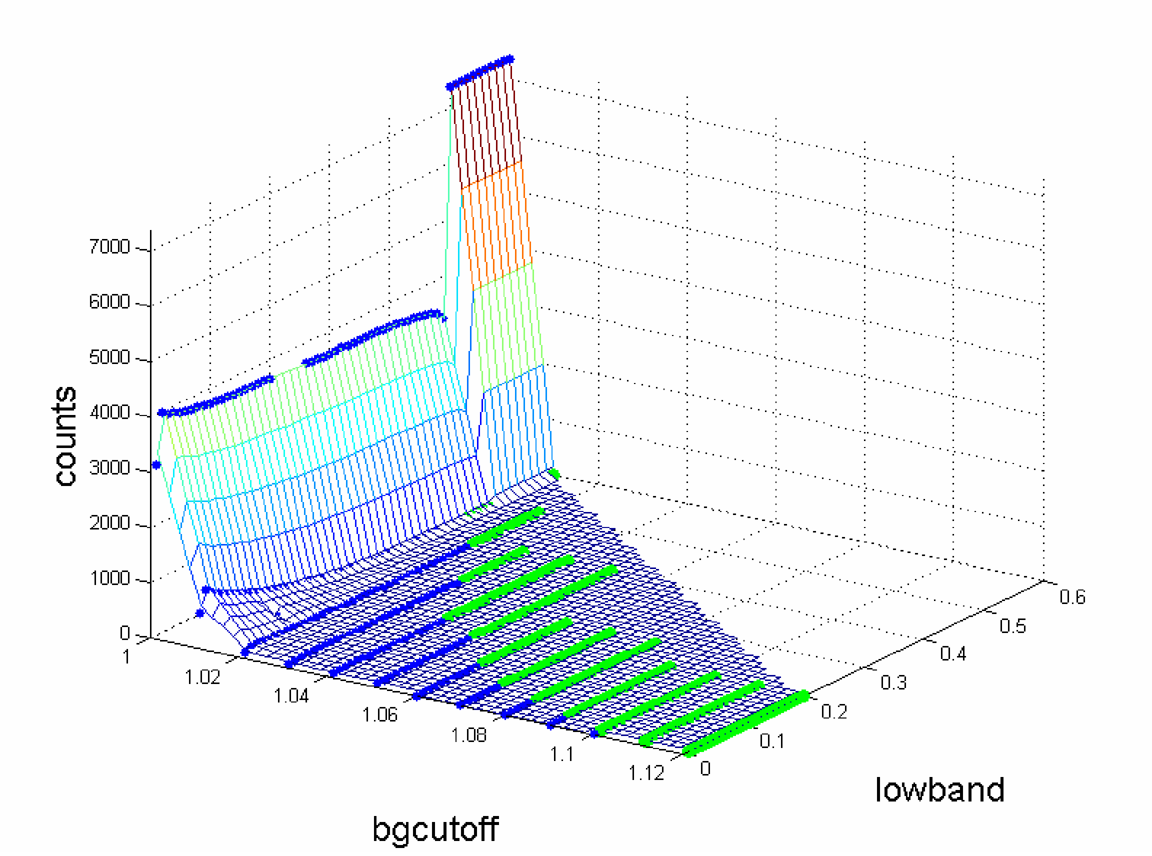

Figure 31: Counts obtained from a blank membrane with varying lowband and bgcutoff. The data points in green indicate zero counts.

Knowing the optimal bgcutoff and lowband values, experiments were performed to determine if these parameters led to better counting consistency among scans of the same cell concentration. The coefficient of variation (CV) was calculated for three scans of membranes that had the same concentration of *E. coli* filtered onto them. Bgcutoff and lowband values were varied over several counting routines and the CV was recalculated for each. The data are presented in Figure 32.

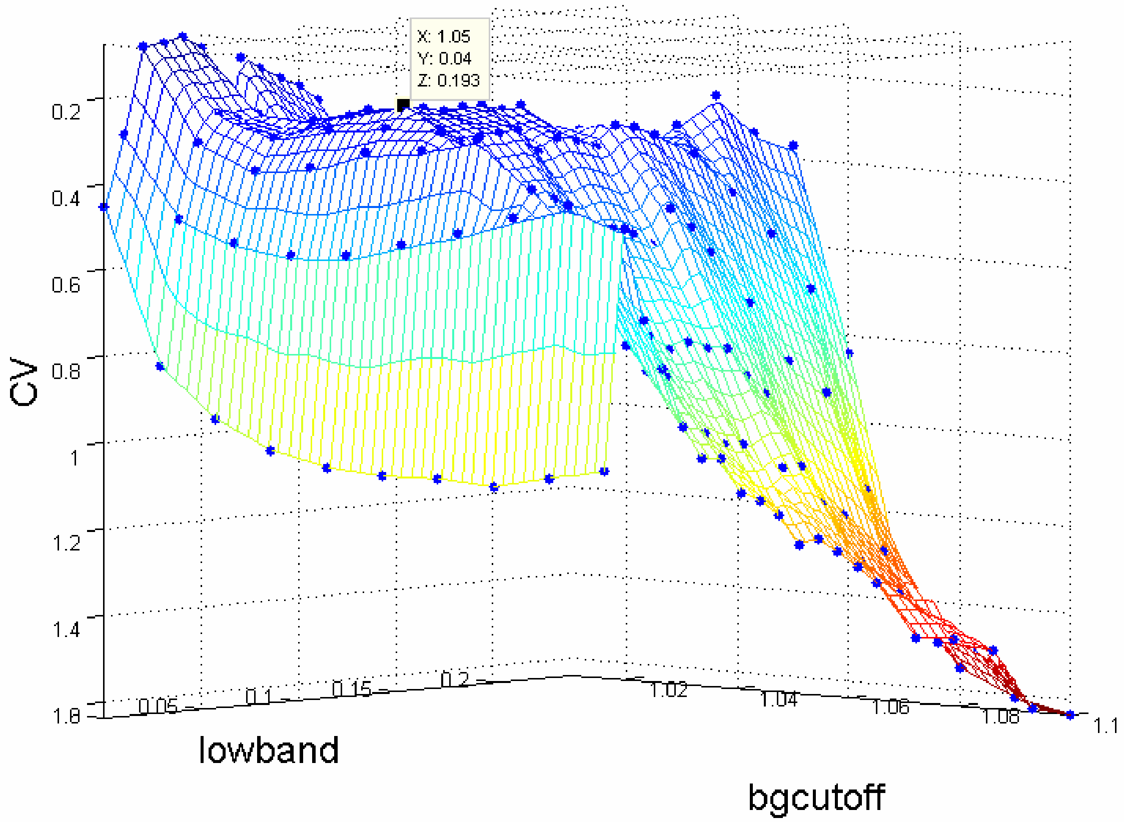

Figure 32: Coefficients of variation (CV) resulting from counting three membranes with the same bacterial concentration, as lowband and bgcutoff were varied. The text box indicates the local maximum and optimal conditions. X corresponds to bgcutoff, Y is lowband, and Z is CV. The CV axis is flipped so the optimal condition (lowest CV) is on top.

In Figure 32 it is apparent that the parameters yielding the lowest CV were bgcutoff equal to 1.05 and lowband equal to 0.04. However, the lowband value was disturbing, as it was much lower than the value (0.2) determined as optimal in previous experiments. More disturbing were the results of looking closely at what happened to the scan data after digital filtration. Figure 33 shows a scan that contained a few large particles, plotted before digital filtration. Figure 34 shows the same scan data, but after digital filtration with a lowband of 0.04. Clearly, the digital filtration inappropriately distorted the data to yield many more counts than were originally present.

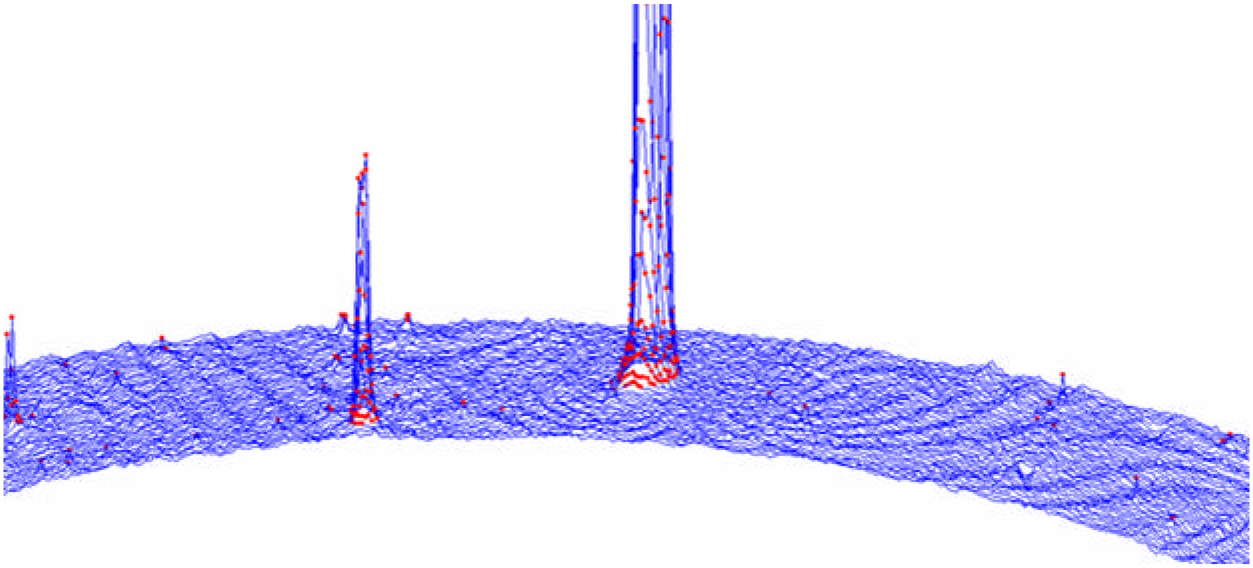

Figure 33: Magnified view of 3D scan data for a membrane with a few large particles present. Red indicates points above the counting threshold.

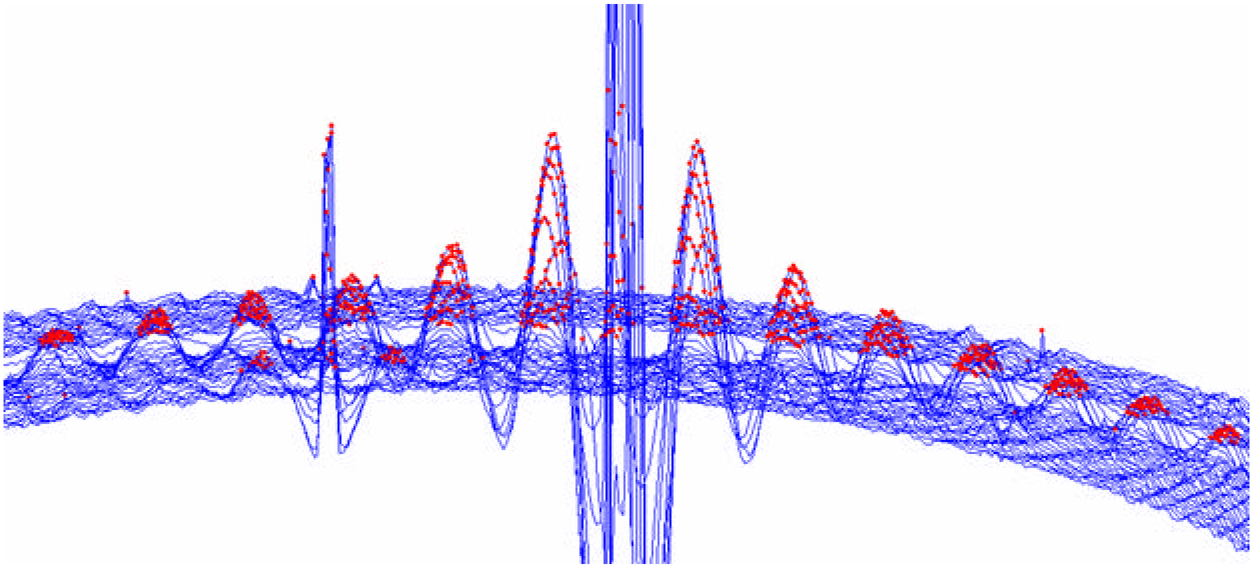

Figure 34: Magnified view of the same scan data in Figure 33, but after digital filtration with lowband = 0.04. Red indicates points above the counting threshold.

It appears that the problem with digital filtration occurred when large particles were present. When the previous experiment was performed, staining was done after filtration, so any particles present would have been stained. Perhaps with only bacteria present there would not be as significant an effect. Another experiment was performed, staining the bacteria before filtration, as was explained in the Staining, Filtering, and Mounting section. In this experiment, four samples were used, all containing the same concentration of bacteria. CV was calculated with varying bgcutoff and lowband, as done previously. However, in this case there was no clear optimum for either bgcutoff or lowband and the trends were not the same as those shown in Figure 32.

In the end, digital filtration failed to improve the counting performance of the prototype LSC. It was useful in some cases, as with the improvement in correlation coefficient for the first experiment in this section, but subsequent data (especially Figure 34) showed that digital filtration could have adverse effects in this cell counting application.

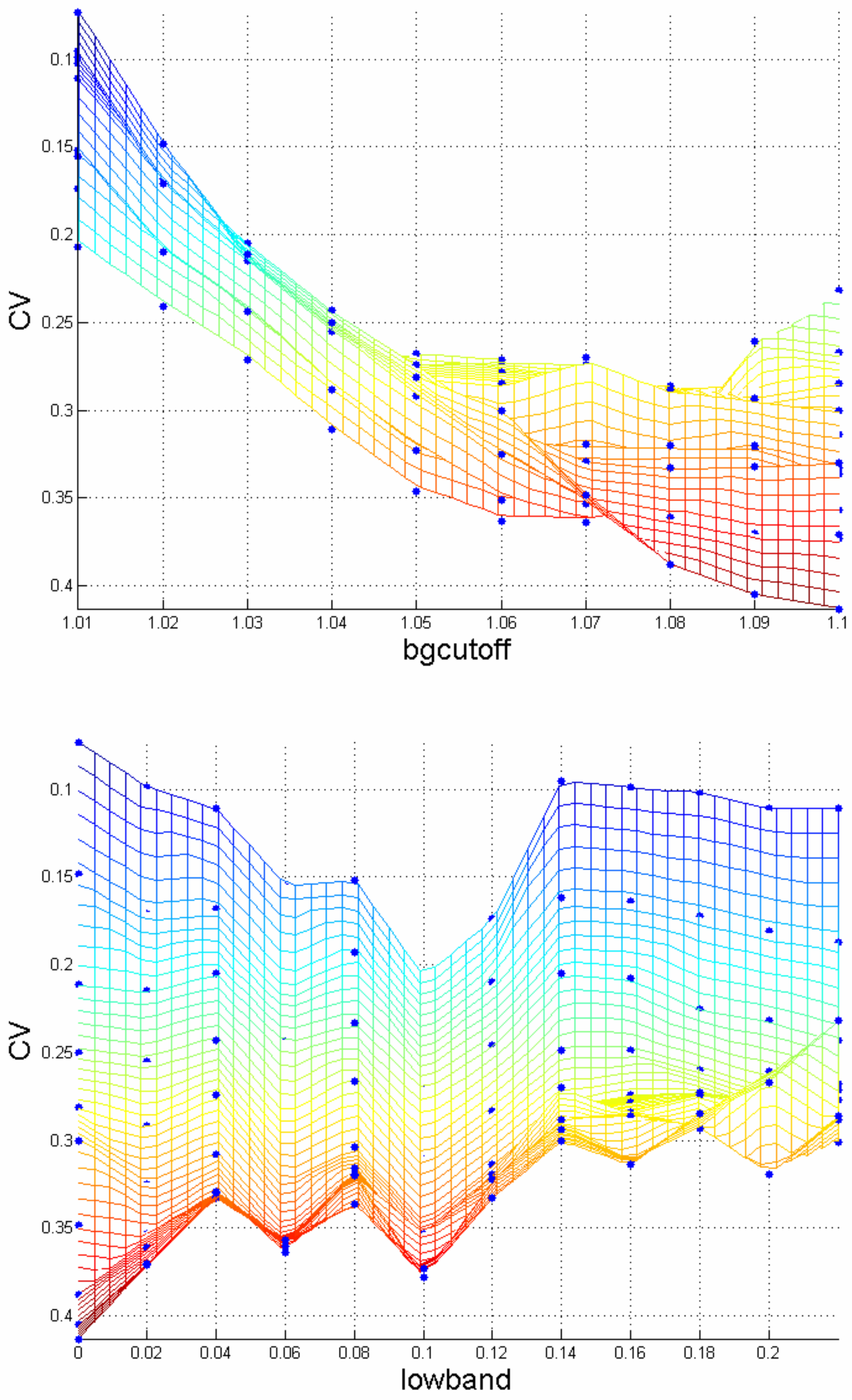

Figure 35: Coefficients of variation (CV) resulting from counting four membranes with the same bacterial concentration, as lowband and bgcutoff were varied. This is comparable with the data in Figure 32, except that these two views were more useful than the 3D view.

Fluorescence Microscopy

To verify the bacterial counting performance of the prototype LSC, Fluorescence Microscopy was employed. The methods were very similar to those used for microsphere counts, except that bacteria did not fluoresce as brightly as microspheres, so more care had to be taken to ensure proper counting. The membrane, mounted between two coverslips with immersion oil, was taped to a glass microscope slide. A 100x microscope objective was used, which resulted in a 6179-µm^2 field of view. At least 10 fields were counted for each membrane. To calculate the cell density (cells per mm^2), the average count per field was divided by the field area. The optimal settings for the microscope are given in Appendix D. These were not used for every experiment. For example, sometimes a 5-second exposure time was used instead of 10 seconds, or the Acceptance Criteria parameter of area greater than 0.5 may have been 1.0. Careful attention was paid to insure that all of the settings were the same for each run, so that counts were consistent.

Experimental Design

The previous sections detail the optimization of the prototype LSC device. Putting the optimal methods together, an experiment was designed to test the performance of the LSC in bacterial counting, compared with fluorescence microscopy. *E. coli* inoculations were incubated in pre-filtered LB broth for 18 hours before being washed in PBS. The PBS solution was also pre-filtered through the 0.2-µm pore size membranes.

A wide range of *E. coli* concentrations was desired for prototype testing. Various amounts of washed *E. coli* solution were added to six samples, as described in Table 4. Each sample had a total concentration of 1 ml and a final SYTO 62 concentration of 0.5 mM. Three 0.2-ml sub-samples were filtered and mounted using the oil sandwich method. They were counted using fluorescence microscopy, with the optimal parameters described in the previous section and shown in Appendix D. When counting, the MCID software gave two values for each frame: “counts” and “est. counts.” In this case, the est. counts values were used. After counting with microscopy, they were scanned in the prototype LSC. The settings were laser power, 10-mW; linear stage velocity, 0.0275 mm/s; rotary stage velocity, 90 degrees/s; inner radius, 1 mm; outer radius, 6.5 mm. This gave 50 tracks, covering most of the surface of the membrane.

Table 4: Volumes of water, *E. coli*, and stain used to make samples of various bacterial concentrations

Sample #	Water (ml)	*E. coli* (ml)	1 mM SYTO 62 (ml)
1	0.250	0.250	0.5
2	0.375	0.125	0.5
3	0.437	0.063	0.5
4	0.469	0.031	0.5
5	0.487	0.016	0.5
6	0.500	0.000	0.5

Results and Discussion

Fluorescence microscope micrographs of one field from each volume sampled are shown in Figure 36. Microscope counting results are given in Figure 37. It appeared that the microscope was successful in counting bacteria over the entire range of *E. coli* concentrations.

LSC counting results are shown in Figures 38 and 39. The counts are reported as "counts per data point," because the true concentration in terms of cells per millimeter squared of membrane area could not be determined. The tracks were very wide compared to the size of a bacterium. It was not clear how much area was actually covered by each track, so the scan area could not be calculated. Instead, the data were reported in terms of the total number of counted peaks normalized to the number of data points collected. This could be used to create a calibration curve with microscope counts and thus derive the number of cells counted by the prototype. The difference between the data in the two figures was the signal processing method used. In Figure 38 the background was calculated automatically, by finding the mode of the PMT data. In Figure 39, the background was not used and the counting threshold was set to 420 mV. The importance of the background setting can be determined by looking at histograms of the PMT data, shown in Figure 40. When the background was calculated from the mode, it was clearly different for the high and low concentration scans. For low concentrations, the automatic calculation gave a background of 405 mV. The counting threshold was then calculated at 1.04 times the background (421 mV in the case of Figure 40). The automation was important because the location of the histogram peak could shift according to PMT temperature, focal distance, laser power, and perhaps other factors of which the user was not aware. However, the width of the peak stayed fairly constant, so it worked well to find the maximum point (providing the mode) and use that to determine the threshold.

For high concentration scans, the automatic calculation would yield a background of about 445 mV for the data in Figure 40, giving a counting threshold of 463. This would clearly be inappropriate, as most of the data representing bacteria would be cut off. Also, when the concentration of bacteria changed, the location of the mode would change drastically, causing an even greater error with automatic background counting. Thus, it was more appropriate for high concentration scans to set the threshold at a specific PMT voltage value, like 420 mV. This did not work well for low concentration scans because the background could change, but with high concentration scans the number of data points counted was very large, making the changes in background insignificant.

Looking again at Figure 38, when the background was calculated automatically, there was less variation in low-concentration counts. In contrast, Figure 39 shows that when the background was set at a specific value (420 mV for this run), there was less variability in high-concentration counts. Despite the counting method, however, fluorescence microscopy was superior to the prototype LSC.

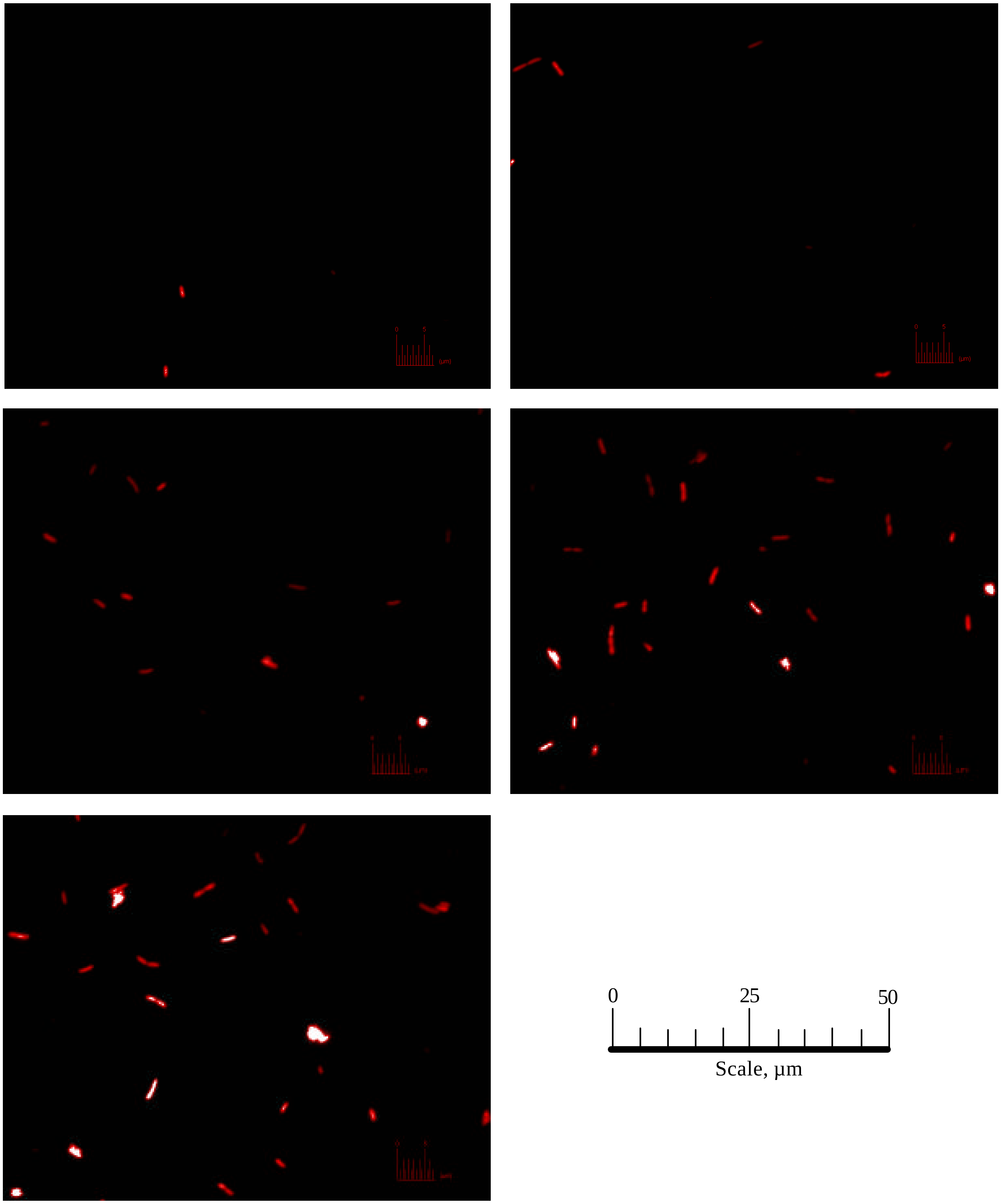

Figure 36: Fluorescence microscope micrographs of 5 concentrations of *E. coli*. These are one frame from each of the concentrations used for microscope direct counts in Figure 37. Concentrations increase from left to right, then down.

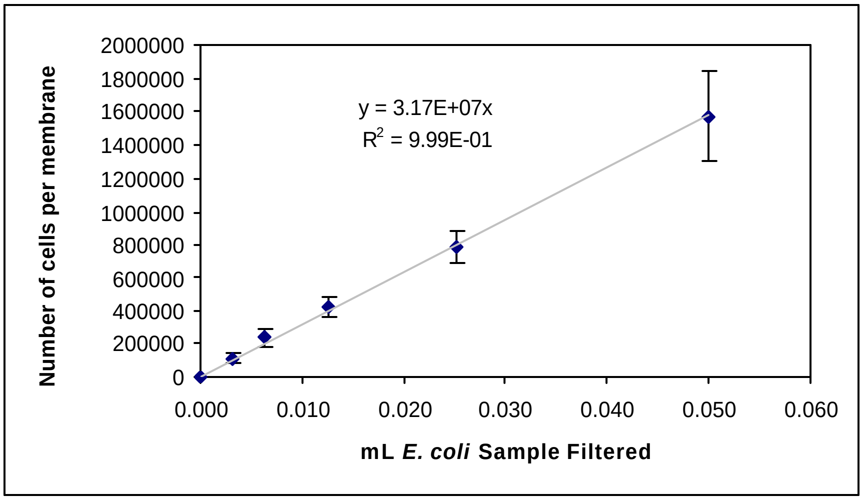

Figure 37: Fluorescence microscope counts of a range of *E. coli* samples stained with SYTO 62. Each data point represents triplicate sub-samples, with error bars showing the standard deviation.

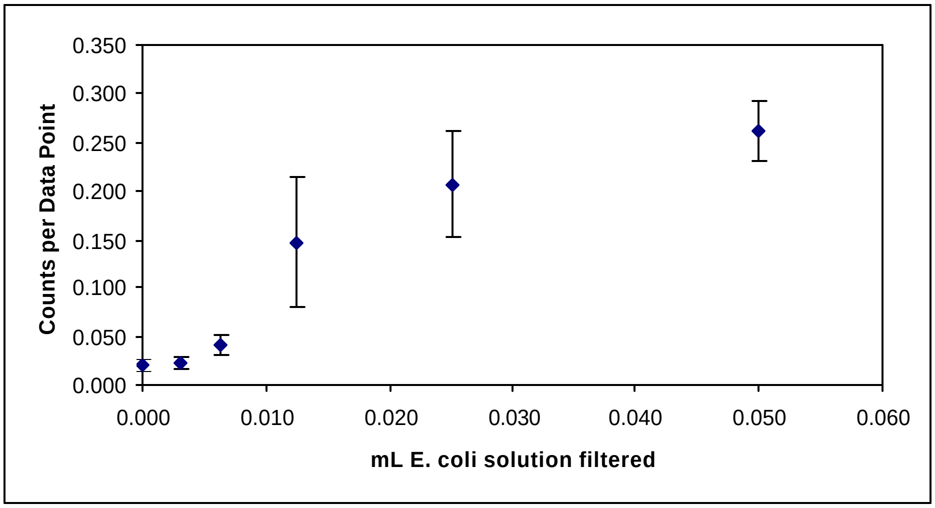

Figure 38: Prototype LSC counts for the same range of *E. coli* samples in Figure 37. These counts were done with the background calculated automatically.

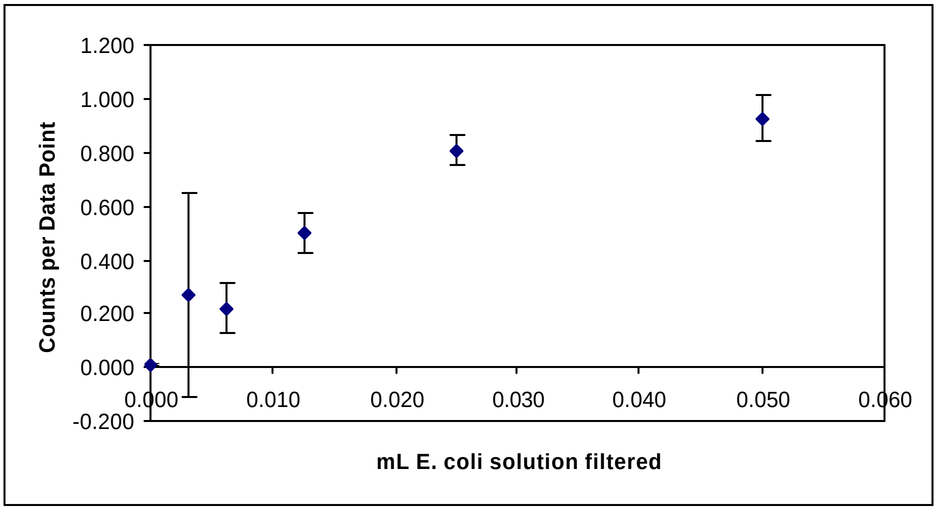

Figure 39: Prototype LSC counts for the same range of *E. coli* samples in Figure 37. These counts were done with the background ignored and the counting threshold set to 420 mV.

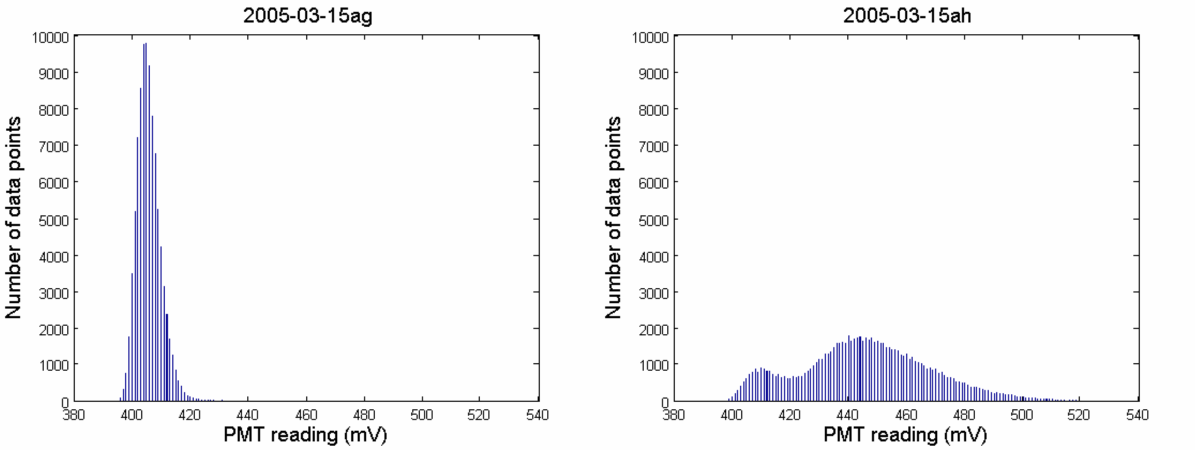

Figure 40: Histograms of PMT data from a blank filter scan (left) and a high *E. coli* concentration scan.

Additional Experiments

Bioreactor Effluent

Beside membrane integrity applications, the prototype LSC could be a valuable tool for any situation where bacteria are counted regularly. One such application is bioreactor experimentation where researchers would like to characterize the amount of biomass being removed from the system over time. A project underway in an adjacent lab during prototype LSC development was studying perchlorate reduction in activated carbon columns augmented with perchlorate-reducing bacteria. A sample of the effluent from this bioreactor was analyzed with both the prototype LSC and fluorescence microscopy. In one LSC scan, a small drop of bioreactor permeate, stained with SYTO 62, was placed on the membrane. The LSC was able to detect this drop and counted only two data points of false positives on the rest of the membrane (Figure 41).

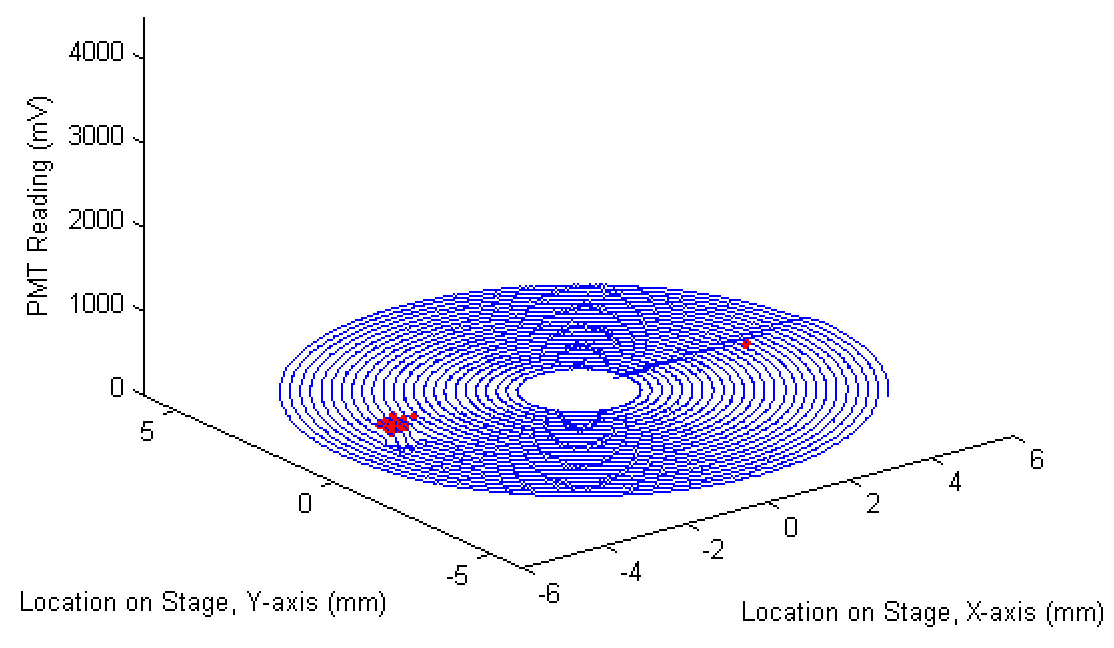

Figure 41: Data from the scan of a small drop of bioreactor effluent stained with SYTO 62. Red indicates counted points, located mainly at the site of the drop. The red points on the right were false positives (there are two points very close together).

Subsequently, a few milliliters of the stained bacterial permeate were filtered onto the entire surface of the membrane and scanned. Figure 42 shows the data. Several of the peaks reached 4500 mV, the maximum for the PMT. Thus, it was clear that effluent from the bioreactor was easily detectable with the prototype LSC.

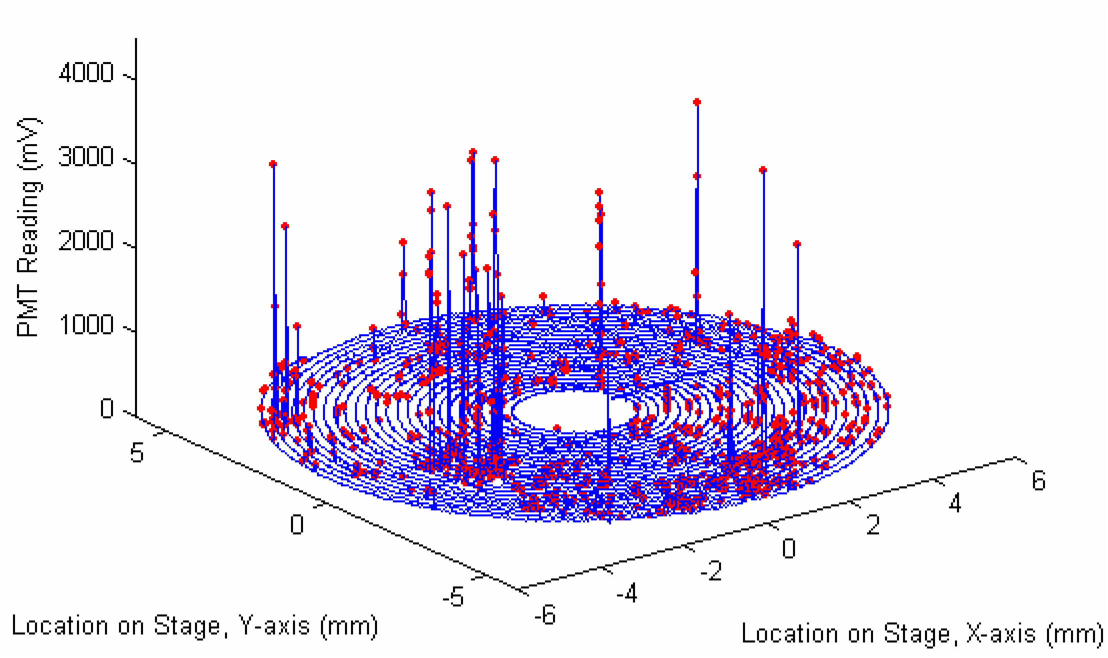

Figure 42: Data from the scan of several milliliters of bioreactor effluent filtered onto the membrane. Red indicates counted data points.

The membrane used for scanning in Figure 42 was also analyzed with fluorescence microscopy. One image from the analysis is given in Figure 43. The bacteria generally appear similar to *E. coli*, but some are more elongated. It seems that the same methods developed for *E. coli* enumeration were applicable for bioreactor effluent characterization.

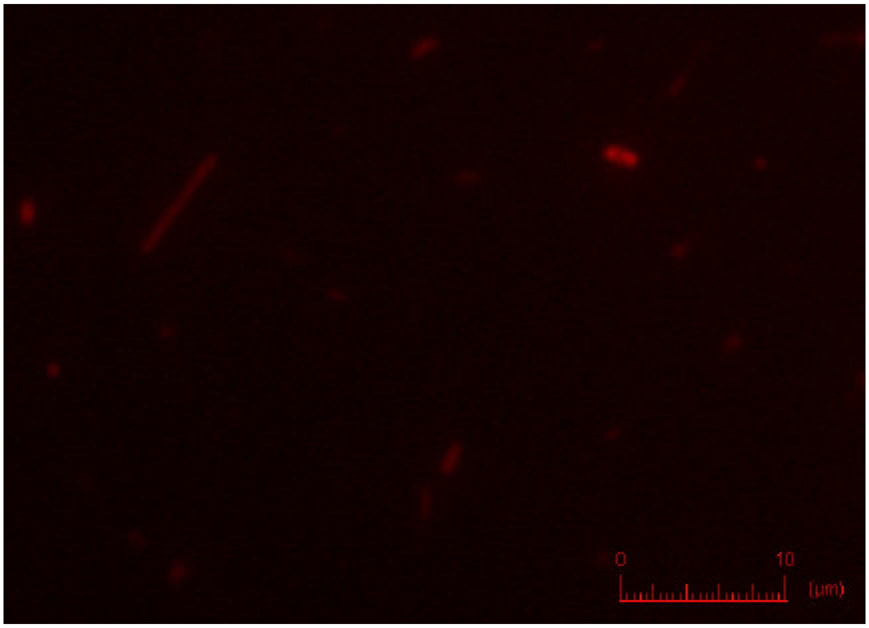

Figure 43: Fluorescence microscope micrograph of bacteria in the effluent of a perchlorate-reducing bioreactor. This was the same sample used in the scan shown in Figure 42.

Lake Water

Ultimately, the goal of this project was to test drinking water with the LSC to ensure that it was free of bacteria. To this end, a sample of Crystal Lake (Urbana, Illinois) water was tested to see if indigenous bacteria were detectable in the LSC. Based on environmental sampling protocols specified for fluorescence microscope counting (Kepner & Pratt, 1994), lake water was sampled and fixed by adding 2% (volume : volume) formalin (37% formaldehyde). Staining was done by placing 0.5 ml of 0.1-mM SYTO 62 into 0.5 ml of sample. Milli-Q water was stained with SYTO 62 in the same manner for blank samples. For scans, 0.2 ml of the stained solution (which is equivalent to 0.1 ml of lake water) was placed in 5 ml of Milli-Q water and filtered, as explained previously for *E. coli* samples. Scans were also performed as explained previously. Plots of the scan data for lake water and blank samples are shown in Figure 44. It appeared that something causing fluorescence was present in even the blank scans. A few of the blips in the data are apparent in all of the scans, indicating that something was present on the stage itself, not on the membranes. Still, it was easy to distinguish between lake water and blank samples. A bar plot of the counts is given in Figure 45, showing that lake water counts were fairly consistent and significantly higher than blank sample counts.

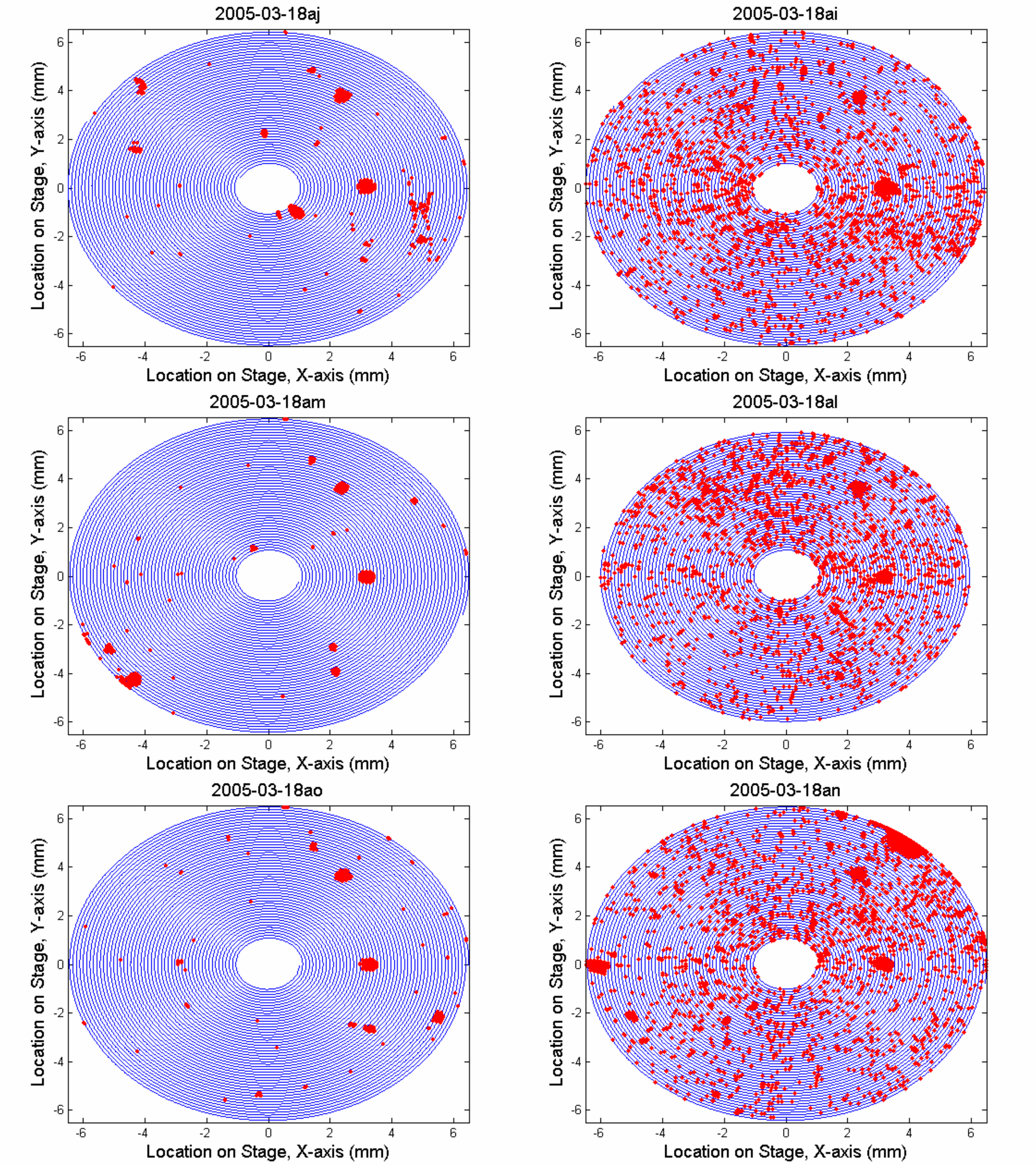
2005-03-18aj

2005-03-18ai

2005-03-18am

2005-03-18al

2005-03-18ao

2005-03-18an

Figure 44: Scan data from blanks (left column) and Crystal Lake samples (right column). Red indicates counted data points.

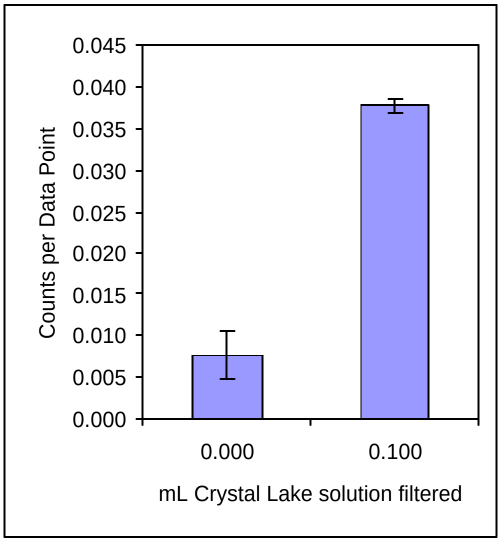

Figure 45: Counting results for blanks and Crystal Lake samples. These are counts of the scans displayed in Figure 44. Error bars show plus and minus one standard deviation. Coefficients of variation were 37% for the blank scans and 2.2% for lake water samples.

Crystal lake water samples and blanks were also counted with fluorescence microscopy. Counts of the triplicate samples averaged 615 cells per mm^2 and the CV was 36.6%. Compared to the CV of 2.2% for LSC scans, the LSC performed more consistently in counting lake water samples. This may have been due to the very low density present. About 40% of the fields counted with fluorescence microscopy had no bacteria present, and the average field had only 3.8 bacteria. For more accurate microscope counts, there should have been about 40 bacteria per field (Kepner & Pratt, 1994). The LSC covered a much larger surface of the membrane, so it could handle lower bacterial densities.

Two micrographs from the fluorescence microscope are shown in Figures 46 and 47. Figure 46 displays bacteria present in the water. Figure 47 shows two larger particles present that were likely not bacteria. These may have been algae or other particles present in the lake water, for which SYTO 62 had an affinity. Many fields of view had similar particles present, and they were almost as ubiquitous as bacteria. Because these particles were so bright compared to bacteria, it is probably these that were counted by the LSC instead of bacteria. Thus, the LSC may not have given a true count of bacteria present, but a count of any particles that could be stained by SYTO 62. It was the same for fluorescence microscopy. It should be noted that blank samples did not have these particles, and all microscope counts of blank samples were zero. Thus, the particles were derived from lake water, not from the laboratory.

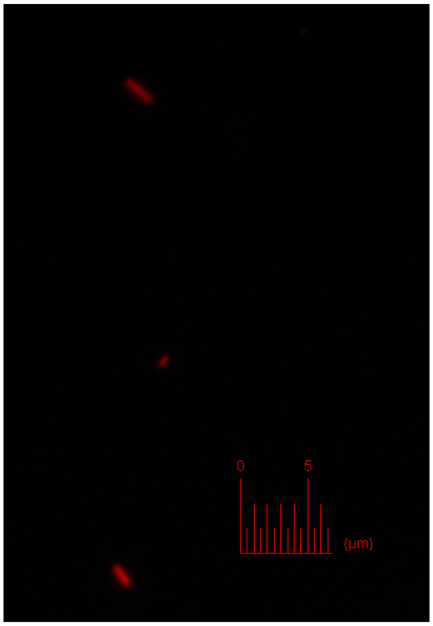

Figure 46: Fluorescence microscope micrograph of Crystal Lake water stained with SYTO 62 showing bacteria.

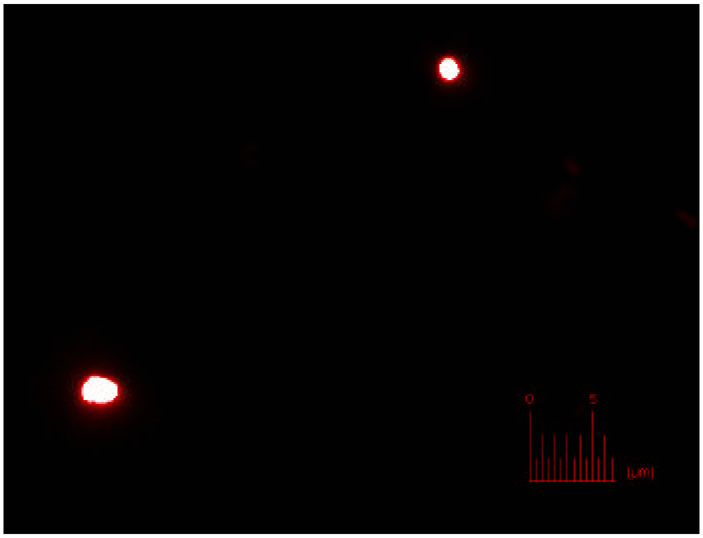

Figure 47: Fluorescence microscope micrograph of Crystal Lake water stained with SYTO 62, showing large, bright particles.

Conclusions and Future Work

The prototype LSC device was effective in counting both microspheres and bacteria. It performed better for microspheres, which fluoresced more brightly than bacteria. This could have been because the microspheres, being 2 µm in diameter, were larger than bacteria. It could also have been that the excitation and emission spectra for SYTO 62 were not optimal for the prototype. The prototype components were selected so that the cutoff frequency of both the dichroic mirror and the emission filter were at 665 nm, exactly between the excitation and emission peaks for SYTO 62 (Figure 48). This also allowed for the laser light to fall at 80% of the peak excitation. Duke microspheres were selected based principally on the emission peak. Notice in Figure 48 that the entire Duke emission peak lay above 665 nm. This could have been the reason Duke microspheres were more easily detected than SYTO 62. Even though the laser light frequency (635 nm) was only at 35% of the Duke excitation peak, the microspheres were excited sufficiently. The more important aspect to consider was the emission peak. This could also be the reason Duke microspheres were easier to detect than Molecular Probes microspheres. Future experiments should use nucleic acid stains with excitation and emission spectra resembling those of the Duke microspheres.

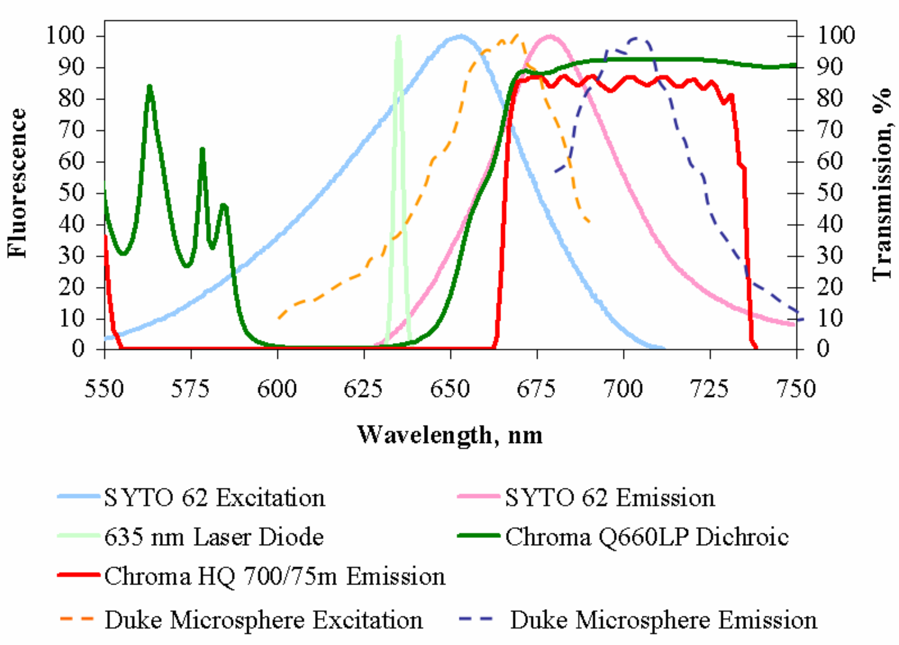

Figure 48: Spectra of prototype LSC components, including Duke microsephere spectra. (Adapted from Lee, 2003).

As for the effectiveness of the prototype as a membrane integrity monitoring device, it has great promise. It not only detected bacteria, but other particles that were in the water. With only 0.1 ml of lake water, the counts were well above blanks. Permeate water in a drinking water treatment plant would be much more dilute than lake water, but one can envision filtering several milliliters of permeate onto the membrane before staining, which would concentrate the particles, making them easy to detect. The project should move to experiments with a pilot membrane system to evaluate this possibility.

It is good that many particles in lake water can be detected, but this means that many particles in the laboratory can be detected, as well. One disadvantage of the prototype LSC is the high degree of false positives caused by particle contamination. False positives increased the lower detection limit of the LSC, decreasing its ability to demonstrate high log removal of particles. For example, in the *E. coli* experiment of Figure 39, the highest concentration detected was 0.93 counts per data point, while the blank samples were 0.01. This was a log removal of 1.97. For the LSC to prove itself, it should demonstrate 4 or 5 log removal. To do this, false positives should be decreased.

One prototype modification that might help remove false positives would be the addition of an excitation filter. This would decrease laser light emitted above 665 nm, which may have been adding to the increased background by reflecting off of the membrane surface. This light could also have been reflecting off of contaminant particles to cause false positives. In fluorescence microscopy, there were very few false positives, because the illumination light was carefully restricted by excitation filters.

Another modification that may help would be the addition of a second emission filter. The dichroic beamsplitter and one emission filter were expected to filter out the very intense laser light reflecting off the membrane surface and allow the much weaker fluoresced light to pass. The high background levels, which increased with stronger laser power, indicated that not all of the laser light was filtered out. An additional emission filter might remove more of the laser light.

It was found that digital filtration was not totally successful in removing oscillations in scan data. Perhaps a closer look at the algorithms and methods used would reveal better signal processing protocols that would achieve the desired results. Another option would be to change the rotary stage. The prototype was very sensitive to focus, as shown in the background variation in Figure 23. Currently, the stage may not be on a perfectly flat plane. This could be the reason for oscillation in scan data. Perhaps the rotational stage should be carefully aligned, or replaced with something that spins more evenly to insure that the entire membrane rotates on the same plane.

Laser scanning cytometry has proven effective in enumerating microspheres and bacteria and shows promise as a membrane integrity verification device. Continued development is possible as with experiments explained above. This technology could be made available for drinking water plant operators to indirectly verify membrane integrity and keep their systems running continuously. They could also directly verify the quality of their water, ensuring that it is bacteria free.

Appendices

Appendix A: Procedure for Reviving and Storing Freeze-Dried *E. coli* cultures

Summary: ATTC freeze-dried cultures are shipped in glass vials that include a dried pellet of microorganisms. Dessicant in the vial helps control moisture and a cotton plug keeps the pellet in place. In order to use the microorganisms in the laboratory, they must be revived. Once rehydrated, the microorganisms should be stored on agar slants until they are need to make laboratory stock solutions.

This procedure outlines methods for opening the ATCC vial, reviving the microorganisms, storing them on agar slants, and making usable laboratory stock solution. Careful use of aseptic techniques is required to maintain pureness of culture.

Materials

E. coli freeze dried culture (MG1655)
Bacto tryptone (Difco)
Yeast extract (Difco)
NaCl
NaOH
Agar granules (Difco)
PBS (recipe is included following this method)
Pasteur pipette
Tweezers
Test tube rack
Sterile (or disposable) 10 ml pipettes and bulb
Bunsen burner
Centrifuge microvials
Microcentrifuge
15 ml centrifuge tubes (Corning)
1 ul inoculating loop
Autoclave
Vortex

Methods

1. Prepare phosphate buffer solutions (and autoclave) before opening culture vial.

2. Prepare agar slants before opening culture vial.
    - 2.1. Make Luria Berari media agar (ATCC 1065LB).
    - 2.2. Fill slant vials.
        - 2.2.1. Place plastic, capped centrifuge tubes in rack.
        - 2.2.2. Pipette about 5 ml of hot agar into each centrifuge tube and cap tightly.
        - 2.2.3. Tilt entire rack to approximately 45 degree angle while agar is still hot.
        - 2.2.4. Allow agar to harden.

3. Revive freeze-dried culture.
    - 3.1. Open the vial.
        - 3.1.1. Heat glass tip of vial in open flame.
        - 3.1.2. Douse tip in cold water to crack glass.
        - 3.1.3. Break off glass tip with sterile tweezers.
        - 3.1.4. Tip the glass vial to remove the outer vial.

        - 3.1.5. Remove cotton plug with sterile tweezers.
    - 3.2. Add growth media.
        - 3.2.1. Use Pasteur pipette to add 0.3 – 0.4 ml liquid media to vial.
        - 3.2.2. Mix well.
        - 3.2.3. Transfer total volume to sterile centrifuge tube with 5-6 ml broth media.

4. Inoculate slants.
    - 4.1. Spread solution on surface of agar slants, using 1 ul inoculation loop.
    - 4.2. Incubate slants at 37C until visible growth is observed, about 24-48 hours.
    - 4.3. Store slants for up to several months for later use at 4C.

5. Create stock solutions from stored slants.
    - 5.1. Create and incubate broth.
        - 5.1.1. Fill sterile vial with about 10 ml liquid media.
        - 5.1.2. Remove sample of visible growth from slant with sterile inoculating loop.
        - 5.1.3. Dip loop into liquid media and move vigorously to dislodge microorganisms.
        - 5.1.4. Vortex sealed vial to disperse microorganisms.
        - 5.1.5. Incubate entire vial at 37C for 20 hours.
    - 5.2. Concentrate microorganisms out of broth suspension.
        - 5.2.1. Pipet 1.5 mL of suspension into each of 6 centrifuge microvials.
        - 5.2.2. Centrifuge vials at 13.2 rpm for 3 minutes.
        - 5.2.3. Decant supernatant with vacuum.
        - 5.2.4. Add 1 ml of autoclaved PBS to each vial.
        - 5.2.5. Resuspend pellet in sealed vial using a vortex.
        - 5.2.6. Repeat steps 5.2.2 – 5.2.5 two additional times.
        - 5.2.7. Combine microvial contents into 15 ml centrifuge vial.

Appendix B: Labview Scanning Programs

Stage Scanning Program

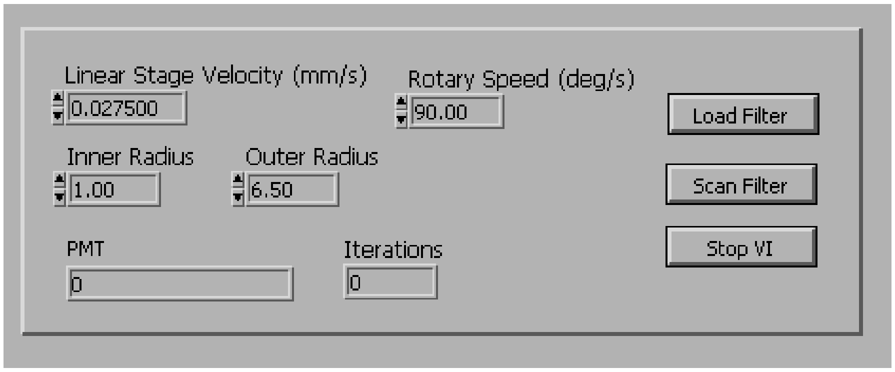

Linear Stage Velocity (mm/s): 0.027500

Rotary Speed (deg/s): 90.00

Inner Radius: 1.00

Outer Radius: 6.50

PMT: 0

Iterations: 0

Load Filter
Scan Filter
Stop VI

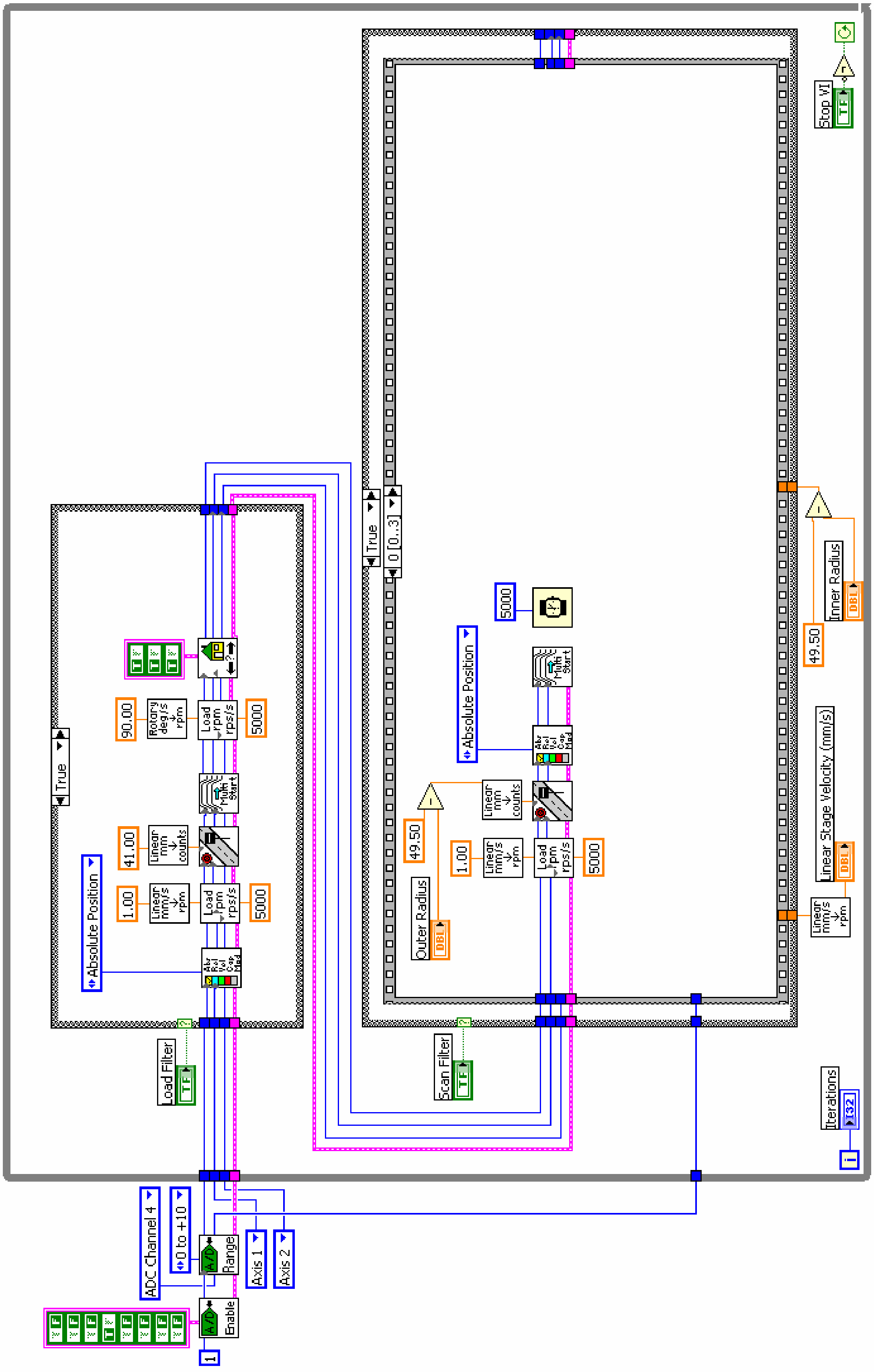

ADC Channel 4
0 to +10
Enable
Range
Axis 1
Axis 2
1
Load Filter
True
Absolute Position
1.00
Linear mm/s → rpm
Load rpm rps/s
5000
41.00
Linear mm → counts
Multi Start
90.00
Rotary deg/s → rpm
Load rpm rps/s
5000
Scan Filter
True
0 [0..3]
Outer Radius
DBL
49.50
1.00
Linear mm/s → rpm
Load rpm rps/s
5000
Linear mm → counts
Absolute Position
Multi Start
5000
Linear Stage Velocity (mm/s)
DBL
Linear mm/s → rpm
49.50
Inner Radius
DBL
Stop VI
TF
Iterations
I32
i

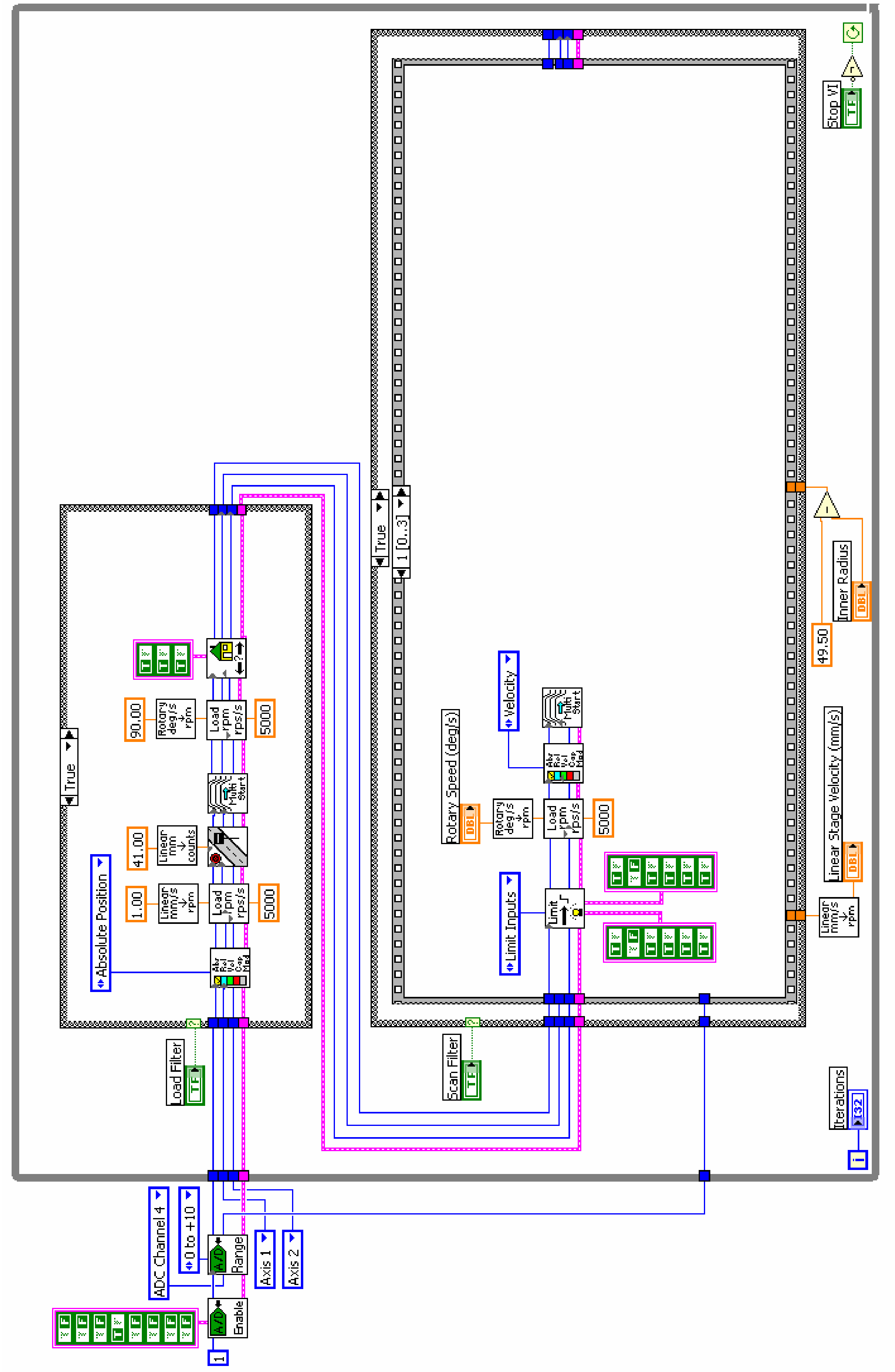
1
Enable
ADC Channel 4
0 to +10
Range
Axis 1
Axis 2
Load Filter
Absolute Position
True
1.00
Linear mm/s → rpm
Load rpm rps/s
5000
41.00
Linear mm → counts
Multi Start
90.00
Rotary deg/s → rpm
Load rpm rps/s
5000
Scan Filter
Limit Inputs
Limit
Rotary Speed (deg/s)
DBL
Rotary deg/s → rpm
Load rpm rps/s
5000
Velocity
Multi Start
True
1 [0..3]
Iterations
I32
i
Linear Stage Velocity (mm/s)
DBL
Linear mm/s → rpm
49.50
Inner Radius
DBL
Stop VI
TF

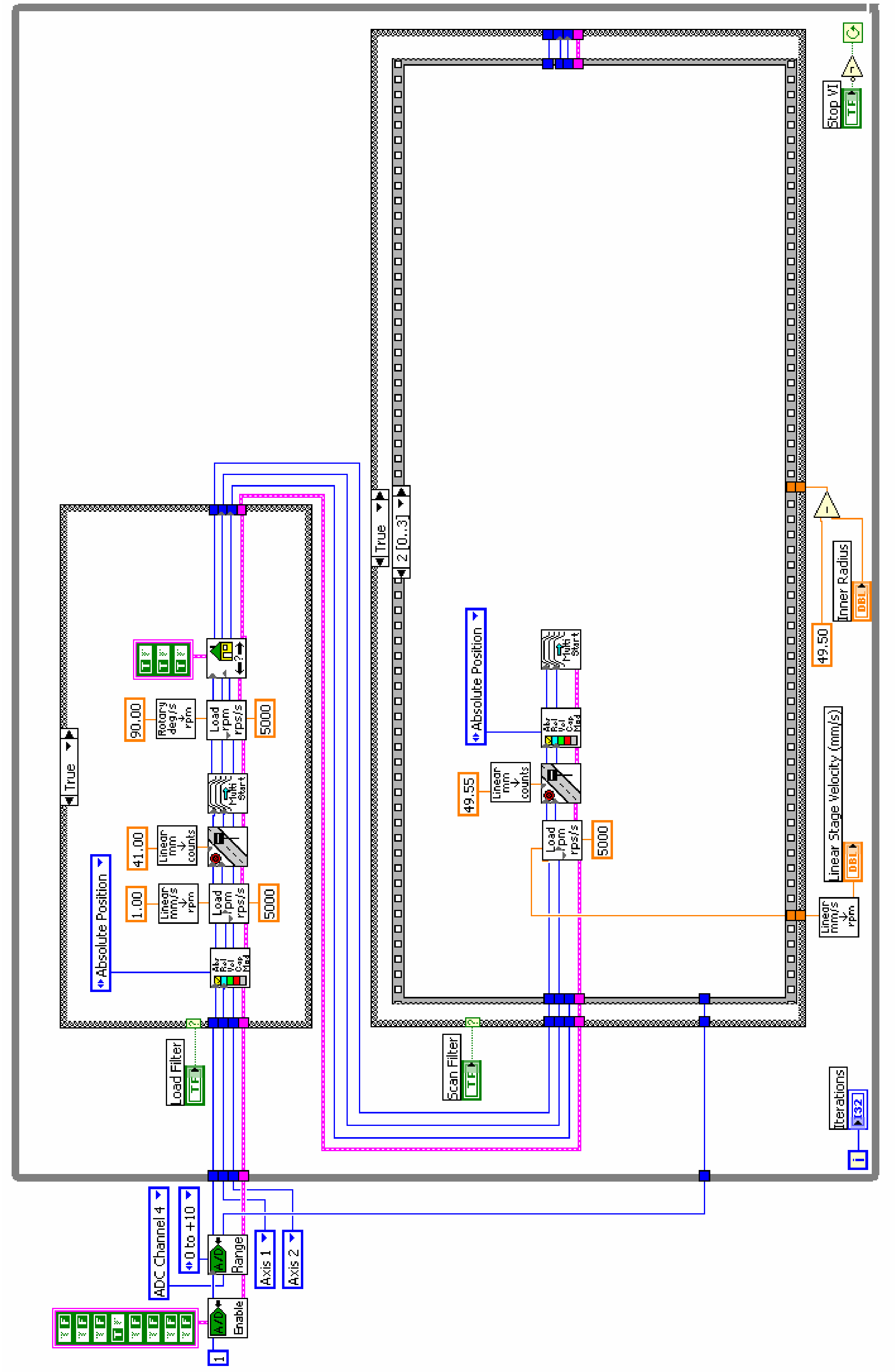
Stop VI
TF
Inner Radius
DBL
49.50
Linear Stage Velocity (mm/s)
DBL
Linear mm/s → rpm
Iterations
I32
i
True
2 [0..3]
Absolute Position
49.55
Linear mm → counts
Load rpm rps/s
5000
Multi Start
Scan Filter
TF
True
Absolute Position
1.00
Linear mm/s → rpm
Load rpm rps/s
5000
41.00
Linear mm → counts
Multi Start
90.00
Rotary deg/s → rpm
Load rpm rps/s
5000
Load Filter
TF
ADC Channel 4
0 to +10
A/D Range
A/D Enable
1
Axis 1
Axis 2

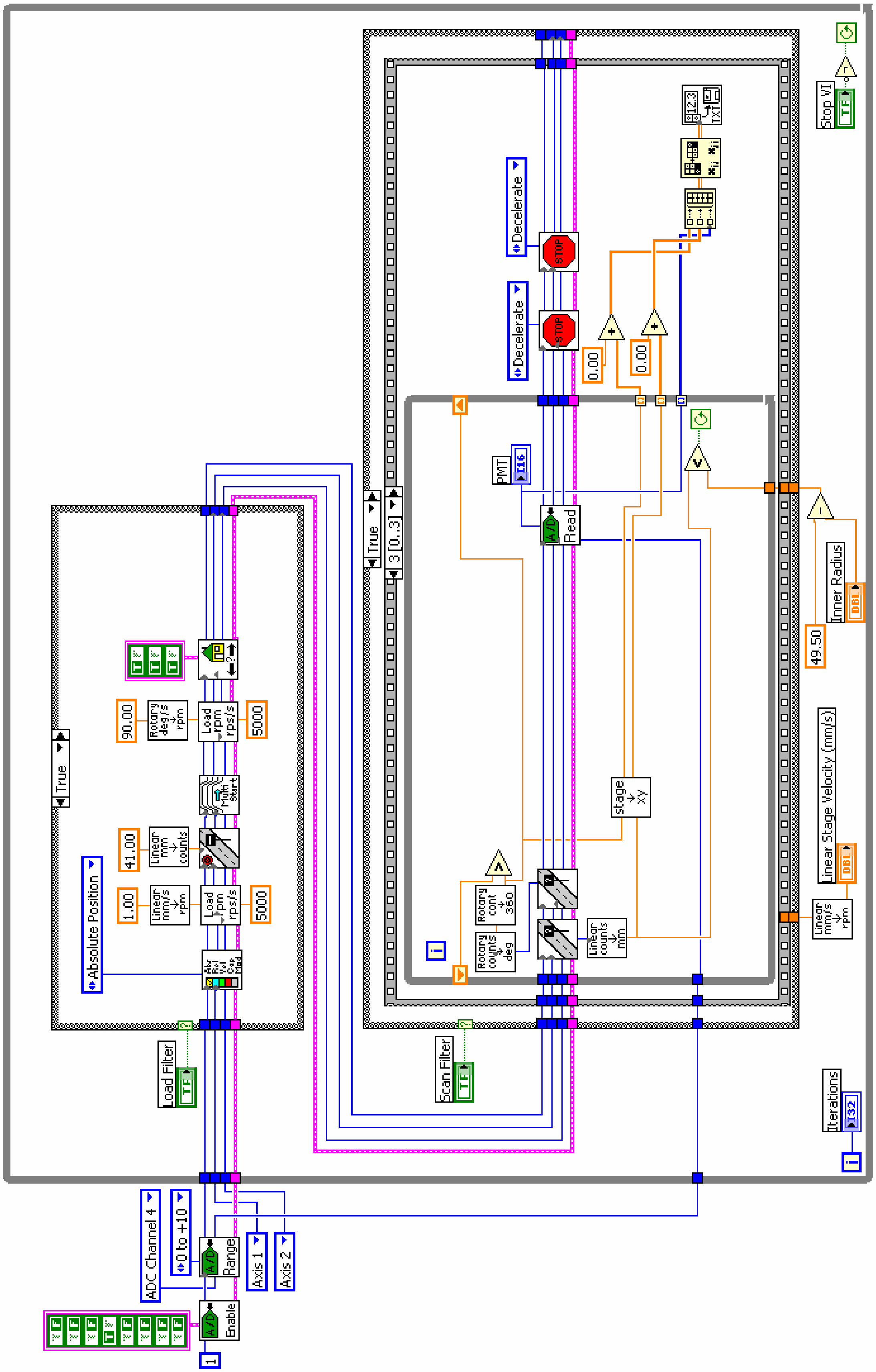
Absolute Position
True
1.00
Linear mm/s → rpm
Load rpm rps/s
5000
41.00
Linear mm → counts
Multi Start
90.00
Rotary deg/s → rpm
Load rpm rps/s
5000
Load Filter
TF
ADC Channel 4
0 to +10
A/D Range
A/D Enable
1
Axis 1
Axis 2
Scan Filter
TF
True
3 [0..3]
Decelerate
Decelerate
STOP
STOP
0.00
0.00
PMT
I16
A/D Read
stage → xy
Rotary counts → deg
Rotary cont → 360
Linear counts → mm
i
Linear mm/s → rpm
Linear Stage Velocity (mm/s)
DBL
49.50
Inner Radius
DBL
Stop VI
TF
12.3 TXT
Iterations
I32
i

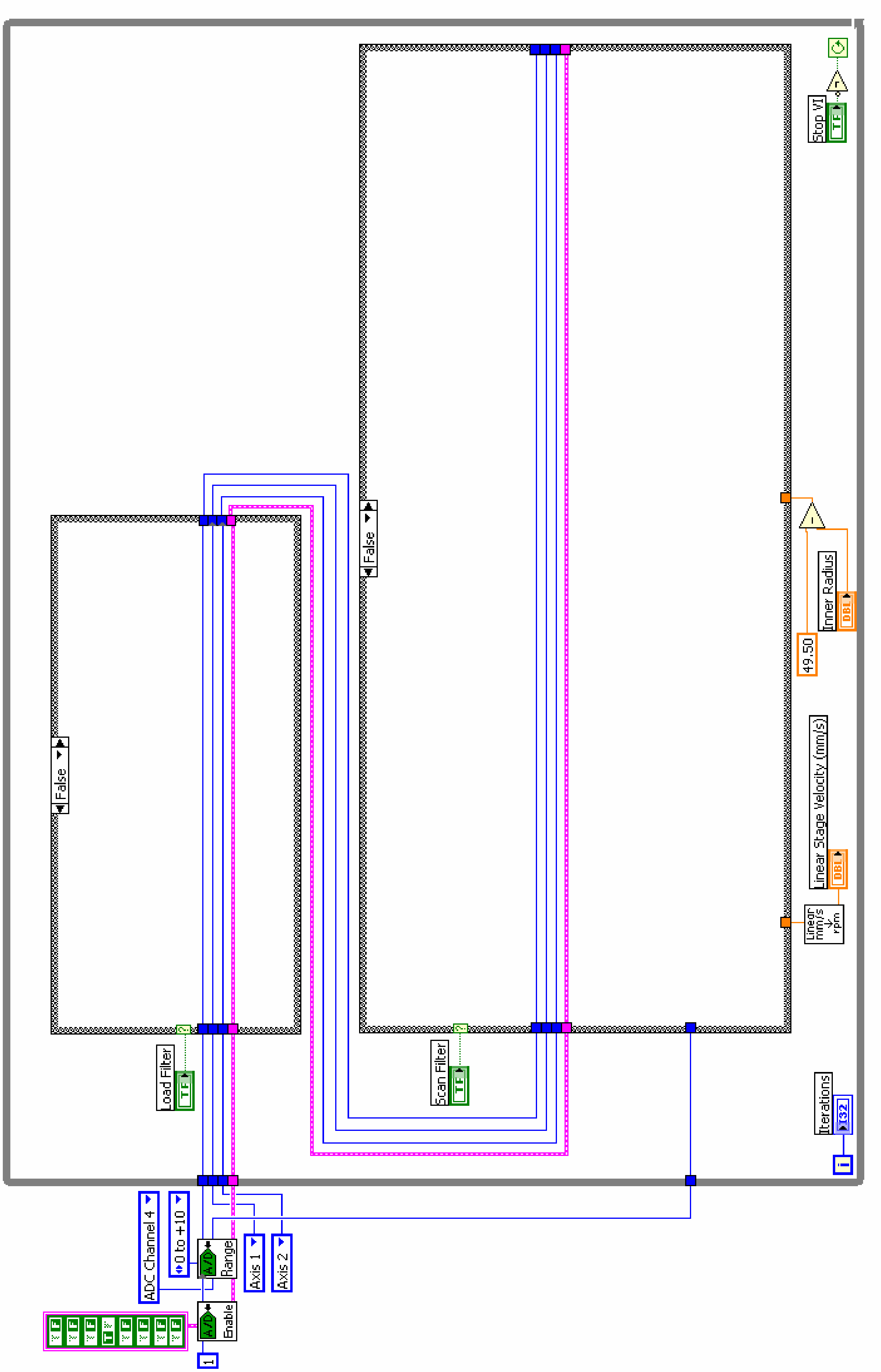

1
A/D
Enable
ADC Channel 4
0 to +10
Range
Axis 1
Axis 2
Load Filter
TF
False
Scan Filter
TF
False
Linear mm/s → rpm
Linear Stage Velocity (mm/s)
DBL
49.50
Inner Radius
DBL
Stop VI
TF
Iterations
I32
i

High Resolution Scanning Program

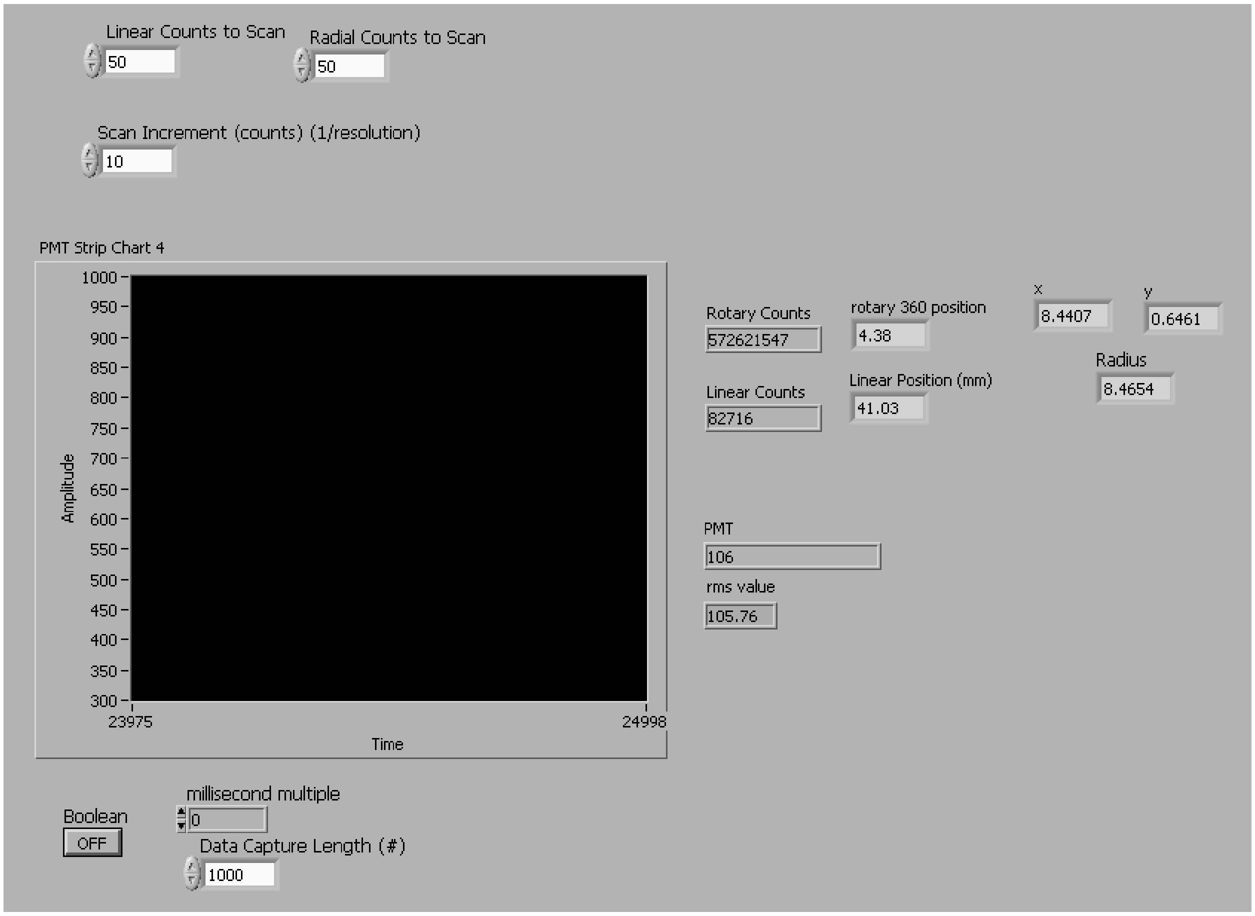
PMT Strip Chart 4
1000
950
900
850
800
750
700
650
600
550
500
450
400
350
300
Amplitude
23975
24998
Time
OFF

Linear Counts to Scan 50

Radial Counts to Scan 50

Scan Increment (counts) (1/resolution) 10

Rotary Counts 572621547

rotary 360 position 4.38

x 8.4407

y 0.6461

Linear Counts 82716

Linear Position (mm) 41.03

Radius 8.4654

PMT 106

rms value 105.76

Boolean OFF

millisecond multiple 0

Data Capture Length (#) 1000

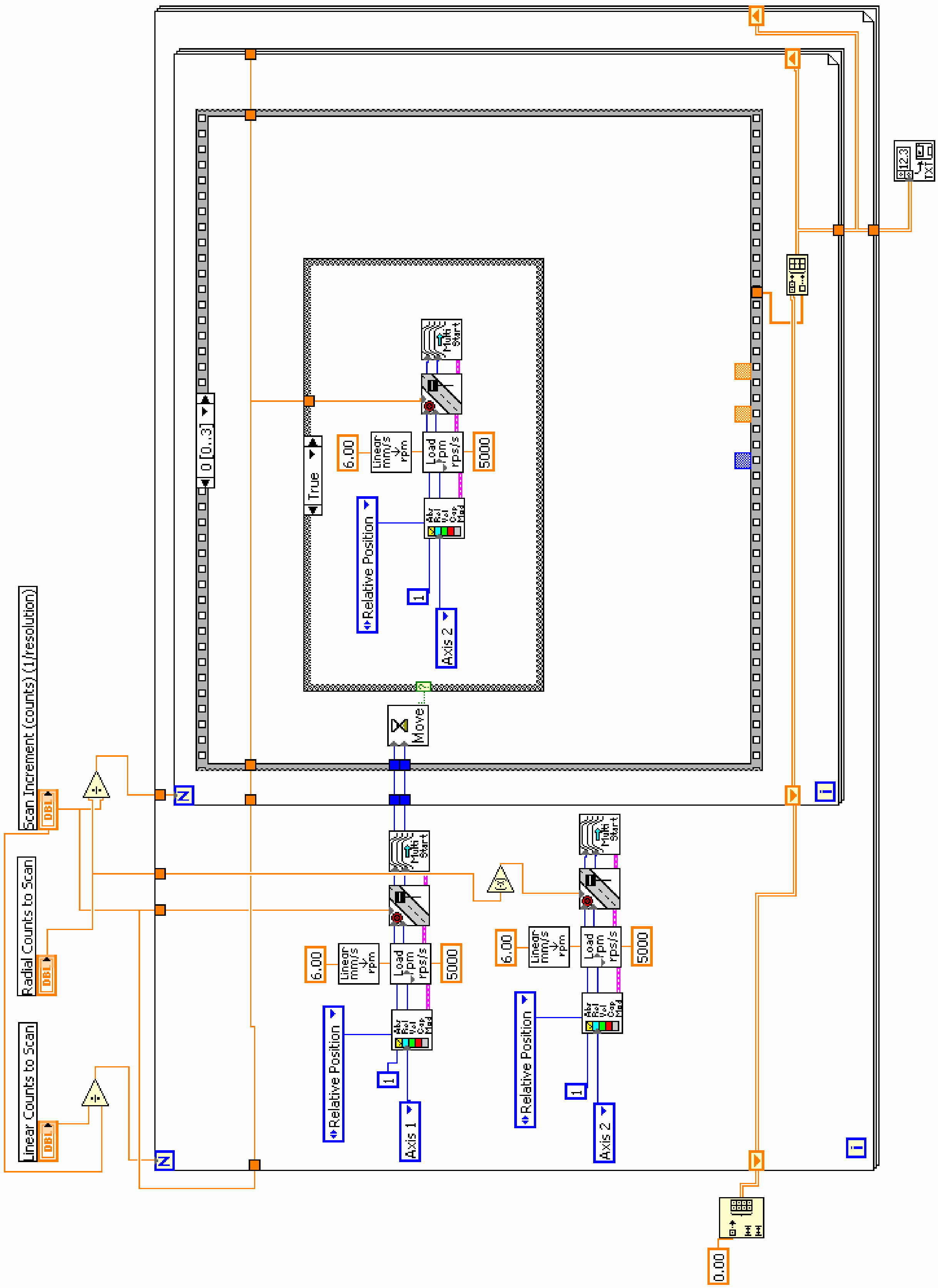
Linear Counts to Scan
Radial Counts to Scan
Scan Increment (counts) (1/resolution)
DBL
DBL
DBL
N
N
i
i
0 [0..3]
True
Relative Position
Relative Position
Relative Position
Axis 1
Axis 2
Axis 2
1
1
1
6.00
6.00
6.00
Linear mm/s → rpm
Linear mm/s → rpm
Linear mm/s → rpm
Load rpm rps/s
Load rpm rps/s
Load rpm rps/s
5000
5000
5000
Multi Start
Multi Start
Multi Start
Move
0.00
12.3

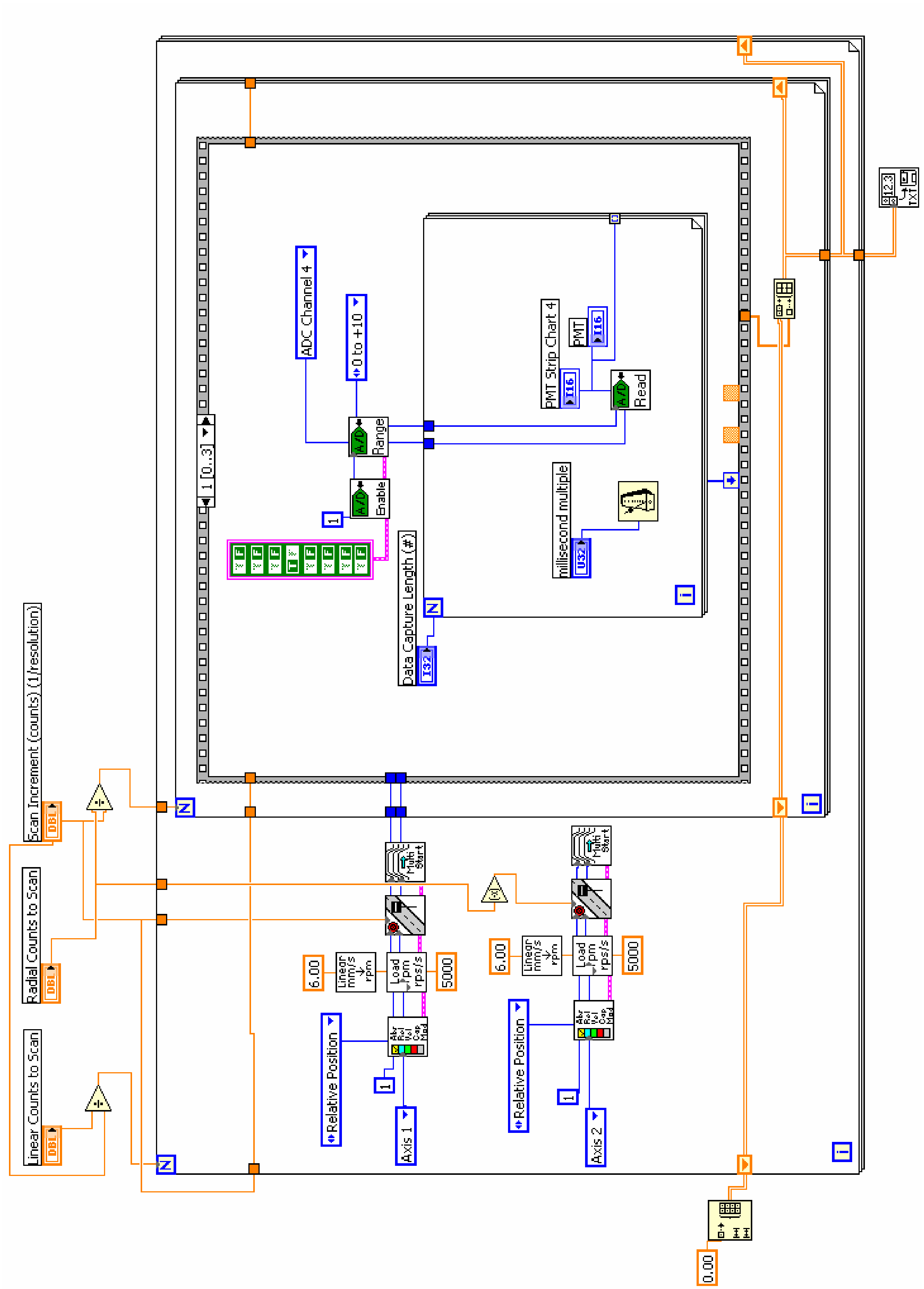
Scan Increment (counts) (1/resolution)
Radial Counts to Scan
Linear Counts to Scan
DBL
DBL
DBL
N
N
1 [0..3]
ADC Channel 4
0 to +10
A/D Range
A/D Enable
1
Data Capture Length (#)
I32
N
PMT Strip Chart 4
I16
PMT
I16
A/D Read
millisecond multiple
U32
i
i
i
Multi Start
Linear mm/s → rpm
Load rpm rps/s
6.00
5000
Relative Position
1
Axis 1
Multi Start
Linear mm/s → rpm
Load rpm rps/s
6.00
5000
Relative Position
1
Axis 2
0.00
123 → TXT

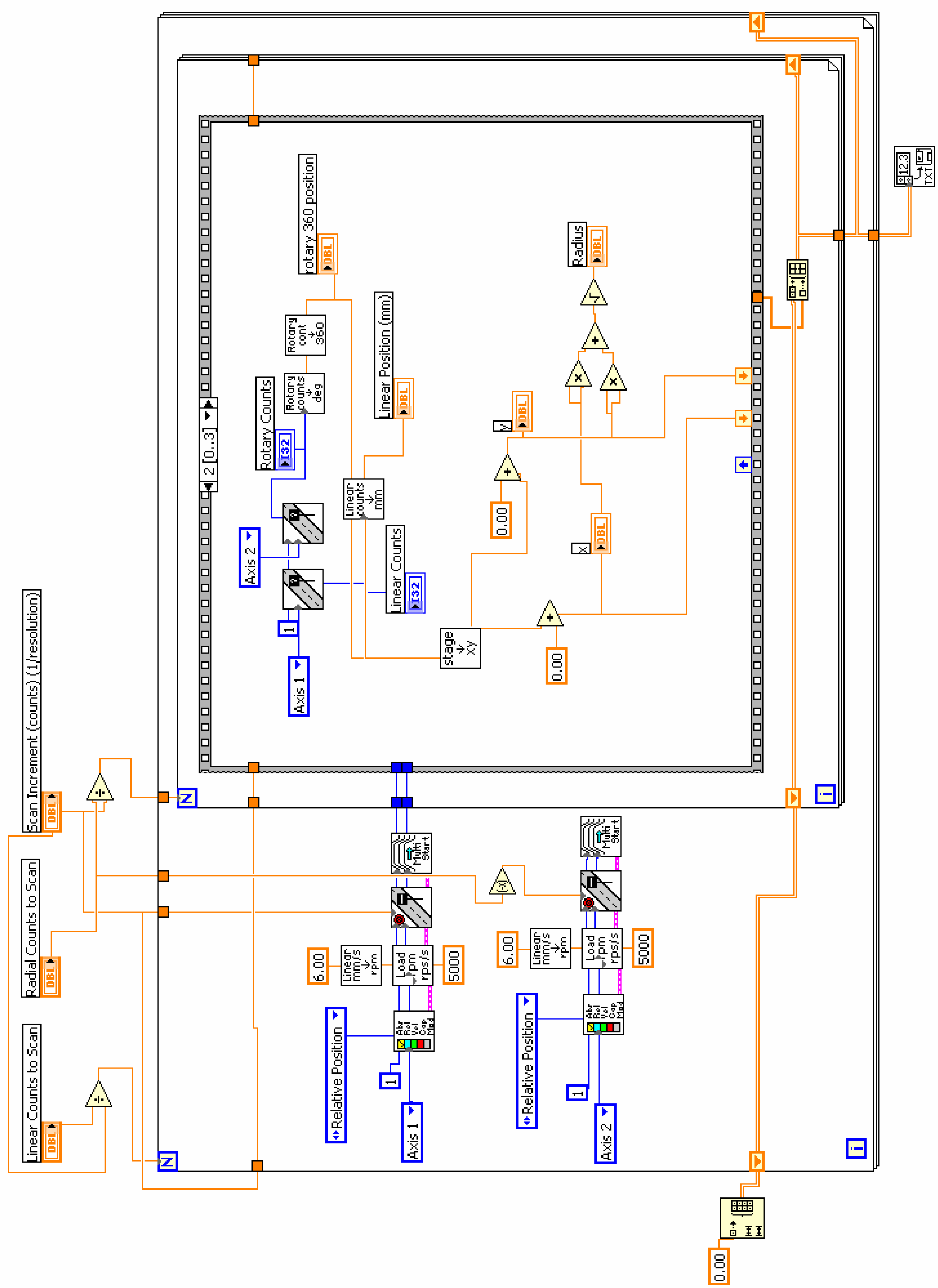
Linear Counts to Scan
DBL
Radial Counts to Scan
DBL
Scan Increment (counts) (1/resolution)
DBL
N
N
2 [0..3]
rotary 360 position
DBL
Rotary Counts
I32
Rotary counts → deg
Rotary cont → 360
Linear Position (mm)
DBL
Linear counts → mm
Linear Counts
I32
Axis 2
Axis 1
1
stage → xy
0.00
0.00
y
DBL
x
DBL
Radius
DBL
Relative Position
Axis 1
1
6.00
Linear mm/s → rpm
Load rpm rps/s
5000
Multi Start
Relative Position
Axis 2
1
6.00
Linear mm/s → rpm
Load rpm rps/s
5000
Multi Start
i
i
0.00
12.3
TXT

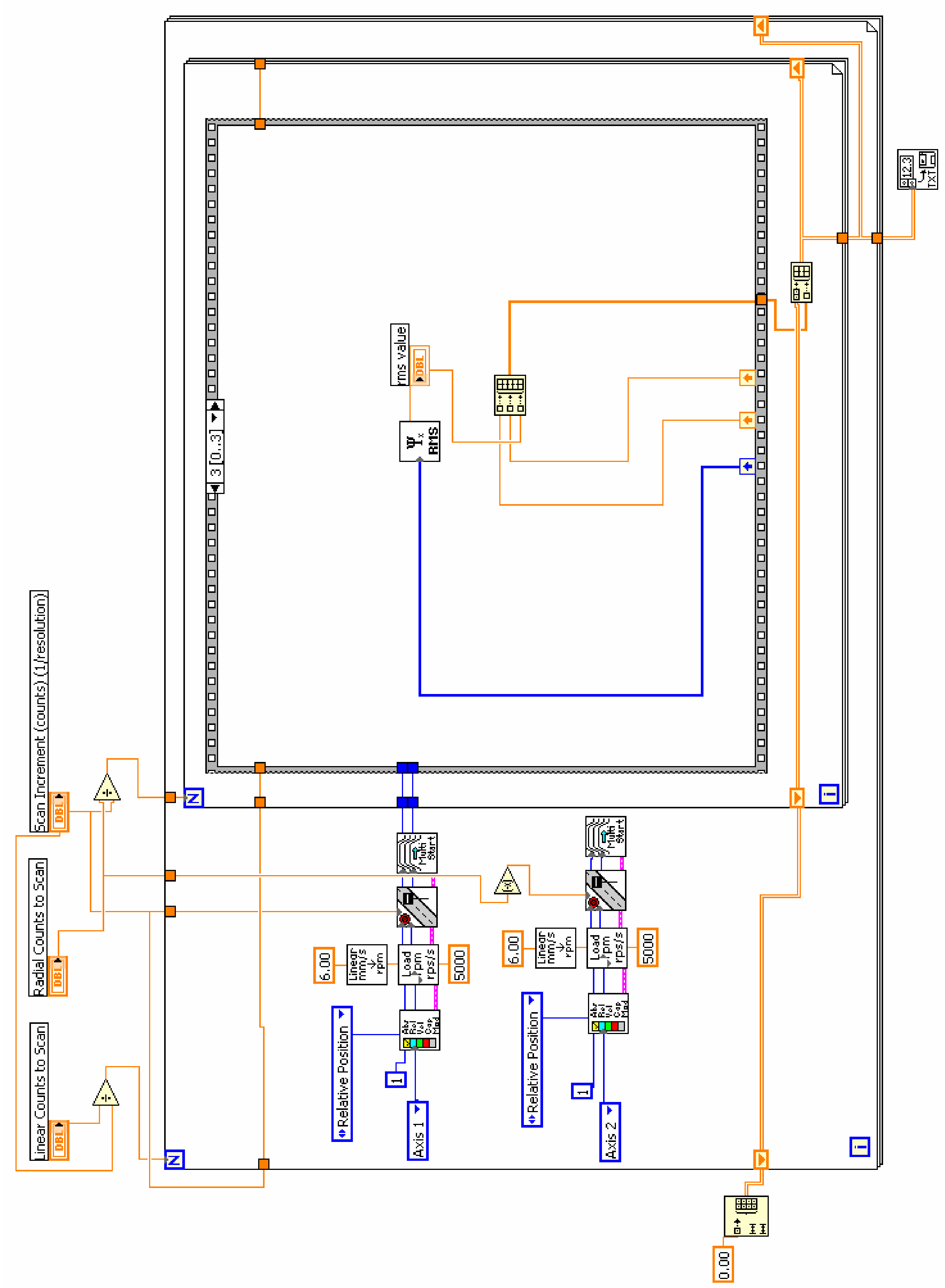
Scan Increment (counts) (1/resolution)
DBL
Radial Counts to Scan
DBL
Linear Counts to Scan
DBL
N
N
3 [0..3]
rms value
DBL
RMS
i
i
Relative Position
Relative Position
Axis 1
Axis 2
1
1
6.00
6.00
Linear mm/s → rpm
Linear mm/s → rpm
Load rpm rps/s
Load rpm rps/s
5000
5000
Multi Start
Multi Start
0.00
12.3

Positioning Program

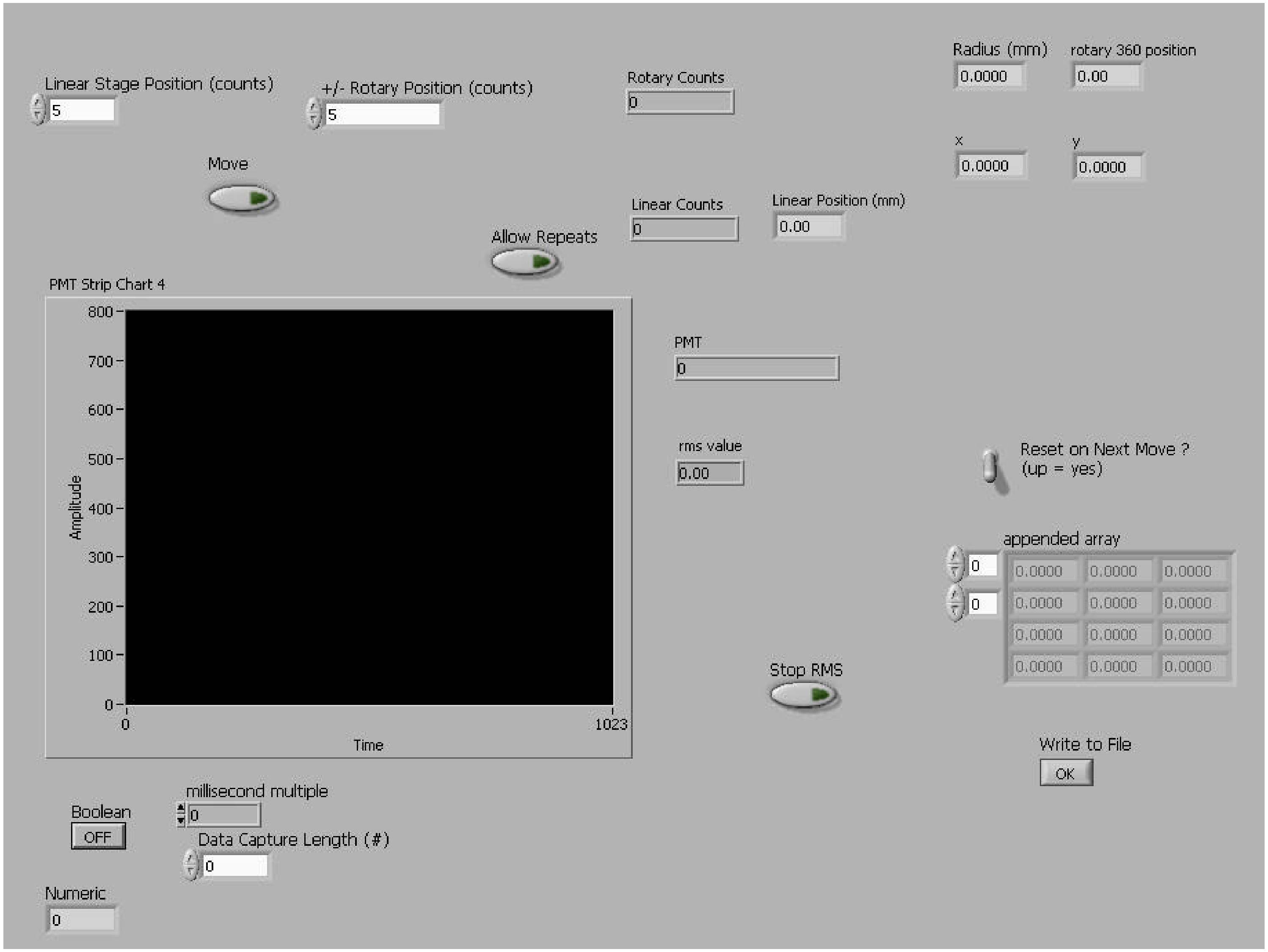

Linear Stage Position (counts): 5

+/- Rotary Position (counts): 5

Rotary Counts: 0

Radius (mm): 0.0000

rotary 360 position: 0.00

x: 0.0000

y: 0.0000

Linear Counts: 0

Linear Position (mm): 0.00

PMT: 0

rms value: 0.00

Reset on Next Move ? (up = yes)

appended array: 0, 0

0.0000	0.0000	0.0000
0.0000	0.0000	0.0000
0.0000	0.0000	0.0000
0.0000	0.0000	0.0000

Boolean: OFF

millisecond multiple: 0

Data Capture Length (#): 0

Numeric: 0

Move
Allow Repeats
PMT Strip Chart 4
Amplitude
800
700
600
500
400
300
200
100
0
0
1023
Time
Stop RMS
Write to File
OK

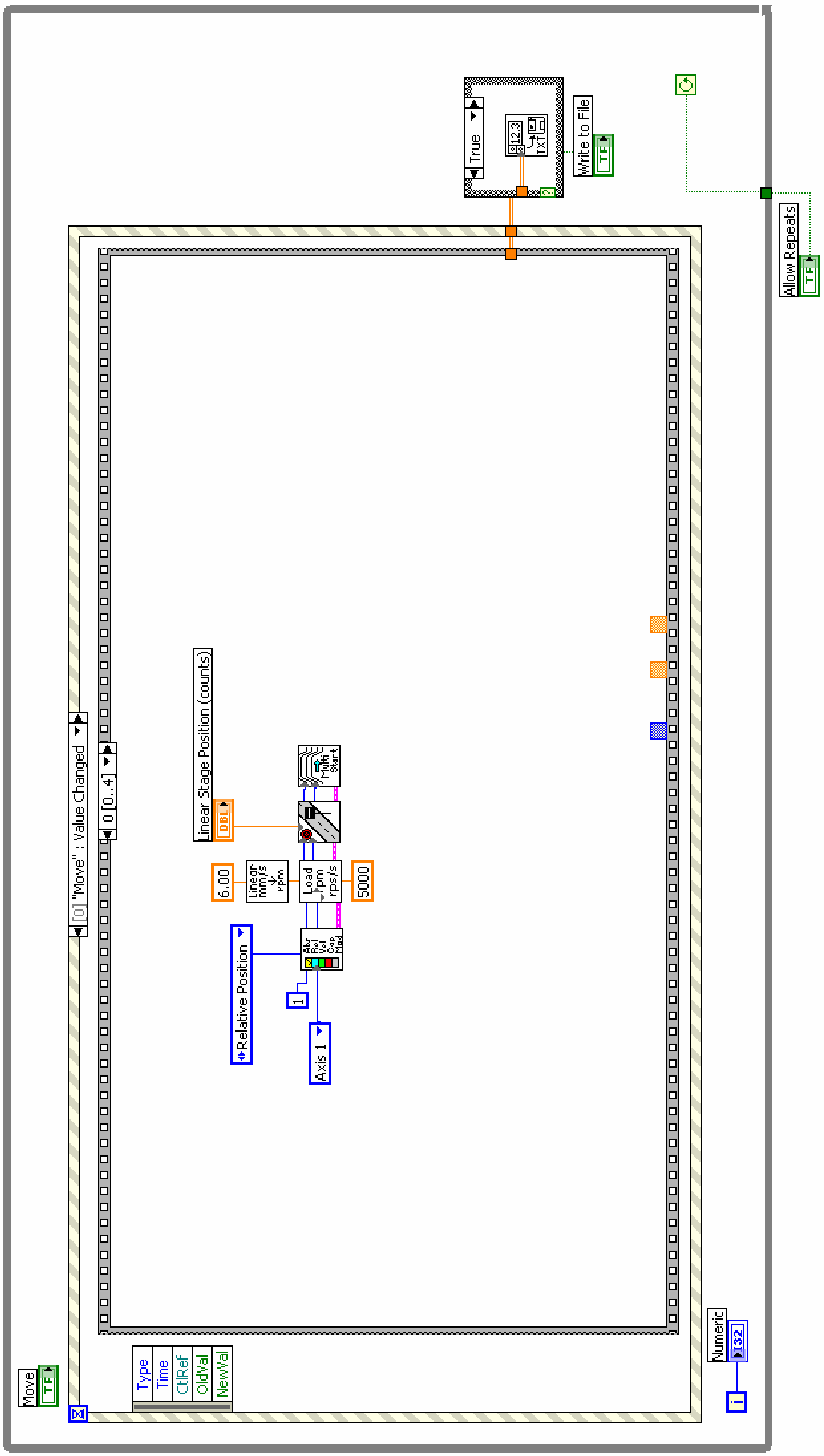
Move
TF
Type
Time
CtlRef
OldVal
NewVal
[0] "Move": Value Changed
0 [0..4]
Linear Stage Position (counts)
DBL
6.00
Linear mm/s → rpm
Load rpm rps/s
5000
Relative Position
1
Axis 1
Multi Start
True
Write to File
TF
Allow Repeats
TF
Numeric
I32
i

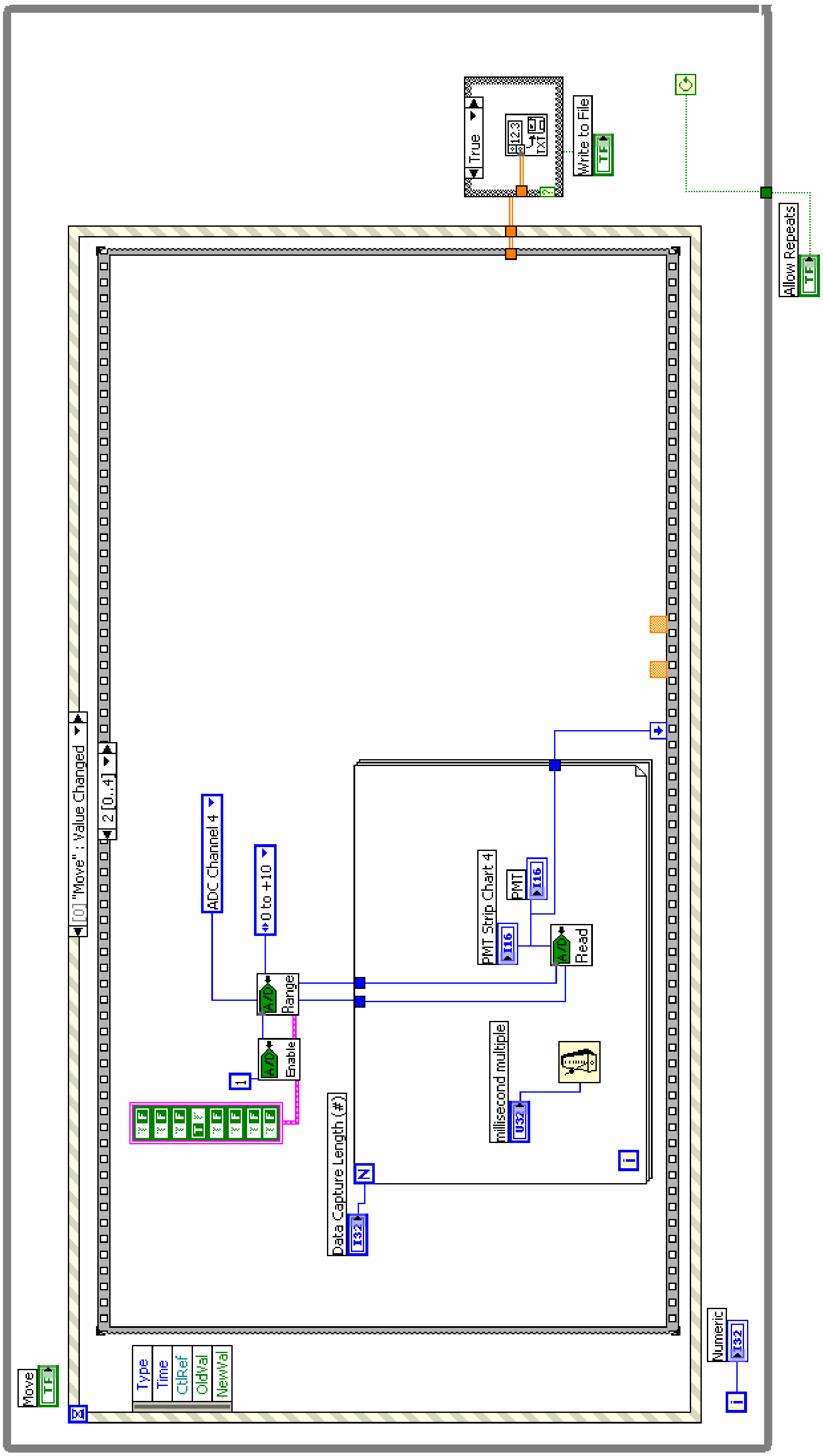

Move
TF
Type
Time
CtlRef
OldVal
NewVal
[0] "Move": Value Changed
2 [0..4]
ADC Channel 4
0 to +10
1
A/D
Enable
A/D
Range
Data Capture Length (#)
I32
N
millisecond multiple
U32
PMT Strip Chart 4
I16
PMT
I16
A/D
Read
i
True
12.3
TXT
Write to File
TF
Allow Repeats
TF
Numeric
I32
i

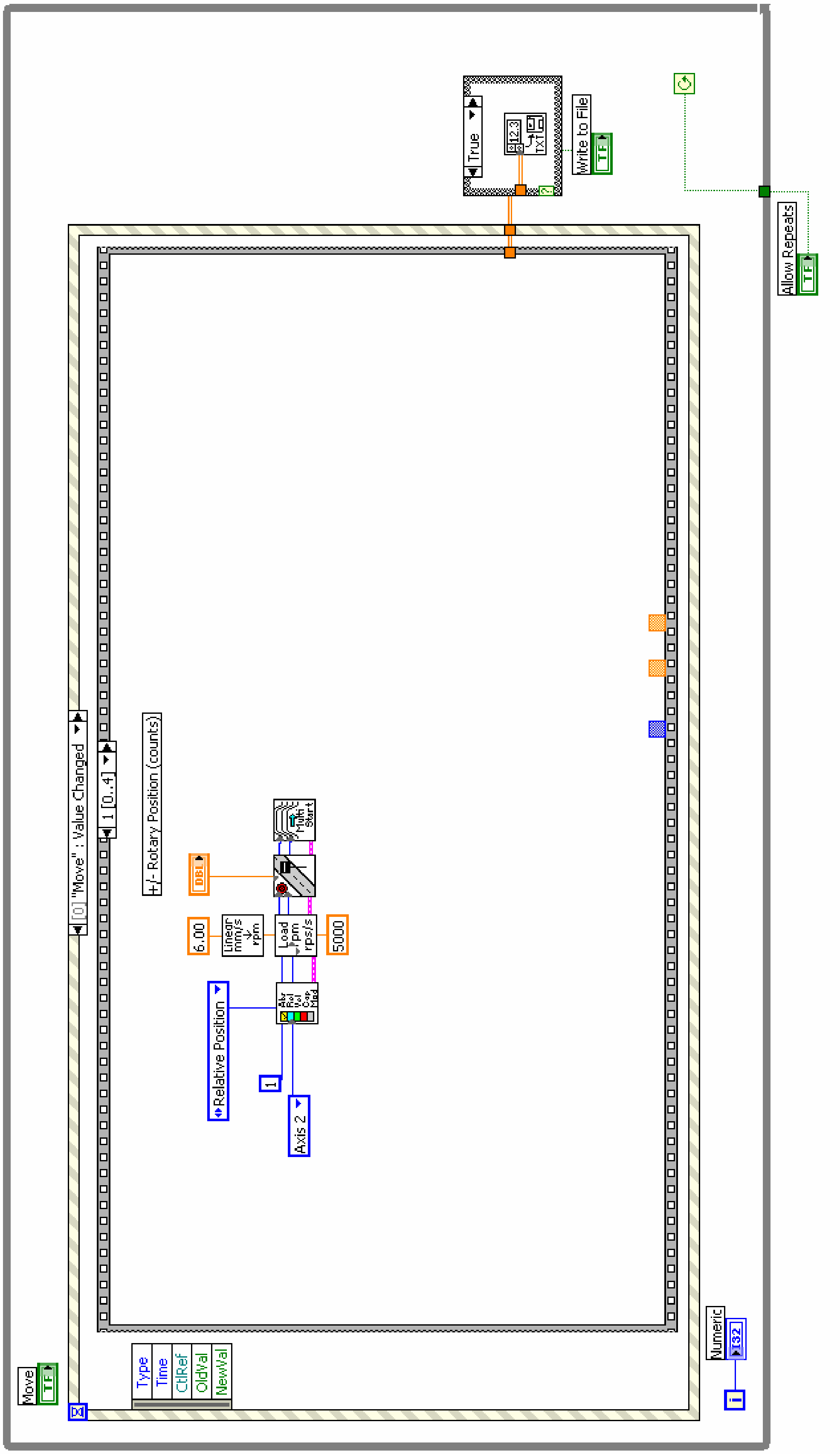
Move
TF
Type
Time
CtlRef
OldVal
NewVal
[0] "Move": Value Changed
1 [0..4]
+/- Rotary Position (counts)
Relative Position
1
Axis 2
6.00
Linear mm/s → rpm
Load rpm rps/s
5000
DBL
Multi Start
Abs Rel Vel Cap Mod
True
12.3
TXT
Write to File
TF
Allow Repeats
TF
Numeric
I32
i

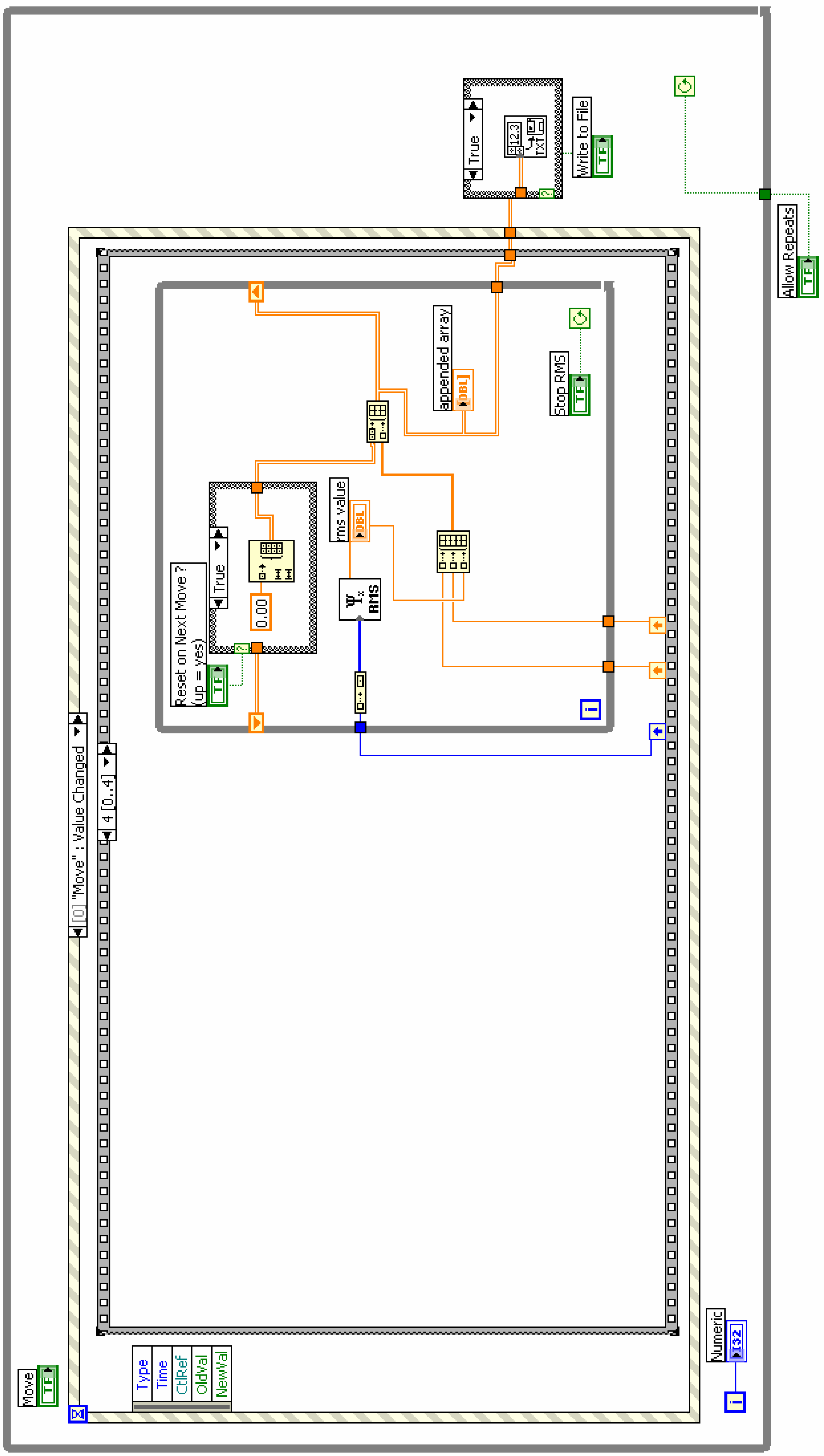
Move
TF
Type
Time
CtlRef
OldVal
NewVal
[0] "Move": Value Changed
4 [0..4]
Reset on Next Move ?
(up = yes)
TF
True
0.00
rms value
DBL
RMS
appended array
[DBL]
Stop RMS
TF
True
12.3
TXT
Write to File
TF
Allow Repeats
TF
Numeric
I32

Appendix C: Matlab Signal Processing Programs

Counting Program used for Microspheres

```
%PeakFinder2

%Tell the program which scan data file to use
TitleText = 'C:\KIST\Dave\Scans2005-01-14Spring05\2005-01-28d';

%Reading in the data
data = textread(TitleText);
cutoff = 1;
x = data(cutoff:length(data),1);
y = data(cutoff:length(data),2);
z = data(cutoff:length(data),3);

%If digital filtration is used, make active the following command:
%FilterScan2;

%Determining the background automatically
bincenters = 1:max(z);
[frequency, bincenters] = hist(z,bincenters);
[bgfrequency, background] = max(frequency);
background

%To set the background to a specific value, make active the following:
%background = 340

%Bgcutoff will be multiplied by the background to determine the minimum
%value that's accepted as a peak point.
bgcutoff = 1.1;

peakX(1) = 0;

k = 1;
for i = 2:length(z);
    if z(i) > background*bgcutoff;
        peakX(k) = x(i);
        peakY(k) = y(i);
        peakZ(k) = z(i);
        k = k+1;
    end
end

%Separation Distance:  how far points have to be away from each other
in
%order to be counted as separate peaks
SepDist = 0.05;

if peakX(1) ~= 0;
m = 1;
for n = 1:length(peakX);
    if m == 1;
        MicroCountX(m) = peakX(n);
        MicroCountY(m) = peakY(n);
        MicroCountZ(m) = peakZ(n);
        m = m + 1;
    elseif sqrt((peakX(n)-MicroCountX(m-1))^2...
        + (peakY(n)-MicroCountY(m-1))^2) < SepDist;
        if peakZ(n) > MicroCountZ(m-1);
            MicroCountZ(m-1) = peakZ(n);
            MicroCountX(m-1) = peakX(n);
            MicroCountY(m-1) = peakY(n);
        end
    else
        MicroCountX(m) = peakX(n);
        MicroCountY(m) = peakY(n);
        MicroCountZ(m) = peakZ(n);
        s=1;

        for p = 2:length(MicroCountX);
            if sqrt((MicroCountX(m)-MicroCountX(p-1))^2...
                + (MicroCountY(m)-MicroCountY(p-1))^2) < SepDist;
                if MicroCountZ(m) > MicroCountZ(p-1);
                    MicroCountZ(p-1) = MicroCountZ(m);
                    MicroCountX(p-1) = MicroCountX(m);
                    MicroCountY(p-1) = MicroCountY(m);
                end
                if s == 1;
                    m = m - 1;
                    s = 2;
                else
                end
            end
        end
        m = m + 1;
    end
end

%Finding the area Scanned
rout = sqrt(x(1)^2 + y(1)^2);
rin = sqrt(x(length(x))^2 + y(length(y))^2);
scanarea = pi*(rout^2 - rin^2);
cpmm2 = length(MicroCountX)/scanarea; %counts per square millimeter

%Plot the data
plot3(x,y,z,'.-');
hold;
plot3(peakX,peakY,peakZ,'or');
plot3(MicroCountX,MicroCountY,MicroCountZ,'or','MarkerFace','g');
hold;

title(TitleText,'Interpreter','none')
xlabel('Location on Stage, X-axis (mm)','FontSize',10)
ylabel('Location on Stage, Y-axis (mm)','FontSize',10)
zlabel('PMT Reading (mV)','FontSize',10)

%Output the summary to the screen
fprintf('\n \nBackground: %4.0f \n', background)
fprintf('Points Above Threshold: %4.0f \n', length(peakX))
fprintf('Number of Peaks Present: %4.0f \n', length(MicroCountX))
fprintf('Sum of peakZ: %4.0f \n', sum(peakZ))
fprintf('Mean of peakZ: %4.0f \n', mean(peakZ))
fprintf('Sum of MicroCountZ: %4.0f \n', sum(MicroCountZ))
fprintf('Mean of MicroCountZ: %4.0f \n', mean(MicroCountZ))
fprintf('Scan Area: %4.0f \n', scanarea)
fprintf('Counts per square millimeter: %4.0f \n', cpmm2)

fprintf('%4.0f\n', background)
fprintf('%4.0f\n', length(peakX))
fprintf('%4.0f\n', length(MicroCountX))
fprintf('%4.0f\n', sum(peakZ))
fprintf('%4.0f\n', mean(peakZ))
fprintf('%4.0f\n', sum(MicroCountZ))
fprintf('%4.0f\n', mean(MicroCountZ))
fprintf('%6.2f\n', scanarea)
fprintf('%6.2f\n', cpmm2)

%If no peaks are counted, the following else statements are activated.
else
RowSize = 48;
for i=1:length(z)./RowSize-1;
    plot3(x(i*RowSize+1:i*RowSize+RowSize),...
          y(i*RowSize+1:i*RowSize+RowSize),...
          z(i*RowSize+1:i*RowSize+RowSize),'r');
end
hold

%Finding the area Scanned
rout = sqrt(x(1)^2 + y(1)^2);
rin = sqrt(x(length(x))^2 + y(length(y))^2);
scanarea = pi*(rout^2 - rin^2);

fprintf('There are no significant Peaks.')
plot3(x,y,z,'.-')
background
title(TitleText,'Interpreter','None')

peakX = [ ];
MicroCountX = [];
peakZ = 0;
MicroCountZ = 0;
cpmm2 = 0;

fprintf('%4.0f\n', background)
fprintf('%4.0f\n', length(peakX))
fprintf('%4.0f\n', length(MicroCountX))
fprintf('%4.0f\n', sum(peakZ))
fprintf('%4.0f\n', mean(peakZ))
fprintf('%4.0f\n', sum(MicroCountZ))
fprintf('%4.0f\n', mean(MicroCountZ))
fprintf('%6.2f\n', scanarea)
fprintf('%6.2f\n', cpmm2)

end
```

Counting Program used for Bacteria

```
%PeakFinder02
%Uses Points Above Threshold to calculate cell concentration
clear

%Tell the program which scan data file to use
TitleText = 'C:\KIST\Dave\Scans2005-01-14Spring05\2005-01-28d';

%Reading in the data
data = textread(TitleText);
cutoff = 1;
x = data(cutoff:length(data),1);
y = data(cutoff:length(data),2);
z = data(cutoff:length(data),3);

%To manually set the digital filter cutoff, activate the following:
%lowband = 0;

%To use digital filtration, activate the following
%FilterScanToCall;

%Automatically determine background
bincenters = 1:max(z);
[frequency, bincenters] = hist(z,bincenters);
[bgfrequency, background] = max(frequency);

%To manually set the background, activate the following
%background = 321;

%Bgcutoff will be multiplied by the background to determine the threshold,
%i.e. the minimum value that's accepted as a peak point.
bgcutoff = 1.04;

%Find all data points above the threshold
keepers = find(z > background.*bgcutoff);
peakX = x(keepers);
peakY = y(keepers);
peakZ = z(keepers);

%Finding the area Scanned and cell concentration
rout = sqrt(x(1)^2 + y(1)^2);
rin = sqrt(x(length(x))^2 + y(length(y))^2);
scanarea = pi*(rout^2 - rin^2);

%To figure the number of cells counted, assume only one spot per bacterium:
cpmm2 = length(peakX)/scanarea; %counts per square millimeter
StoN = mean(peakZ)/background;
cpp = length(peakX)/length(z);

%Display a histogram of PMT data
figure
hist(z,length(z))
```

```
axis([350 450 0 9000])
title(TitleText,'Interpreter','none')

%Display a 3D plot of the data, with counted points in red
figure
plot3(x,y,z);
hold;
plot3(peakX,peakY,peakZ,'.r');

hold;

title(TitleText,'Interpreter','none')
xlabel('Location on Stage, X-axis (mm)','FontSize',10)
ylabel('Location on Stage, Y-axis (mm)','FontSize',10)
zlabel('PMT Reading (mV)','FontSize',10)

%Output a summary of important data to the screen
fprintf('\n \nBackground: %4.0f \n', background)
fprintf('Points Above Threshold: %4.0f \n', length(peakX))
fprintf('Scan Area: %4.0f \n', scanarea)
fprintf('Counts per square millimeter: %6.2f \n', cpmm2)
fprintf('Signal to Noise ratio: %6.2f \n', StoN)
fprintf('Counts per Data Points: %6.5f \n', cpp)

fprintf('%4.0f\n', background)
fprintf('%4.0f\n', length(peakX))
fprintf('%6.2f\n', scanarea)
fprintf('%6.2f\n', cpmm2)
fprintf('%6.2f\n', StoN)
fprintf('%6.5f\n', cpp)
```

Digital Filtering Program

```
%FilterScanToCall
%This program can be called by others in annulus scan data interpreters.

SampleSize = length(z);

%Fast Fourier Transform used to convert data to the frequency domain
Z = fft(z,SampleSize);

%Determine the distance between data points for
%Only 1/5 of the data is used, which decreases run time
for ij = 2:length(z)/20
    i = ceil(ij + length(z)/2 - length(z)/40);
    dist(ij) = sqrt((x(i)-x(i-1)).^2 + (y(i)-y(i-1)).^2);
end

%Find the outer radius of the scanned annulus
rout1 = sqrt(x(1)^2 + y(1)^2);
%Find the inner radius of the scanned annulus
rin1 = sqrt(x(length(x))^2 + y(length(y))^2);
%Determine the average radius in the annulus
meanRad = mean([rout1,rin1]);

%Determine number of data points in one circumference
circ = meanRad*2*pi/mean(dist);

%harmonic is the number of harmonics in the frequency spectrum that the
%user would like to filter out.
%When calling this program, harmonic is set by the calling program.
%To set the harmonic value manually, activate the following:
%harmonic = 2.5;

%Determine how much of the frequency domain data to remove, based on the
%harmonic value.  The number of data points in one circumference (circ)
%is used to determine where the harmonics actually lie.
lowband = ((1/circ)-1/(length(z)))/(1-1/length(z))*harmonic;

%Filter out the low frequency data, up to the number of harmonics desired
Zfilt = Z;
Zfilt(2:round(length(Z)*lowband)) = 0;
Zfilt(round(length(Z)*(1-lowband)):length(Z)) = 0;

%convert the data back to the time domain
zi = ifft(Zfilt);
z = real(zi);
```

The Graphical output was done by another program, whose pertinent code is given below.

```
%FilterScan

Zfiltout = Z;
Zfiltout(round(length(Z)*lowband):round(length(Z)*(1-lowband))) = 0;
```

```
ziout = ifft(Zfiltout);

PZ = Z.*conj(Z);
PZfilt = Zfilt.*conj(Zfilt);
PZfiltout = Zfiltout.*conj(Zfiltout);

frequency = 1./[1:length(z)];
frequency = fliplr(frequency);

figure
Plength=700;
subplot(2,1,1);
semilogy(frequency(1:Plength),PZ(1:Plength));
hold
semilogy(frequency(1:Plength),PZfilt(1:Plength),':r','LineWidth',2);
axis([min(frequency) frequency(Plength/2) 10^2 10^15])
hold
xlabel('Frequency','Fontsize',14)
ylabel('Amplitude','Fontsize',14)
legend('Original Frequencies','Filtered Frequencies')
harmonicString = num2str(harmonic)
plottitle = ['Harmonic Cutoff = ', harmonicString]
title(plottitle,'Fontsize',14)

Zlength = 7000;
subplot(2,1,2);
plot(z(1:Zlength));
hold
plot(real(zi(1:Zlength)),'r');
plot(real(ziout(1:Zlength)),'g','LineWidth',2);
hold

xlabel('Data Point #','Fontsize',14)
ylabel('PMT Reading (mV)','Fontsize',14)
legend('Original Data','Filtered Data','Data Subracted')
```

Appendix D: Fluorescence Microscope Settings

Screen shots of fluorescence microscope settings were taken and are pasted below.

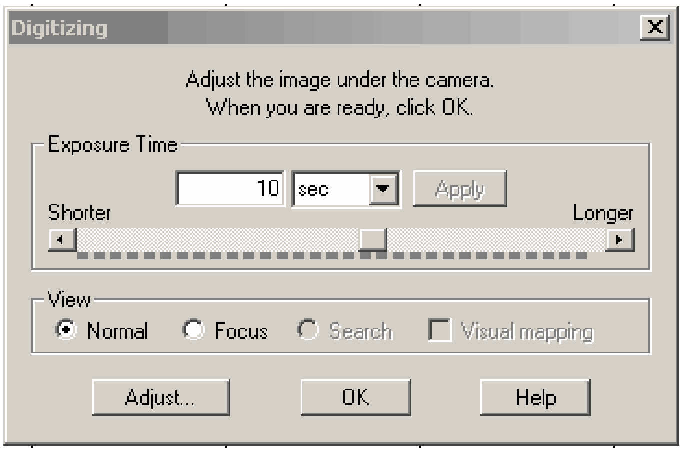

Digitizing

Adjust the image under the camera.
When you are ready, click OK.

Exposure Time: 10 sec

View: ● Normal ○ Focus ○ Search ☐ Visual mapping

Apply
Shorter
Longer
Adjust...
OK
Help

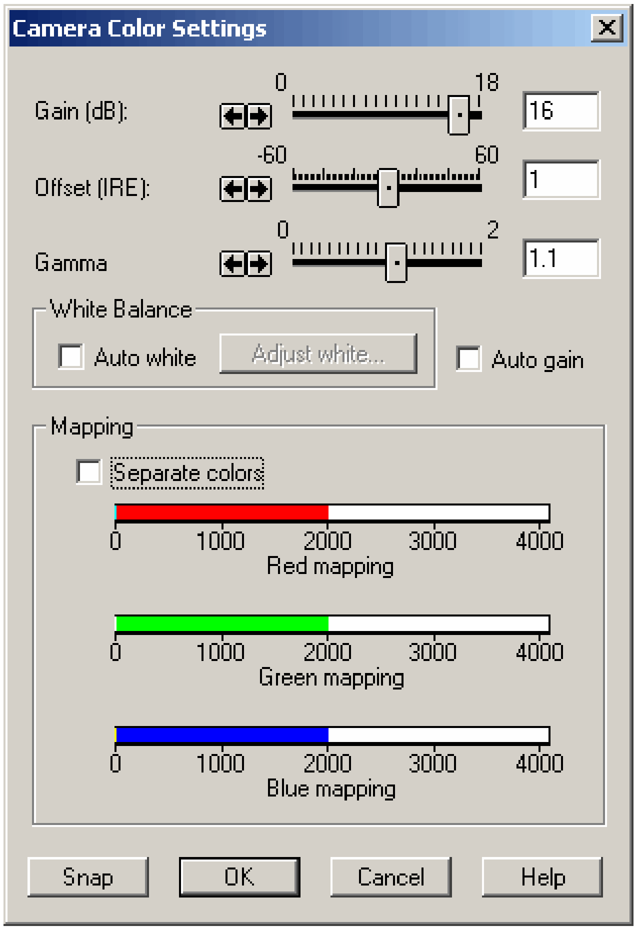

Camera Color Settings

Gain (dB): 16

Offset (IRE): 1

Gamma: 1.1

White Balance: ☐ Auto white

☐ Auto gain

Mapping: ☐ Separate colors

0
18
-60
60
0
2
Adjust white...
0
1000
2000
3000
4000
Red mapping
0
1000
2000
3000
4000
Green mapping
0
1000
2000
3000
4000
Blue mapping
Snap
OK
Cancel
Help

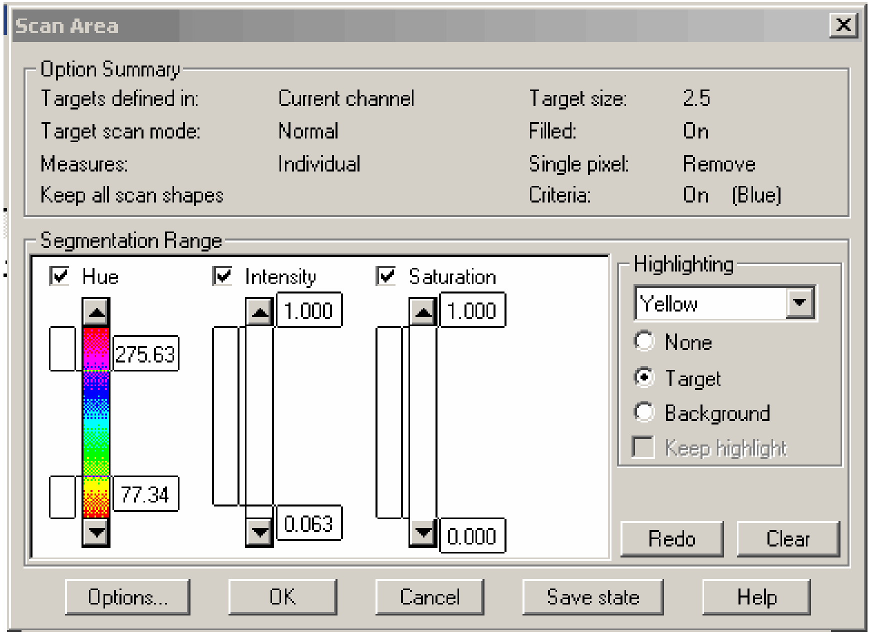

Scan Area

Option Summary

Targets defined in:	Current channel	Target size:	2.5
Target scan mode:	Normal	Filled:	On
Measures:	Individual	Single pixel:	Remove
Keep all scan shapes		Criteria:	On (Blue)

Segmentation Range

☑ Hue 275.63 77.34

☑ Intensity 1.000 0.063

☑ Saturation 1.000 0.000

Highlighting: Yellow

○ None

● Target

○ Background

☐ Keep highlight

Redo
Clear
Options...
OK
Cancel
Save state
Help

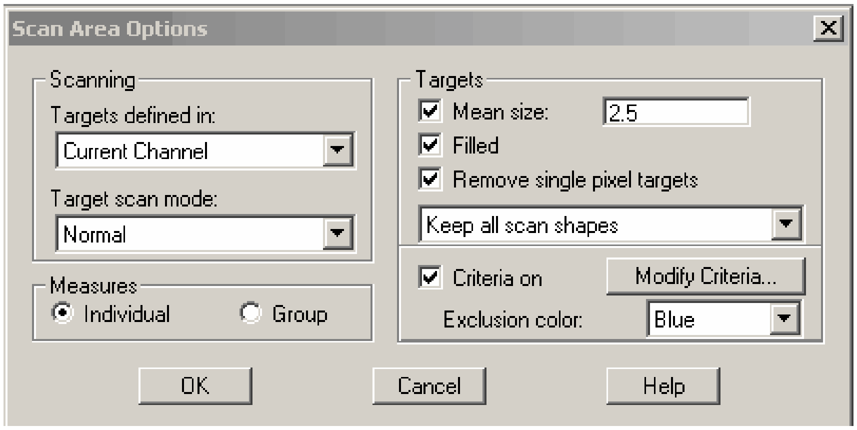

Scan Area Options

Scanning

Targets defined in: Current Channel

Target scan mode: Normal

Measures: ● Individual ○ Group

Targets

☑ Mean size: 2.5

☑ Filled

☑ Remove single pixel targets

Keep all scan shapes

☑ Criteria on

Exclusion color: Blue

Modify Criteria...
OK
Cancel
Help

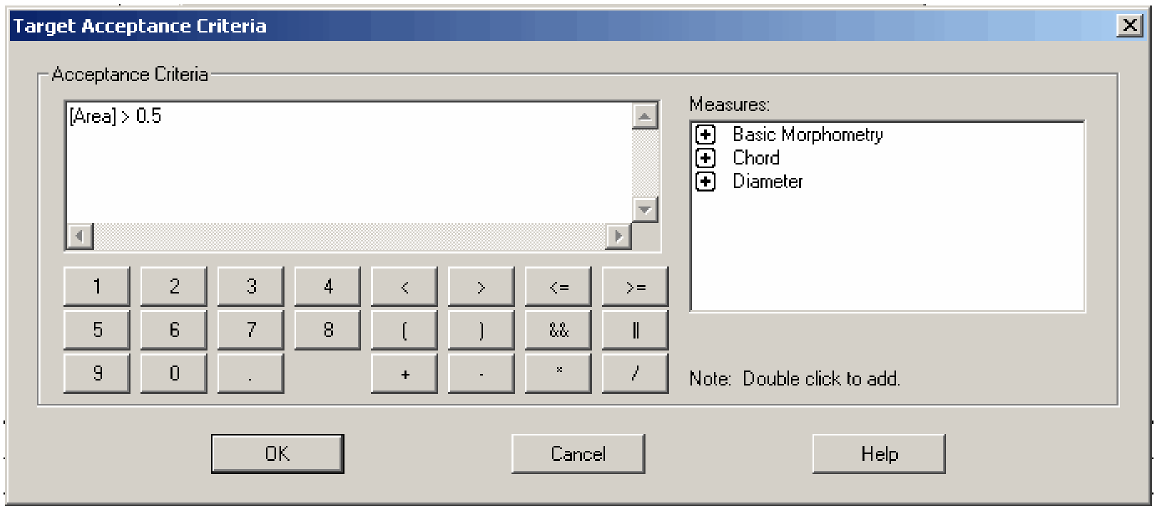

Target Acceptance Criteria

Acceptance Criteria

[Area] > 0.5

Measures:

- Basic Morphometry
- Chord
- Diameter

Note: Double click to add.

1
2
3
4
<
>
<=
>=
5
6
7
8
(
)
&&
||
9
0
.
+
-
*
/
OK
Cancel
Help

Bibliography

Acker, C. L., C. K. Colvin, B. J. Marinas, and J. C. Lozier. 2001. Assessing the Integrity of Reverse Osmosis Spiral-Wound Membrane Elements with Biological and Non-Biological Surrogate Indicators.

Aurell, H., P. Catala, P. Farge, F. Wallet, M. Le Brun, J. H. Helbig, S. Jarraud, and P. Lebaron. 2004. Rapid Detection and Enumeration of Legionella pneumophila in Hot Water Systems by Solid-Phase Cytometry. *Applied and Environmental Microbiology* 70:3, 1651-1657.

Braga, P. C., C. Bovio, M. Culici, and M. Dal Sasso. 2003. Flow cytometric assessment of susceptibilities of Streptococcus pyogenes to erythromycin and rokitamycin. *Antimicrobial Agents and Chemotherapy* 47:1, 408-412.

Broadaway, S. C., S. A. Barton, and B. H. Pyle. 2003. Rapid staining and enumeration of small numbers of total bacteria in water by solid-phase laser cytometry. *Applied and Environmental Microbiology* 69:7, 4272-4273.

Carr, M. C., K. H. Carlson, and M. Sadar. 2003. Membrane integrity monitoring with distributed laser turbidimetry. *Journal / American Water Works Association* 95:6, 83-94.

Chiou, C. F., M. Torres-Lugo, B. J. Marinas, and J. Q. Adams. 1997. Nonbiological surrogate indicators for assessing ozone disinfection. *Journal / American Water Works Association* 89:8, 54-66.

Comas, J., and J. Vives-Rego. 1997. Assessment of the effects of gramicidin, formaldehyde, and surfactants on Escherichia coli by flow cytometry using nucleic acid and and membrane potential dyes. *Cytometry* 29:1, 58-64.

Comas-Riu, J., and J. Vives-Rego. 2002. Cytometric monitoring of growth, sporogenesis and spore cell sorting in Paenibacillus polymyxa (formerly Bacillus polymyxa). *Journal of Applied Microbiology* 92:3, 475-481.

Crozes, G. F., S. Sethi, B. Mi, J. Curl, and B. Marinas. 2002. Improving membrane integrity monitoring indirect methods to reduce plant downtime and increase microbial removal credit. *Desalination* 149:1-3, 493-497.

Dai, X., and R. M. Hozalski. 2003. Evaluation of microspheres as surrogates for Cryptosporidium parvum oocysts in filtration experiments. *Environmental Science and Technology* 37:5, 1037-1042.

Darzynkiewicz, Z., E. Bedner, X. Li, W. Gorczyca, and M. R. Melamed. 1999. Laser-scanning cytometry: A new instrumentation with many applications. *Experimental Cell Research* 249:1, 1-12.

Degrooth, B. G., T. H. Geerken, and J. Greve. 1985. The Cytodisk - A Cytometer Based Upon A New Principle of Cell Alignment. *Cytometry* 6:3, 226-233.

Deininger, R. A., and J. Lee. 2001. Rapid determination of bacteria in drinking water using an ATP assay. *Field Analytical Chemistry and Technology* 5:4, 185-189.

Eckner, K. F., S. Jullien, I. D. Samset, and J. D. Berg. 1999. Rapid, enzyme-based, fluorometric detection of total and thermotolerant coliform bacteria in water samples. *Water Supply* 17:2, 73-79.

Fang, Y., and B. E. Logan. 1999. Bacterial transport in gas-sparged porous medium. *Journal of Environmental Engineering* 125:7, 668-673.

Farahbakhsh, K., S. S. Adham, and D. W. Smith. 2003. Monitoring the integrity of low-pressure membranes. *Journal / American Water Works Association* 95:6, 95-107.

Farinas, J., A. W. Chow, and H. G. Wada. 2001. A microfluidic device for measuring cellular membrane potential. *Analytical Biochemistry* 295:2, 138-142.

Guindulain, T., J. Comas, and J. Vives-Rego. 1997. Use of nucleic acid dyes SYTO-13, TOTO-1, and YOYO-1 in the study of Escherichia coli and marine prokaryotic populations by flow cytometry. *Applied and Environmental Microbiology* 63:11, 4608-4611.

Guindulain, T., and J. Vives-Rego. 2002. Involvement of RNA and DNA in the staining of Escherichia coli by SYTO 13. *Letters in Applied Microbiology* 34:3, 182-188.

Hobbie, J. E., R. J. Daley, and S. Jasper. 1977. Use of Nucleopore Filters for Counting Bacteria by Fluorescence Microscopy. *Applied and Environmental Microbiology* 33:5, 1225-1228.

Hong, S. K., F. A. Miller, and J. S. Taylor. 2001. Assessing pathogen removal efficiency of microfiltration by monitoring membrane integrity. *Water Science and Technology: Water Supply* 1:4, 43-48.

Jacangelo, J. G., J. M. Laine, K. E. Carns, E. W. Cummings, and J. Mallevialle. 1991. Low-pressure membrane filtration for removing Giardia and microbial indicators. *Journal of the American Water Works Association* 83:9, 97-106.

Kamentsky, L. A., and L. D. Kamentsky. 1991. Microscope-Based Multiparameter Laser Scanning Cytometer Yielding Data Comparable to Flow-Cytometry Data. *Cytometry* 12:5, 381-387.

Katsuragi, T., and Y. Tani. 2001. Single-cell sorting of microorganisms by flow or slide-based (including laser scanning) cytometry. *Acta Biotechnologica* 21:2, 99-115.

Kepner, R. L., and J. R. Pratt. 1994. Use of Fluorochromes for Direct Enumeration of Total Bacteria in Environmental-Samples - Past and Present. *Microbiological Reviews* 58:4, 603-615.

Kitis, M., J. C. Lozier, J. H. Kim, B. Mi, and B. J. Marinas. 2003. Microbial removal and integrity monitoring of RO and NF membranes. *Journal / American Water Works Association* 95:12, 105-119.

Kramer, T. A., and M. M. Clark. 1996. The Measurement of Particles Suspended in a Stirred Vessel Using Microphotography and Digital Image Analysis. *Particles and Particle Systems Characterization* 13:3-9.

Latt, S. A., M. Marino, and M. Lalande. 1984. New Fluorochromes, Compatible with High Wavelength Excitation, for Flow Cytometric Analysis of Cellular Nucleic-Acids. *Cytometry* 5:4, 339-347.

Lebaron, P., P. Servais, H. Agogue, C. Courties, and F. Joux. 2001. Does the high nucleic acid content of individual bacterial cells allow us to discriminate between active cells and inactive cells in aquatic systems? *Applied and Environmental Microbiology* 67:4, 1775-1782.

Lee, B. W. 2003. Indirect Membrane Integrity Monitoring through Bacteria Detection. Masters Thesis, University of Illinois at Urbana-Champaign, Urbana, Illinois.

Lisle, J. T., M. A. Hamilton, A. R. Willse, and G. A. McFeters. 2004. Comparison of fluorescence microscopy and solid-phase cytometry methods for counting bacteria in water. *Applied and Environmental Microbiology* 70:9, 5343-5348.

Mignon-Godefroy, K., J. G. Guillet, and C. Butor. 1997. Solid phase cytometry for detection of rare events. *Cytometry* 27:4, 336-344.

Niehren, S., and W. Kinzelbach. 1998. Artificial colloid tracer tests: Development of a compact on-line microsphere counter and application to soil column experiments. *Journal of Contaminant Hydrology* 35:1-3, 249-259.

Norton, S. M., J. Winkler, and L. J. Dietz. 2000. Cell enumeration and characterization in Microvolume Laser Scanning Cytometry: A multicolor image processing package. Proceedings of SPIE - The International Society for Optical Engineering 3921:20-30.

Pinder, A. C., P. W. Purdy, S. A. G. Poulter, and D. C. Clark. 1990. Validation of Flow-Cytometry for Rapid Enumeration of Bacterial Concentrations in Pure Cultures. *Journal of Applied Bacteriology* 69:1, 92-100.

Seyde, V., D. Clark, E. Akiyoshi, A. Kalinsky, and C. Spangenberg. 1999. Nanofiltration process microbial challenge studies.

Shapiro, H. M., and S. Stephens. 1986. Flow-Cytometry of Dna Content Using Oxazine-750 Or Related Laser-Dyes with 633-Nm Excitation. *Cytometry* 7:1, 107-110.

Shaw, N., and P. L. Haddix. Video Counting Devices Save Time, Reduce Injuries. Opflow , 10-12. 2004. American Water Works Association. (GENERIC)
Ref Type: Magazine Article

Smith, S. W. 1999. *The Scientist and Engineer's Guide to Digital Signal Processing*. 2 ed. California Technical Publishing, San Diego.

States, S., J. Newberry, J. Wichterman, J. Kuchta, M. Scheuring, and L. Casson. 2004. Rapid Analytical Techniques for Drinking Water security investigations. *Journal / American Water Works Association* 96:1, 52-64.

Thein, E., S. Raab, A. G. Harris, and K. Messmer. 2000. Automation of the use of fluorescent microspheres for the determination of blood flow. *Computer Methods and Programs in Biomedicine* 61:1, 11-21.

Tibbe, A. G. J., B. G. de Grooth, J. Greve, P. A. Liberti, G. J. Dolan, and L. W. M. M. Terstappen. 1999. Optical tracking and detection of immunomagnetically selected and aligned cells. *Nature Biotechnology* 17:12, 1210-1213.

Van Poucke, S. O., and H. J. Nelis. 2000. A 210-min solid phase cytometry test for the enumeration of Escherichia coli in drinking water. *Journal of Applied Microbiology* 89:3, 390-396.

Varga, V. S., J. Bocsi, F. Sipos, G. Csendes, Z. Tulassay, and B. Molnar. 2004. Scanning fluorescent microscopy is an alternative for quantitative fluorescent cell analysis. *Cytometry Part A* 60A:1, 53-62.

Walton, I. D., L. J. Dietz, G. Frenzel, J. Chen, J. Winkler, S. M. Norton, and A. B. Kantor. 2000. Microvolume laser scanning cytometry platform for biological marker discovery. *Proceedings of SPIE - The International Society for Optical Engineering* 3926:192-201.